

Copyright  
by  
Jason Kelly Allison  
2012

**The Dissertation Committee for Jason Kelly Allison Certifies that this is the  
approved version of the following dissertation:**

**The Rev-mediated Dimerization of HIV RRE RNA**

**Committee:**

---

Robert O. Fox, PhD

---

Henry Epstein, PhD

---

Miles Cloyd, PhD

---

James Briggs, PhD

---

Junji Iwahara, PhD

---

Dean, Graduate School

**The Rev-mediated Dimerization of HIV RRE RNA**

**by**

**Jason Kelly Allison, BS**

**Dissertation**

Presented to the Faculty of the Graduate School of

The University of Texas Medical Branch

in Partial Fulfillment

of the Requirements

for the Degree of

**Doctor of Philosophy, Biochemistry and Molecular Biology**

**The University of Texas Medical Branch**

**December, 2012**

## **Dedication**

I would like to dedicate this work to my father, Bucky Allison, who passed away in 2007, and to my daughter, Paris Celeste Allison. Both have been in my thoughts and given me the motivation to persevere.

## **ACKNOWLEDGEMENTS**

I would like to extend gratitude to my mentor Dr. Robert O. Fox for his direction, experience and knowledge, as well as giving me the opportunity to learn and study in his laboratory. I would also like to thank lab members Deqian Liu, Dr. Raza Khan, Dr. Kris Tesh, Dr. Kevin Mackenzie, and Dr. Aditya Hindupur for offering their expertise and experience toward my education. I would also like to thank Debora Botting for her commitment and support.

## LIST OF TABLES

<b>Table 1</b> Calculated analytical ultracentrifugation parameters for Rev:sIIB-tRNA <sup>Phe</sup> Complexes using SEDFIT .....	101
<b>Table 2</b> Measured hydrodynamic properties of tRNA, sIIB-tRNA <sup>Phe</sup> , and its complexes with Rev and RevN70 using Hydropro.....	112
<b>Table 3</b> Calculated hydrodynamic properties of models for sIIB-tRNA <sup>Phe</sup> with Rev ...	112

## LIST OF FIGURES

Figure 1 Functional Motifs of Rev.....	7
Figure 2 Canonical Rev-RRE Transport Cycle. ....	8
Figure 3 Rev-RRE Transport Cycle with Cellular Cofactors. ....	11
Figure 4 NMR structure of the 34 nucleotide Stem Loop-IIB complexed with ARM peptide of Rev. ....	14
Figure 5 Crystal structure of the Rev dimer.....	15
Figure 6 Crystal structure of the Rev dimer.....	15
Figure 7 Representation of full-length RRE secondary structural elements.....	17
Figure 8 Minimally functional RRE (240 nucleotides) as described in 1989.....	18
Figure 9 Minimally functional RRE as described in 1994 .....	19
Figure 10 Properties of RevWT.....	24
Figure 11 Properties of RevN70. ....	26
Figure 12 Properties of RevN60.. ....	27
Figure 13 Properties of Rev103a peptide.....	28
Figure 14 Map of YP001 vector .....	30
Figure 15 SDS-PAGE of purified and TEV cut RevN60, RevN70, and RevWT. ....	33
Figure 16 Schematic for expression of chimeric tRNA from pBS(SK+) containing target RNA sequences. ....	35
Figure 17 Gel shift experiment comparing Rev binding to RWZ1 and RWZ2 (sIIB). ....	37
Figure 18 Lysyl tRNA (Human).....	38
Figure 19 Lysyl tRNA (Human).. ....	40
Figure 20 Phenylalanyl tRNA (Yeast).....	41
Figure 21 Phenylalanyl tRNA (Yeast).....	43
Figure 22 Initiator methionyl tRNA ( <i>E. coli</i> ). ....	44
Figure 23 Initiator methionyl tRNA ( <i>E. coli</i> ) .....	46
Figure 24 Position of the IIB sequence within the context of the truncated Rev Response Element. . ....	48
Figure 25 Annotated gene sequence for IIB-tRNA <sup>Phe</sup> construct.....	49
Figure 26 Postion of the RRE contained within IIB sequence .....	50
Figure 27 sIIB-tRNA <sup>Phe</sup> . ....	51
Figure 28 Expression of sIIB-tRNA <sup>Lys</sup> .. ....	53
Figure 29 pBS(SK+) vector.. ....	54
Figure 30 Q-Sepharose chromatogram showing purification of sIIB-tRNA <sup>Lys</sup> .....	63
Figure 31 Native PAGE (12%) of Q-Sepharose fractions of sIIB-tRNA <sup>Lys</sup> elution profile. ....	64

Figure 32 Elution profile of MonoQ 16/10 purification of sIIB-tRNA <sup>Lys</sup> .....	65
Figure 33 Native PAGE (7%) of fractions from MonoQ 16/10 purification of sIIB-tRNA <sup>Lys</sup> . .....	66
Figure 34 7% Native-PAGE of IIB-tRNA <sup>Phe</sup> and sIIB-tRNA <sup>Phe</sup> .....	67
Figure 35 Elution profile of Q-Sepharose purification of sIIB-tRNA <sup>Phe</sup> .....	68
Figure 36 Elution profile of MonoQ 16/10 purification of sIIB-tRNA <sup>Phe</sup> .....	69
Figure 37 Native PAGE (7%) of fractions from MonoQ 16/10 purification of sIIB-tRNA <sup>Phe</sup> .....	70
Figure 38 Elution profile from MonoQ 16/10 purification of sIIB-tRNA <sup>MetI</sup> .....	71
Figure 39 Native PAGE (7%) of fractions from MonoQ 16/10 purification of sIIB-tRNA <sup>MetI</sup> .....	73
Figure 40 Elution profile from Q-Sepharose purification of IIB-tRNA <sup>Phe</sup> .....	74
Figure 41 Native PAGE (7%) representing fractions from Q-Sepharose elution for purification of IIB-tRNA <sup>Phe</sup> .....	75
Figure 42 Elution profile from MonoQ 16/10 purification of IIB-tRNA <sup>Phe</sup> .....	76
Figure 43 7% Native-PAGE of MonoQ purified IIB-tRNA <sup>Phe</sup> .....	77
Figure 44 Gel shift of Rev:sIIB <sup>MetI</sup> complexes. ....	80
Figure 45 Standards for Shodex KW803 size-exclusion column. ....	83
Figure 46 SEC elution profiles of Rev:tRNA <sup>Phe</sup> .....	84
Figure 47 SEC elution profiles of Rev:tRNA <sup>Phe</sup> .....	85
Figure 48 SEC elution profiles of Rev:sIIB-tRNA <sup>Phe</sup> .....	86
Figure 49 Shodex KW803 elution profile of purified sIIB-tRNA <sup>Phe</sup> .....	87
Figure 50 Shodex KW803 elution profiles of Rev:sIIB-tRNA <sup>Phe</sup> .....	88
Figure 51 SEC Elution profiles complexed sIIB-tRNA <sup>Phe</sup> .....	89
Figure 52 SEC Elution RevN70 complexed sIIB-tRNA <sup>Phe</sup> .....	91
Figure 53 SEC Elution profiles of Rev <sup>Fluo</sup> :sIIB-tRNA <sup>Phe</sup> .....	93
Figure 54 SEC Elution profiles of Rev <sup>Fluo</sup> :sIIB-tRNA <sup>Phe</sup> .....	94
Figure 55 495 nm absorbance across the Rev <sup>Fluo</sup> :sIIB-tRNA <sup>Phe</sup> .....	95
Figure 56 SEC Elution profiles of sIIB-tRNA <sup>Phe</sup> monomer in the presence of 1 $\mu$ M Rev 97	
Figure 57 S-values extracted from SV-AUC data for the sIIB-tRNA <sup>Phe</sup> monomer in 100 $\mu$ M and 5 mM MgCl <sub>2</sub> .....	102
Figure 58 S-values extracted from SV-AUC data for Rev/sIIB-tRNA <sup>Phe</sup> mixtures. ....	103
Figure 59 Model of sIIB-tRNA <sup>Phe</sup> monomer.....	106
Figure 60 Model of sIIB-tRNA <sup>Phe</sup> monomer rotated 90° .....	107
Figure 61 Model of a Rev <sub>2</sub> : sIIB-tRNA <sup>Phe</sup> <sub>2</sub> .....	110
Figure 62 Model of a Rev <sub>2</sub> : sIIB-tRNA <sup>Phe</sup> <sub>2</sub> .....	110
Figure 63 Model of a Rev <sub>2</sub> : sIIB-tRNA <sup>Phe</sup> <sub>2</sub> .....	111

Figure 64 Model of a Rev <sub>2</sub> : sIIB-tRNA <sup>Phe</sup> .....	111
Figure 65 Log(I) vs. s plot(s) from SAXS data on tRNA <sup>Phe</sup> .....	116
Figure 66 Kratky Plot (I*s <sup>2</sup> vs. s). Overlay of experimental and theoretical Kratky plots (I*s <sup>2</sup> vs. s) of tRNA <sup>Phe</sup> .....	117
Figure 67 Guinier Plot for tRNA <sup>Phe</sup> .....	118
Figure 68 D <sub>Max</sub> determination for tRNA <sup>Phe</sup> .....	119
Figure 69 Bead model of tRNA <sup>Phe</sup> derived from SAXS data compared with the crystal structure.....	120
Figure 70 Bead model of tRNA <sup>Phe</sup> derived from SAXS data compared with the crystal structure.....	121
Figure 71 Log(I) vs. s plot(s) from X-ray scattering curves on sIIB-tRNA <sup>Phe</sup> .....	124
Figure 72 Kratky Plot (I*s <sup>2</sup> vs. s). Overlay of Kratky plots (I*s <sup>2</sup> vs. s) plots of experimental and theoretical scattering curves of tRNA <sup>Phe</sup> ..	125
Figure 73 Guinier plot for sIIB-tRNA <sup>Phe</sup> .....	126
Figure 74 P(r) Curve for sIIB-tRNA <sup>Phe</sup> .....	127
Figure 75 Bead model of sIIB-tRNA <sup>Phe</sup> .....	128

## **The Rev-Mediated Dimerization of HIV RRE RNA**

Publication No. \_\_\_\_\_

Jason Kelly Allison, PhD

The University of Texas Medical Branch, 2011

Supervisor: Robert O. Fox, PhD

The HIV-1 Regulator of Virion Expression (Rev) a regulatory protein which is critical for the late-phase development of the Human Immunodeficiency Virus-1 (HIV-1). During early-phase development of HIV-1, Rev accumulates in the cytoplasm and is transported into the nucleus through interactions with Importin- $\beta$  via its Nuclear Localization Sequence (NLS). Following sufficient accumulation in the nucleus, Rev recognizes and assembles on the Rev Response Element (RRE), a 351nt region contained within singly and unspliced HIV RNAs. This ribonucleoprotein (RNP) complex allows for the export of these RNA transcripts encoding viral structural proteins and genomic RNA to the cytoplasm. Of particular interest is the interaction of Rev with the Rev Response Element (RRE) RNA. It is known that Rev initially binds to a structured Stem Loop-IIB on the RRE and subsequently assembles along flanking sequences of the RRE; however, details of this interaction are not completely understood. RRE-containing tRNAs were designed for biophysical studies of Rev:RRE complexes. The tRNA chimeras employ natural tRNA from human lysyl tRNA, bacterial initiator methionyl tRNA, and baker's yeast (*S. cerevisiae*) phenylalanyl tRNA for use as scaffolds to

express RRE sequences. Using size-exclusion chromatography (SEC), analytical ultracentrifugation (AUC), and small angle X-ray scattering (SAXS), I demonstrate the formation of a discrete Rev:RRE RNA complex. Data analysis presented in this work suggests that Rev is mediating a dimer of RRE RNA.

## TABLE OF CONTENTS

ACKNOWLEDGEMENTS.....	V
LIST OF TABLES.....	VI
LIST OF FIGURES.....	VII
LIST OF ABBREVIATIONS.....	XIV
<b>CHAPTER 1: HIV AND THE REV PROTEIN.....</b>	<b>1</b>
Section 1.1 HIV-1 Replication.....	3
Section 1.2 Rev and the HIV-1 Life Cycle.....	5
Section 1.3 Biophysical Properties of Rev.....	12
Section 1.4 Rev and the Rev Response Element (RRE).....	16
Section 1.5 Rev-mediated RRE RNA Dimerization.....	21
<b>CHAPTER 2: MATERIALS AND METHODS.....</b>	<b>23</b>
Section 2.1 Rev Constructs.....	23
Section 2.1.1 Proteins and Peptides: RevWT, RevN70, RevN60, and Rev 103a.....	23
Section 2.1.1.1 RevWT.....	23
Section 2.1.1.2 RevN70.....	25
Section 2.1.1.3 RevN60.....	26
Section 2.1.1.4 Rev103a.....	28
Section 2.2 Expression, Purification, and Characterization of Rev Constructs.....	29
Section 2.2.1 Rev (WT, N60, and N70) Step by Step Purification Protocol.....	31
Section 2.3 Chimeric tRNA Constructs.....	34
Section 2.3.2 Design of sIIB-containing -tRNA <sup>Lys</sup> , -tRNA <sup>Phe</sup> , and tRNA <sup>Met</sup> I, sIIB-.....	38
Section 2.3.2.1 tRNA <sup>Lys</sup> .....	38
Section 2.3.2.2 sIIB-tRNA <sup>Phe</sup> .....	41

Section 2.3.2.3 sIIB-tRNA <sup>MetI</sup> .....	44
Section 2.3.2.4 IIB-tRNA <sup>Phe</sup> .....	47
Section 2.4 Expression and Purification of RRE-containing Chimeric tRNAs.....	52
Section 2.4.1 Protocol for Chimeric tRNA Expression and Purification .....	55
Section 2.4.2 Protocol for (Chimeric) tRNA:Rev Complex Gel Shift, and Size- Exclusion Chromatography .....	59
Section 2.4.3 Expression and Purification of sIIB-tRNA <sup>Lys</sup> , sIIB-tRNA <sup>MetI</sup> , sIIB- tRNA <sup>Phe</sup> , and IIB- tRNA <sup>Phe</sup> .....	62
<b>CHAPTER 3: REV-MEDIATED DIMERIZATION OF RRE RNA.....</b>	<b>78</b>
Section 3.1 Gel Shift Analysis: Rev forms a discrete complex with sIIB-tRNA <sup>MetI</sup>	78
Section 3.2 Biophysical Measurements on Rev:sIIB-tRNA <sup>Phe</sup> Complexes .....	80
Section 3.2.1 SEC of sIIB-tRNA <sup>Phe</sup> Monomer and Rev:sIIB-tRNA <sup>Phe</sup> Complexes.....	81
Section 3.2.1.1 SEC of Purified sIIB-tRNA <sup>Phe</sup> .....	87
Section 3.2.1.2 SEC of Rev:sIIB-tRNA <sup>Phe</sup> Complexes.....	88
Section 3.2.1.3 SEC of RevN70:sIIB-tRNA <sup>Phe</sup> Complexes.....	90
Section 3.2.1.4 SEC of Rev <sup>Fluo</sup> :sIIB-tRNA <sup>Phe</sup> Complexes.....	92
Section 3.2.2 Analytical Ultracentrifugation: sIIB-tRNA <sup>Phe</sup> and Rev:sIIB- tRNA <sup>Phe</sup> Complexes .....	98
Section 3.2.3 Modeling of the sIIB-tRNA <sup>Phe</sup> Monomer.....	104
Section 3.2.4 Modeling the Rev-mediated sIIB-tRNA <sup>Phe</sup> Dimer .....	108
Section 3.2.5 SAXS: tRNA <sup>Phe</sup> and sIIB-tRNA <sup>Phe</sup> .....	113
Section 3.2.4.1 SAXS Analysis: tRNA <sup>Phe</sup> .....	114
Section 3.2.4.2 SAXS Analysis: sIIB-tRNA <sup>Phe</sup> .....	122
<b>CHAPTER 4: SUMMARY AND IMPLICATIONS.....</b>	<b>129</b>
<b>REFERENCES.....</b>	<b>135</b>

## LIST OF ABBREVIATIONS

AIDS: Acquired Immunodeficiency Syndrome

AUC-SV: Analytical ultracentrifugation-Sedimentation Velocity

CA: Capsid protein

CCR5: Chemokine Receptor 5

env: Envelope protein

FI: Fusion Inhibitor

gag: Group associated antigen

gp120: Glycoprotein 120

gp41: Glycoprotein 41

HAART: Highly Affective Antiretroviral Therapy

HIV-1: Human Immunodeficiency Virus

II: Integrase Inhibitor

IN: Integrase

LTR: Long Terminal Repeat

MA: Matrix protein

NC: Nucleocapsid protein

NLS: Nuclear Localization Sequence

NNTRIs: Non-Nucleoside Reverse Transcriptase Inhibitor

nTRIs: Nucleotide Reverse Transcriptase Inhibitor

ORF: Open Reading Frame

pBS(SK+): pBlueScript(SK+), Vector used for Expression of Chimeric tRNA Constructs

PI: Protease Inhibitor

PR: Protease

Rev: Regulator of Virion Expression

Rev103a: Arginine-rich Peptide of Rev containing residues 34-50

RevN60: C-terminal truncation of Rev containing residues 1-60

RevN70: C-terminal truncation of Rev containing residues 1-70

RNP: Ribonucleoprotein

RRE: Rev Response Element

RT: Reverse Transcriptase

SDS-PAGE: Sodium Dodecyl Sulfate-Polyacrylamide Gel Electrophoresis

SEC: Size-exclusion Chromatography

sIIB-tRNA<sup>Lys</sup>: Chimeric tRNA containing lysyl tRNA (human origin)

sIIB-tRNA<sup>MetI</sup>: Chimeric tRNA containing initiator methionyl tRNA (ecoli) with hairpin sequence RWZ2 replacing anticodon loop

sIIB-tRNA<sup>Phe</sup>: Chimeric tRNA containing phenylalanyl tRNA (Baker's Yeast) with hairpin sequence RWZ2 replacing anticodon loop

SL-IIB: Stem Loop-IIB of RRE, High-affinity binding site for Rev

SU: Surface protein

TM: Transmembrane protein

tRNA: Transfer RNA

## CHAPTER 1: HIV AND THE REV PROTEIN

Human Immunodeficiency Virus (HIV), the causative agent of Acquired Immunodeficiency Syndrome (AIDS), is in the genus *Lentivirus* belonging to the family Retroviridae [1,2]. This virus specifically disrupts the immune system by infecting T-helper cells via the surface CD4+ receptors as well as macrophages and dendritic cells [1,3].

The first clinical case of the virus was recorded in 1981 the Centers for Disease Control (CDC). The CDC received first reports of immunocompromised patients presenting with the opportunistic infections *Pneumocystis carinii* and Kaposi's sarcoma. Later in 1982, the disease was identified as Acquired Immunodeficiency Syndrome (AIDS). HIV is believed to have entered the human population via Chimpanzees and/or Sooty Mangabeys by retroviral transfer of the Simian Immunodeficiency Virus (SIV) [4,5,6]. The virus is considered a pandemic by the World Health Organization (WHO, 2011), and in 2011 there were 33,000,000 persons infected with HIV worldwide, ~2.6 million new infections each year, and with ~1.8 million deaths [7]. HIV is acquired and transmitted via unprotected sexual intercourse, contaminated needles, breast milk, and infected mother to her baby at birth with sexual intercourse being the primary mode of transmission. Lifetime treatment of an infected individual costs about \$155,000 in the United States (WHO, 2011). The current treatment for HIV infection is known as Highly Active Anti-Retroviral Therapy (HAART) which was

introduced in 1996 [8,9]. The therapy consists of 5 classes of chemotherapies which attack the virus at different stages of the viral life-cycle. These classes include: Nucleoside Reverse Transcriptase Inhibitors (nTRIs), Non-Nucleoside Reverse Transcriptase Inhibitors (NNTRIs), Protease Inhibitor (PI), Integrase Inhibitor (II), and the Fusion Inhibitor (FI) [8,10,11,12].

HAART is the most effective treatment against HIV thus far. This is in part due to the use of drug combinations that decrease the probability of selecting viral copies which contain multiple mutations and become resistant. However, this regimen depends upon the efficacy and efficiency of each drug and the naïve resistance of each patient [13]. Rev has proven to be critical in progression from early- to late-phase replication of HIV. The amino acid sequence and functional domains are highly conserved making random mutation an unlikely event. The protein interacts with a structure contained within HIV RNA known as the Rev Response Element but details of this interaction are limited to one NMR structure of the arginine rich motif (ARM) region complexed with the RRE high affinity binding site known as stem loop-IIB [14,15,16,17,18,19,20,21]. It is also established that without functional Rev there is an accumulation of small, ~2 kB transcripts in the cytoplasm of infected cells with no production of structural proteins rendering the virus unviable, unable to replicate [22,23]. A better understanding of the Rev/RRE interaction may allow the development of chemotherapies which disrupt this critical part of HIV replication. This work should provide more insight into how Rev interacts with Rev Response Element RNA.

## Section 1.1 HIV-1 Replication

The Human Immunodeficiency Virus (HIV) belongs to the genus Lentivirus (family Retroviridae), and displays tropism for T-cells, macrophages, and dendritic cells [1,3]. Upon infection, the virus interacts with the cell surface CD4+ receptor (primary) via gp120 (glyco-protein) followed by interaction with chemokine receptor 5 (CCR5) or another secondary receptor, CXCR4, through glycoprotein 41 (gp41) which allows for fusion and subsequent entry into the host. Following cell entry, the viral RNA is reverse-transcribed into proviral DNA by the action of viral reverse transcriptase (RT) and integrase (IN) [22,24]. This pre-integration complex is transported into the nucleus for inclusion into the infected cell's chromosome where the virus can remain latent or begin replicating. The genome is ~9 kilobases in length and encodes 15 proteins from 9 open reading frames (ORFs) [24]. Beginning at the 5' end, the genome contains a 5' long terminal repeat (LTR) followed by *gag* (group-associated antigens), *pol* (polymerase), *env* (envelope) genes and finally a 3' LTR. The group associated antigen (*gag*) ORF houses genes encoding the matrix (MA), capsid (CA), nucleocapsid (NC), and p6 proteins. The polymerase (*pol*) transcripts encode the protease (PR), reverse transcriptase, integrase, along with a spliced gene product, *vif* (function not well understood, may play a role in nucleocapsid assembly). The envelope (*env*) region encodes surface (SU) and transmembrane (TM) proteins, as well as spliced transcripts *tat*, *rev*, *vpu*, *nef*, and *vpr*. The envelope contains surface protein (SU), *gp120* and transmembrane (TM) proteins, *gp41*, which is responsible for fusion of the virus with its

host. During replication of the virus, singly and doubly spliced transcripts (~4kb and ~2kb transcripts, respectively) are produced allowing for the production of regulatory proteins and structural proteins. The nucleocapsid is surrounded by MA (matrix) protein and encases a diploid copy of the RNA genome, viral protease (PR), reverse transcriptase (RT), integrase (IN), vif, vpr, nef, and p6 [22,25].

The replication of HIV may be (generically) categorized by cell entry, replication (early- and late- phase), assembly of viral proteins and genomic RNA at the plasma membrane followed by release of mature virions from the infected cell surface. Following host exposure to the virus, gp120 on the envelope surface interacts with CD4+ receptors. This initial event is followed by interaction of gp41 with chemokine receptors (CCR5, CXCR4) allowing for envelope-membrane fusion and entry of the nucleocapsid into the cytosol. Subsequent to release of the nucleocapsid into the cytosol, RT (reverse transcriptase) and integrase begin transcribing proviral DNA from the genomic RNA. These proviral DNA transcripts are then transported to the nucleus of the infected cell and subsequently integrated into the cell's chromosome by the action of the virally-encoded IN (integrase) and RT (reverse transcriptase). Following integration, the virus may remain latent or begin producing viral proteins and particles responsible for the production of an infectious virion. During the permissive or replication phase, the virus "hi-jacks" transcriptional machinery from the host and begins the production of "early-phase" or accessory proteins responsible for enhanced transcription (tat), down regulation of CD4+ receptor production, and transport of partially-spliced (doubly- spliced) and

genomic-length RNA which encodes the regulatory proteins, *tat*, *rev*, and *nef* [26,27,28,29,30,31]. Following the production of a sufficient quantity of regulatory proteins during early phase replication, the virus can then begin late-phase development and production of singly- and doubly- spliced mRNA transcripts which encode *env*, *gag*, and *pol* proteins as well as full-length, 9kB genomic RNA. After sufficient accumulation of viral proteins and genomic-length RNA at the cell membrane, the virus is packaged and released as a mature, infectious virion [22,32].

### **Section 1.2 Rev and the HIV-1 Life Cycle**

The Regulator of Virion Expression or Rev is a regulatory protein produced during the early-phase of HIV replication. It was discovered in 1986 and has proven to be critical for the production of a mature HIV virion [33,34]. In its absence, the virus is unable to replicate efficiently and there is a decreased production of *gag* and *pol* encoded proteins (structural) and genomic-length RNA [35,36,37]. Rev is 116 residues in-length and ~13kDa with defined functional motifs responsible for its operation within infected cells [23,35,38,39]. These motifs include the nuclear localization sequence (NLS), arginine-rich motif (ARM) or RNA binding region, multimerization domains which flank the ARM motif, and the nuclear export sequence (NES) [35,40,41]. These functional motifs define Rev's interaction with Importin- $\beta$  via the nuclear localization sequence (NLS), Exportin-1 (chromosome remodeling protein-1) through the nuclear export sequence (NES), Ran-GTP (provides energy for dissociation from RNA), and the ARM region which binds to the Rev Response Element (RRE) [42,43,44,45,46]. The protein is

highly basic with an isoelectric point of about 9, perfectly suited for RNA-binding and contains serine residues which may serve as phosphorylation sites driving the association and dissociation reactions involved with its import and export function within infected cells [33]. It is classified as a *trans*-activating and shuttle protein which interacts with a specific RNA sequence known as the Rev Response Element (RRE) (*cis*-target) contained within a ~351 nucleotide sequence within genomic HIV RNA and shuttles between the nucleus and cytoplasm of an infected cell [23]. Rev is encoded by a doubly spliced product of the *env* gene where the mRNA transcripts are translated in the cytoplasm and Rev is subsequently shuttled into the nucleus where it recognizes and binds the RRE (Rev Response Element) via the ARM with nanomolar affinity [47]. The RRE is a ~351 nucleotide sequence contained within the *env* encoding region between nucleotides 7706-8068 of HIV-1 genomic RNA. This region contains many secondary structural elements which Rev recognizes and subsequently assembles on the RRE. Once there is a sufficient accumulation of Rev in the nucleus of the infected cell, Rev recognizes Stem Loop-IIB within the RRE with high-affinity ( $K_D = 1$  to  $5$  nM) and subsequently assembles along Stem Loop-I, followed by the interaction with exportin-1 and Ran-GTP for the transport of singly-spliced and genomic-length RNA [14,33,48].

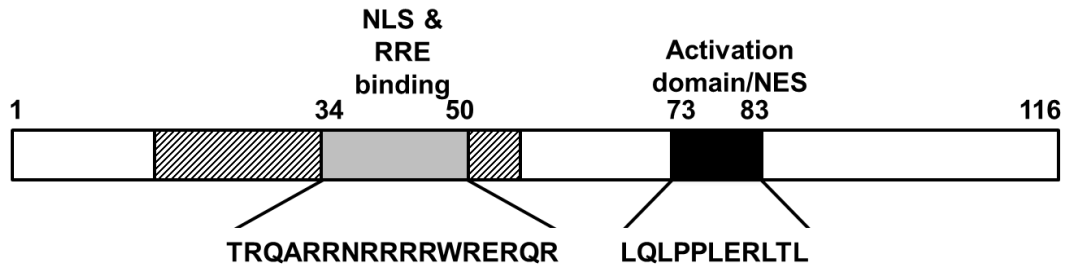


**Figure 1 Functional Motifs of Rev.** Rev is 116 residues in length. The N-terminal residues 34-50 function as the nuclear localization sequence (NLS) and Rev Response Element (RNA) binding region. This region is flanked on both sides by oligomerization domain(s) (cross-hatched). The C-terminal residues 73-83 function as the nuclear export sequence (NES) and activation domain.

Subsequent to the transport of the Rev/Importin- $\beta$ /RanGDP complex into the nucleus, RanGDP is converted to RanGTP which is mediated by RCC1. This causes Rev to dissociate from Importin- $\beta$ . Following dissociation, Rev recognizes and binds to the RRE. Rev initially binds to the high-affinity binding site known as stem loop-IIB followed by assembly of up to 12 monomers of Rev along Stem I of the RRE. The Rev/RRE complex then recognizes and binds to Exportin-1 (CRM1) via the Rev leucine-rich nuclear export sequence (NES). Export of this complex through nuclear pores is energy dependent. Increased levels of Ran-GTP in the nucleus promote the interaction of Ran-GTP and Rev with CRM1. CRM1 interacts with and localizes the Rev/RRE complex to the nuclear pores for export [44,46,49]. The Rev/RRE/CRM1 complexes are kinetically very stable, and the dissociation of these complexes is mediated by the action of RanGAP1 and RanBP1 (cellular GTPases) which hydrolyze Ran-GTP to Ran-GDP

[43,50]. Once Rev is in the cytoplasm, it is targeted back to the nucleus by the immediate binding of importin- $\beta$  via the NLS of Rev, preventing further interaction with RRE RNA.

The canonical Rev-RRE shuttle cycle is shown in Figure 2.

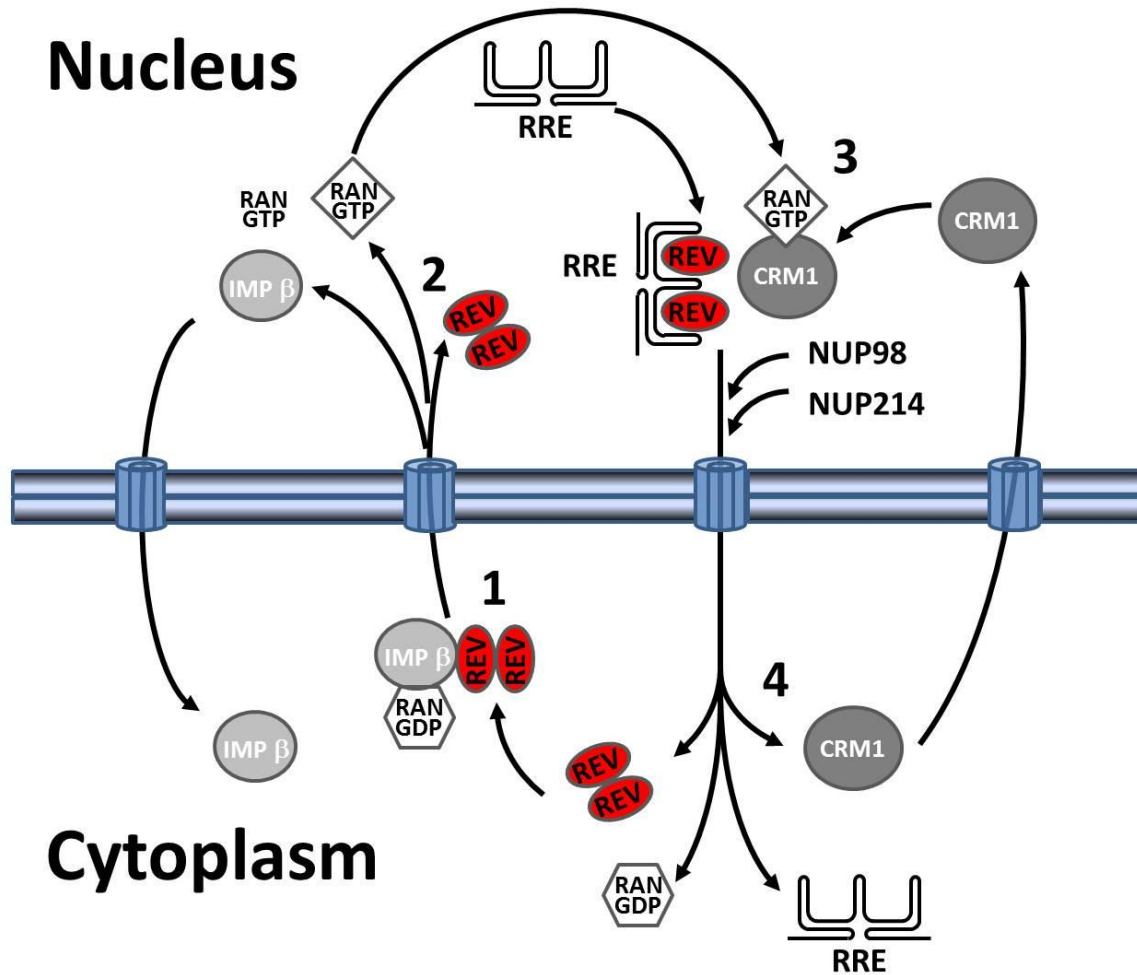


Figure 2 Canonical Rev-RRE Transport Cycle. (1) Rev interacts with Importin- $\beta$ /RanGDP complex, (2) Rev dissociates from the Importin- $\beta$ /RanGDP complex following phosphorylation of RanGDP, (3) Rev associates with the RRE followed by binding to the RanGTP/Exportin-I complex, (4) Rev dissociates from RanGTP/Exportin I (CRM1) complex following dephosphorylation of RanGTP (Figure adapted from [23]).

The major cellular proteins involved in the nuclear import of Rev and the export of Rev-mediated transport of RRE RNA have been established (Figure 2). These include CRM1, RanGDP, RanGTP, Importin- $\beta$ , and Exportin-1. However, additional cellular cofactors have been identified which enhance the function of Rev and the subsequent export of RRE RNA. These proteins interact either with Rev directly via the conserved NES functional motif, bind directly to RRE RNA or interact with CRM1 to synergistically enhance the export of RRE RNA.

The eukaryotic initiation factor-5A (eIF-5A) is a 17-kDa acidic protein evolutionarily conserved from archaeobacteria to mammals [51]. It contains hydroxyhypusine in the N-terminus which is a post-translationally modified lysine catalyzed by Deoxyhypusine synthase (DHS). It was shown to be a cellular partner of Rev via UV-crosslinking experiments [52]. Further implications for its role in HIV replication were indicated when mutants of eIF-5A were capable of binding the Rev/Exportin I complex but blocked the export of the Rev/RRE complex. Although the explicit role of eIF-5A is not understood, it is known to interact with CRM1 and nucleoporins making it essential for export of Rev/RRE complexes [42,52,53,54].

An additional cellular cofactor implicated in Rev-mediated RRE export is human Rev interacting protein (hRIP). Overexpression of hRIP enhanced Rev activity and function was compromised in the presence of suboptimal levels of Rev. An RNAi

experiment revealed the accumulation of RRE-containing RNA at the nuclear perinuclear region, preventing the release of RRE RNA into the cytoplasm [55,56,57].

Src-associated protein or Sam68 is 68 kDa classified as a RNA binding protein. It contains the 70 residue KH domain and a RGG box found in many nucleic acid binding proteins [58,59]. Recently it has been established as being absolutely necessary for the nuclear export of the Rev/RRE complex. C-terminal deletions of Sam68 showed a transdominant negative effect on Rev function for the export of RRE RNA. Overexpression of Sam68 in astrocytes restored Rev function. Sam68 was originally thought to replace the function of Rev by direct interaction with RRE RNA. However, it is now believed that Sam68 binds directly to the RRE and Rev and acts synergistically to enhance the export of RRE RNA [56,60,61]. The precise manner in which Sam68 participates in the export of RRE RNA is not well understood.

RNA helicases A (RHA), DDX3 (RNA helicase), and DDX1 (RNA helicase) represent other cellular proteins implicated in the transactivation of Rev [62,63]. RHA is believed to cause the premature release of unspliced and singly-spliced RNA viral RNA from the splicing machinery enhancing the ability of unspliced HIV mRNA transcripts to be transported to the cytoplasm [62]. DDX3 is a nucleo-cytoplasmic shuttling protein which binds to CRM1 and promotes the cytoplasmic accumulation of Rev/RRE dependent *gag* transcripts. Dominant-negative mutants of DDX3 inhibit Rev/RRE transport. DDX1 binds to the Rev/RRE complex and ameliorate Rev activity in RRE

gene expression. The down regulation of DDX1 decreases the concentration of Rev in the nucleus with Rev

being predominantly located in the cytoplasm [63,64]. The Rev-RRE transport cycle including cellular cofactors is shown in Figure 3.

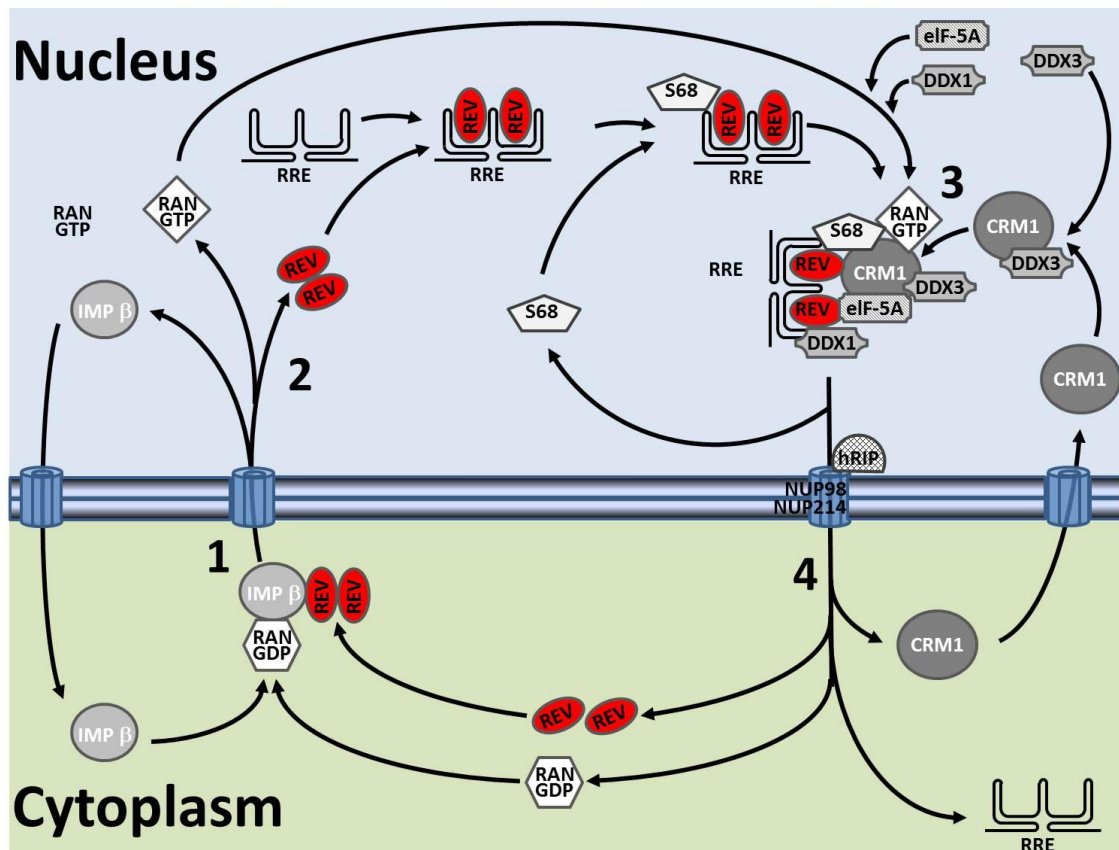


**Figure 3 Rev-RRE Transport Cycle with Cellular Cofactors.** Additional cellular cofactors have been identified which act synergistically with the Rev-RRE complex to enhance the export of RRE RNA from the nucleus. These include Sam68, eIF-5A, DDX3, and DDX1. The full function of these proteins in the context of the Rev-RRE complex are not fully understood (Figure adapted from [23,56].

### Section 1.3 Biophysical Properties of Rev

Following the discovery of Rev in 1986, solution biophysical experiments used circular dichroism (CD) to examine the conformation of Rev and Rev in complex with RRE sequences. Rev alone was determined to contain 50% alpha helices and 25% beta-sheet content with double minima at 222nm and 210nm, respectively [65,66]. Rev in complex with RRE-RNA retained almost identical secondary structural elements. It was discovered that the disordered C-terminus was critical for assembly onto the RRE. Gel shift analysis demonstrated that removal of C-terminal residues 92-116 was sufficient to disrupt Rev's ability to assemble the RRE [67]. The C-terminus contains the NES which interacts with Importin- $\beta$  for export from the nucleus. More recently, NMR data has shown that the C-terminal residues are disordered although its function regarding Rev assembly on the RRE is not understood.

In 1996, Battiste, *et al* reported an NMR structure of the ARM (Arginine Rich Motif) peptide of Rev bound to a 34-nucleotide fragment of stem loop-IIB (SLIIB) [25] (Figure 4). The structure showed the  $\alpha$ -helical, Rev-derived peptide positioned into the major groove of the RNA fragment with conserved arginine residues in positions 35, 39, 40, and 44 making base-specific interactions with the RRE RNA (Battise, 1996 and Gosser 2001). In 2001, a series of genetic experiments mapped residues which were important for dimerization and subsequent assembly on the RRE. A helix-loop-helix model was proposed for Rev which suggested that residues important for dimerization were located at the A interface and residues at the B interface were required for oligomerization or Rev

assembly. Using the ARM peptide-stem loop-IIB NMR structure, Rev was superposed as an A:A interface (Leu18 and Ile55) mediated dimer followed by assembly on the RNA via B:B interactions (Leu12 and L60). Gel shift analysis with mutant Rev/RRE complexes supported the model [68].

In 2010, two crystal structures of Rev were reported. The first structure was of full-length Rev bound to F<sub>ab</sub> fragments flanking the hydrophobic B interfaces and the Rev dimer interacting via B:B or assembly interface [69] (Figure 5). The F<sub>ab</sub> fragments prevented assembly of the protein by disabling the oligomerization domain via A:A interface interference. The two monomers had an obtuse crossing angle of  $\sim 140^\circ$  in which the ARM domains protruded in a prong-like manner from the V-shaped dimer. The second crystal structure was of a Rev (residues 1-70) mutant (Figure 6). The crystallized Rev clone was designed based upon the protein's propensity for aggregation at concentrations above 10 $\mu$ M and previously discussed genetic data which defined residues (Leu12 and Leu60) responsible for higher-order assembly. These B:B interface residues were mutated to prevent higher-order oligomerization. Additionally, 46 residues were removed from the C-terminus based upon NMR data and the previous crystal structure which suggests that these residues are disordered and may not be amenable to crystallization. The mutant was 70 residues in length with L12S and L60R double mutations. The protein crystallized as a dimer with the protein interacting via A:A interface residues as previously described. The designed Rev clone proved to be soluble and crystallized as a dimer [70] (Figure 6). In summary, both of the crystal structures

offered atomic resolution data on the interaction of the A:A and B:B interfaces involved with dimerization and subsequent assembly of Rev.

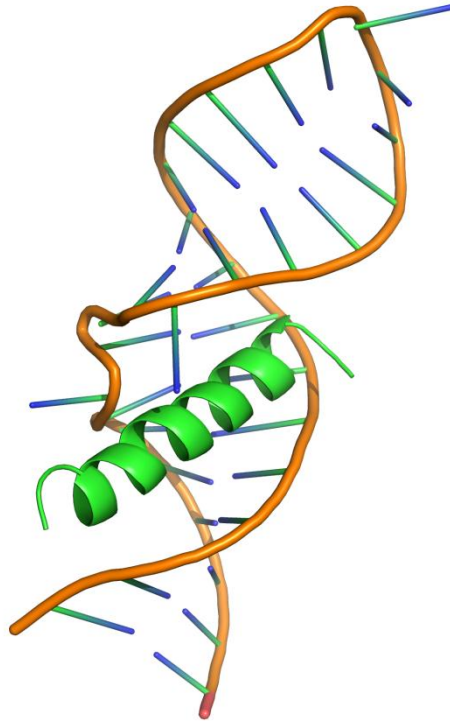


**Figure 4 NMR structure of the 34 nucleotide Stem Loop-IIB complexed with ARM peptide of Rev.** Stem loop-IIB is the high-affinity binding site on the RRE recognized by Rev. This represents the structural information which is available on the Rev-RRE complex [25].

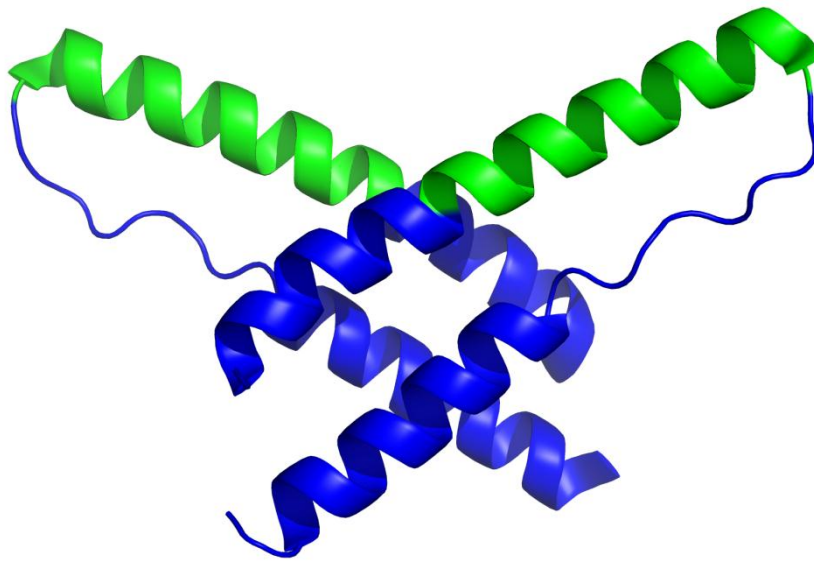


**Figure 5 Crystal structure of the Rev dimer (Residues 1-70, L12S and L60R mutations).** RNA binding residues highlighted in green. Crystal structure of the Rev dimer with monomers interacting via the defined A:A interface.

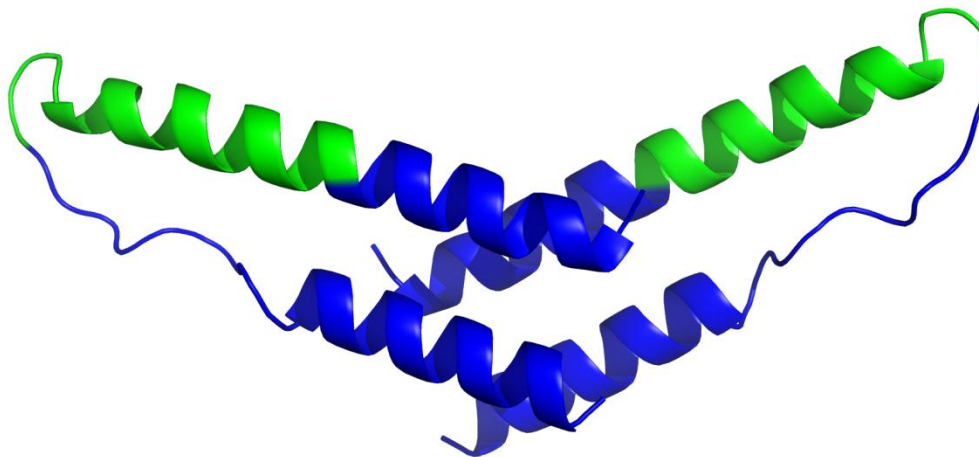


**Figure 6 Crystal structure of the Rev dimer.** Crystal structure of the Rev dimer with monomers interacting via the defined B:B interface (residues Leu18 and Ile55). The Rev dimer was flanked by F<sub>ab</sub> fragments at the putative A:A dimerization interface.

## Section 1.4 Rev and the Rev Response Element (RRE)

The RRE or Rev Response Element (RRE) is a *cis*-activating ~351 nucleotide sequence contained within the *env* encoding region of the ~9kB genome [15,18,20,24,71]. It is characterized by a series of stem loops and extensive secondary structure which recognizes and binds the Rev protein (*trans*-activator) with high affinity and specificity (Figure 7). The minimally functional RRE was discovered in 1989 and determined to be 241 nucleotides in length [18,19,20] (Figure 8). Later in 1994, functional assays using systematic truncations of the RRE determined the fully active molecule to be 351 nucleotides in length [37]. This included an additional 58 nt on the 5' end and 59 nt on the 3' end beyond the sites initially proposed (Figure 9). The additional residues allowed for the increased production of late-phase structural *gag* (group-associated antigen), and *pol* (polymerase) polyproteins. Upon sufficient accumulation of Rev in the nucleus, it initially recognizes stem loop-IIIB (SLIIB) as a dimer followed by assembly of 8-11 monomers along Stem I [70,72,73,74,75,76].

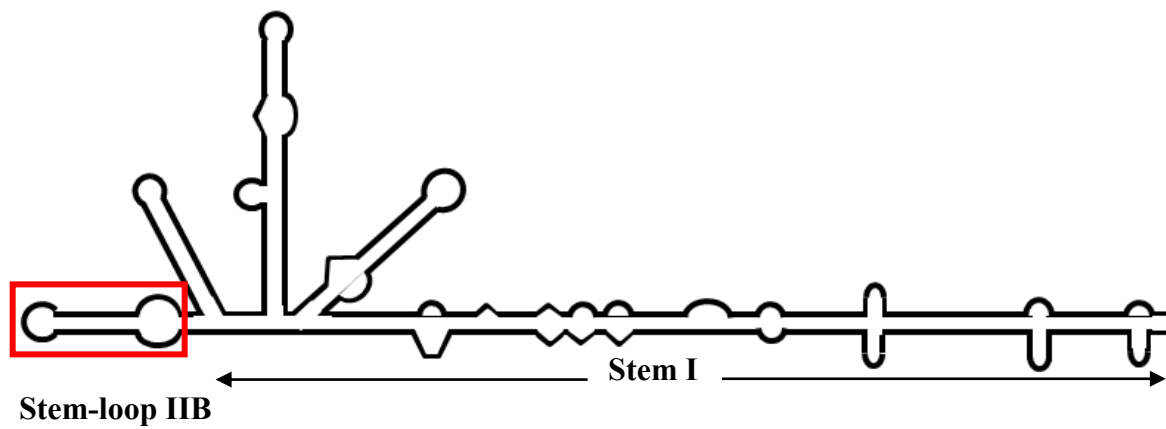


**Figure 7 Representation of full-length RRE secondary structural elements.** 2-dimensional representation of hairpin and stem loop structures within in the 351 nucleotide Rev Response Element sequence. The high-affinity binding site, stem loop-IIB is outlined in red.

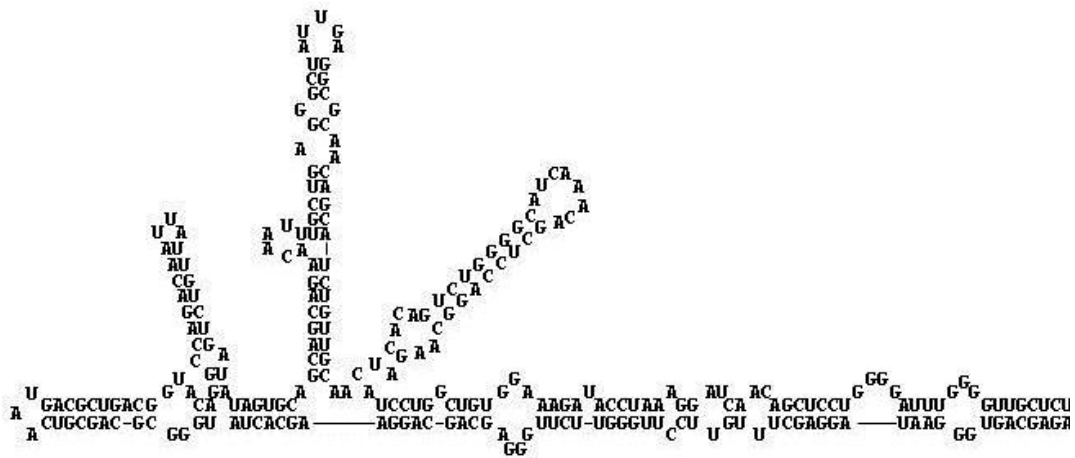


**Figure 8 Minimally functional RRE (240 nucleotides) as described in 1989 [20].** The minimally functional RRE was initially examined to be 240 nucleotides.



Many experiments have been performed to understand the mechanism underlying the interaction and assembly of Rev on the RRE. The assembly of Rev on the RRE has proven to be critical for the export of intron-containing HIV RNA from an infected cell. One experiment employed ribonuclease T1 digestion of a full-length RRE molecule in the presence and absence of Rev. Locations on the RRE which were accessible to Rev were inaccessible by the ribonuclease and therefore remained intact. Regions “unoccupied” by Rev were accessible to the enzyme and were cleaved at specific nucleotide residues. The titration data supported the initial interaction of Rev at stem loop-IIB followed by the sequential “filling” or binding to the unpaired nucleotides along Stem Loop-I. Experiments using truncated versions of the RRE demonstrated the reduction in the number of Rev/RRE complexes achieved with varying truncations of the RRE. This data illustrated the importance for the entire sequence of the RRE for the assembly of Rev [37,72]. Additional experiments examined the residues involved with Rev-Rev interactions on a full-length RRE molecule. Random mutations were generated and gel-shift experiments were performed on each single or double mutant in the presence of the RRE to determine the stoichiometry on the RNA fragment. This data enabled the construction of an *in silico* model of multiple Rev molecules (trimer) bound to the RRE due to the mutated residue positions within the sequence [68]. However, it remains unclear whether Rev interacts directly with sites distant from Stem Loop-IIB or if protein-protein interactions dictated the oligomerization along Stem Loop-I.

## Section 1.5 Rev-mediated RRE RNA Dimerization

It is known that a mature HIV-1 virion carries a diploid copy of genomic RNA in the capsid. The dimerization of the RNA is mediated by cis-acting signals contained within secondary structural elements of HIV RNA synergistically with transactivating viral proteins. The cis-acting signals for encapsidation and RNA dimerization are contained within the 5' untranslated region (UTR) and include the “kissing” loop ( $\Psi$ ), dimer linkage structure (DLS), primer binding site (PBS), and the dimerization initiation site (DIS) [77,78,79]. The transactivating proteins promoting HIV RNA dimerization are nucleocapsid (NC) and the group associated antigen (gag) proteins. Recently, it was shown using a Murine Leukemia virus (MLV)-derived viral vector that the Rev/RRE system is required with the 5' UTR cis elements to augment encapsidation of heterologous RNA into a HIV-1 viral particle (Cockrell et al. 2011). For these experiments, the Rev/RRE system as well as 5' UTR *cis* packaging elements were reconstructed in a retroviral vector RNA to investigate the additive, and independent, impact on the gain of encapsidation function into HIV-1 derived viral particles. The Rev/RRE system increased the packaging efficiency of a diploid copy of the heterologous RNA ~100 fold. Although the physical basis by which the Rev/RRE system increases the efficiency of packaging a diploid copy of genomic RNA is unknown

Experiments performed on Rev/RRE complexes since the discovery of the RRE in 1989 have all suggested that Rev interacts with one copy of RRE RNA. The position of the RNA binding regions of the Rev dimer(s) as revealed by the two crystal structures

solved suggest that an oligomer of Rev could bridge a dimer or bind a single copy of RRE RNA [69,70]. Both crystal structures reveal that Rev monomers interact at a  $\sim 140^\circ$  angle to each other with the RNA binding residues (residues 34-50) which protrude in a prong-like manner and could bridge two copies of RRE RNA in an antiparallel fashion. Dimattia suggests that Rev binds to one copy of the RRE in a manner in the first monomer binds to stem loop-IIB followed by stem loop-I of the RRE “wrapping” around and interacting with the oligomer of Rev via the available RNA binding regions. Gel shift experiments performed by Daugherty and colleagues suggest that Rev binds to one stem loop-IIB (34 nucleotides) and an extended version of stem loop-IIB (42 nucleotides) as a dimer.

Gel retardation data published in 1996 demonstrated that a radio-labeled sequence of RNA containing a modified stem loop-IIB sequence (named RWZ2) with the introduction of a UC bulge flanking the unpaired residues produced a soluble, discrete Rev:RNA species at a Rev/RNA molar ratio of 16/1 [48,72]. The disparity of the migration position of the unbound RWZ2 RNA and the Rev:RWZ2 complex was curious. The authors claim that the upper band was a dimer of Rev bound to RWZ2. However, from the position of the complex band on the gel, this did not seem consistent. It seemed plausible that Rev may have been binding two copies of the RWZ2 RNA hairpin. To investigate this, the RWZ2 fragment, which was later named sIIB was fused to tRNA scaffolds and Rev:sIIB-tRNA complexes were analyzed by SEC, AUC, and the monomeric sIIB-tRNA<sup>Phe</sup> was examined by SAXS.

## CHAPTER 2: MATERIALS AND METHODS

This chapter will include details on the Rev constructs, sIIB-tRNA<sup>Lys</sup>, sIIB-tRNA<sup>MetI</sup>, sIIB-tRNA<sup>Phe</sup>, and IIB-tRNA<sup>Phe</sup> chimeric tRNAs used to study the Rev-RRE interaction, and purification protocols for these molecules. I will describe in detail the tRNA scaffold technology followed by the methodologies for expression of Rev and RRE-containing tRNAs. Protocols for native PAGE gel shift, size-exclusion chromatography, and small angle X-ray scattering experiments will also be covered.

### Section 2.1 Rev Constructs

Various constructs of Rev were used to study the Rev-RRE interaction. These included the full-length protein, Rev103a, RevN60, and RevN70. Rev103a is a synthetic peptide which includes the arginine-rich stretch of amino acids of the ARM or RNA-binding region. RevN60 and RevN70 are C-terminal truncations of Rev which represent the first 60 and 70 N-terminal residues, respectively. Masses of all protein constructs were verified via ESI-MS. Section 2.1.1 Proteins and Peptides: RevWT, RevN70, RevN60, and Rev 103a

#### Section 2.1.1.1 RevWT

Strain HXB2 HIV-1 wild-type Rev is 116 amino acids in length with a mass of 13.26 kDa, and has a pI of 9.23 as in Figure 10. The additional N-terminal glycine and histidine residues are part of the TEV protease recognition sequence and remain following 6X histidine tag removal. It contains functional domains consistent with its function. The Arginine Rich Motif (ARM) region (residues highlighted in red) also

serving as the Nuclear Localization Sequence (NLS) is a 17 amino acid sequence located between residues 34-50. It recognizes stem loop-IIB of RRE RNA as well as Importin- $\beta$ . The Nuclear Export Sequence (NES, highlighted in blue) interacts with Exportin I (CRM1) which serves to facilitate the export of RRE RNA from the nucleus to the cytoplasm. The yield is ~80 mg per 2L of 2xYT culture media. The protein was analyzed for purity and mass via SDS PAGE (15%) in Figure 16.

**Number of amino acids:** 118  
**Molecular weight:** 13260.9  
**Theoretical pI:** 9.23

```
          10          20          30          40
GHMAGRSGDS DEDLLKAVRL IKFLYQSNPP PNPEGTRQAR
          50          60          70          80
RNRRRRWREER QRQIHSISER ILSTYLGRSA EPVPLQLPPL
          90          100         110
ERLTLDCNED CGTSGTQGVG SPQILVESPT VLESGTKE
```

**Figure 10 Properties of RevWT.** Number of residues, molecular weight, pI, and sequence of RevWT. The ARM and NES sequences are highlighted in red and blue, respectively.

### Section 2.1.1.2 RevN70

RevN70 includes the first 70 N-terminal residues of HIV-1 Rev from Strain HBX2. This construct was designed based on the recent crystal structure solved of the Rev dimer [70]. It contains the N-terminal helical hairpin region of Rev without the disordered C-terminal region which made it more amenable to crystallization. The sequence in the crystal structure (PDB 3LPH) includes the arginine-rich domain (ARM) motif which is specific for recognizing RRE-containing RNA and mutations L12S and L60R which have been shown to prevent higher-order assembly *in vitro* [68]. Our sequence (RevN70) is purified using the same protocol as wild-type Rev described in Section 2.2. The yield is ~80 mg per 2L 2xYT media. The mass measured with ESI-MS is 8.32 kDa and agrees with the theoretical mass of 8.44 kDa. This construct was used for gel filtration experiments and crystallization trials in complex with sIIB-tRNA<sup>Phe</sup>. Figure 11 shows the sequence, pI, and molecular weight of RevN70. The protein was analyzed via SDS PAGE (15%) in Figure 15.

## RevN70

**Number of amino acids:** 72

**Molecular weight:** 8443.7

**Theoretical pI:** 11.46

```
          10          20          30          40
GHMAGRSGDS DEDLLKAVRL IKFLYQSNPP PNPEGTRQAR
          50          60          70
RNRRRRWREER QRQIXSISER ILSTYLGRSAEP
```

**Figure 11 Properties of RevN70. Represents N-terminal residues 1-70 of Rev.** The ARM sequence is highlighted in red.

### Section 2.1.1.3 RevN60

RevN60 represents the first 60 N-terminal residues of HIV-1 Rev strain HBX2. The additional glycine and histidine residues at the N-terminus are from the Tobacco Etch Virus (TEV) protease recognition sequence and remain following the 6X his-tag removal by TEV. This construct was designed to include the N-terminal helical hairpin region of Rev without the disordered C-terminal region [67,73,80] (Figure 12). The sequence includes the arginine-rich domain (ARM) motif which is specific for recognizing RRE-containing RNA [81,82,83]. The protein is very basic and is purified using the same protocol as wild-type Rev as described in Section 2.2. The yield was ~80

mg per 2L of 2xYT culture medium. Following Ni-NTA affinity purification, the protein was HPLC purified for enrichment and removal of RNA contamination. SDS-PAGE gel analysis of the purified protein is shown in Figure 16. All Rev constructs are loaded onto the SDS-PAGE gel in guanidine-HCl which disrupts migration through the gel matrix. The mass measured with ESI-MS was in agreement with the theoretical mass of 7.83 kDa. RevN60 was used for size-exclusion chromatography experiments and crystallization trials in complex with sIIB-tRNA<sup>Phe</sup>, sIIB-tRNA<sup>Lys</sup>, and sIIB-tRNA<sup>Met</sup>

## RevN60

**Number of amino acids:** 62

**Molecular weight:** 7381.5

**Theoretical pI:** 11.66

```
          10          20          30          40
GHMAGRSGDS DEDLLKAVRL IKFLYQSNPP ENPEGTRQAR
          50          60
RNRRRRWRER QRQIXSISER IL
```

**Figure 12 Properties of RevN60.** The figure represents the C-terminal residues 1-60 from Rev. The ARM or RNA binding sequence is highlighted in red.



## Section 2.2 Expression, Purification, and Characterization of Rev Constructs

Rev fusions are cloned into a pUC (YP001) plasmid under the control of a T7 promoter (Figure 14). The plasmid is transformed into *E. coli* cell line BL21(DE3). Cells were grown in 2L of ampicillin supplemented (50 µg/ml) 2xYT media and induced at  $A_{600} = 0.6$  with 1 mM IPTG. Cells were pelleted by centrifugation at 5,000 rpm in a swing bucket rotor for 30 min. Cell pellets were suspended and sonicated in 100 mL of denaturing buffer (8M Urea, 100 mM NaCl, 10 mM Imidazole, 10 mM Tris, 5 mM beta-mercaptoethanol, pH 7.2). Following sonication, cell debris is cleared via centrifugation @ 17000 rpm for 30 min in 50 ml centrifuge tubes at 25°C. Supernatant was loaded onto Ni-NTA resin (Qiagen) equilibrated in sonication buffer, washed with sonication buffer, and eluted with buffer containing 1M imidazole (8M Urea, 100 mM NaCl, 1 M Imidazole, 10 mM Tris, 5 mM beta-mercaptoethanol, pH 7.2). For nucleic acid removal, Rev was subjected to cation-exchange chromatography (SP-Sepharose 16/10-GE Life Sciences, 20 mL CV) and eluted with 10 CV of 5M guanidine-HCl, 1 M NaCl, 10 mM Tris, 5 mM beta-mercaptoethanol, pH 7.2) at a flow rate of 3 mL/min. For removal of TEV-6X his-tag, the eluate is diluted to  $[Rev] = 60 \mu\text{M}$  (~1 mg/ml, OD measured using  $E_{260} = 8400 \text{ M}^{-1} \text{ cm}^{-1}$ ) to prevent aggregation and dialyzed O/N against TEV proteolysis buffer (1 M guanidine-HCl, 50 mM Tris- HCl, 5 mM beta-mercaptoethanol, pH 7.2). Subsequent to O/N dialysis, TEV protease is added (1 mg TEV/10 mg protein) to Rev-WT solution and allowed to incubate O/N at room temperature (RT) for cleavage of the TEV-6x histidine tag sequence, followed by the addition of 5 M guanidine-HCl to

dissolve any precipitate. The Rev-TEV solution is then loaded onto Ni-NTA resin (Qiagen) equilibrated in sonication buffer and flow through was collected and analyzed for purity via SDS-PAGE and ESI-MS. The propensity of Rev to bind nucleic acid makes it necessary to improve the 260nm/280nm ratio. The protein was acidified in 0.1% trifluoroacetic acid (TFA) and loaded onto a C18 HPLC column. A gradient of 5-70% acetonitrile was applied over 10 column volumes for enrichment. Subsequently, the protein was characterized via ESI-MS, aliquoted, lyophilized and stored at -20°C.

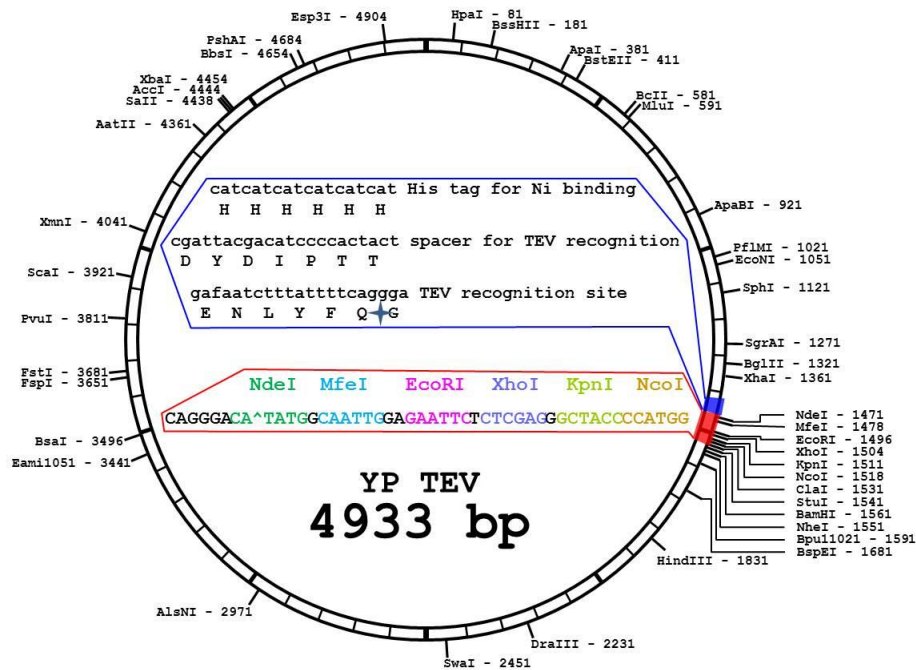


**Figure 14 Map of YP001 vector (4933 bp) used for expression of Rev constructs.** The plasmid is a modified pUC vector where a new multiple cloning site (red) was cloned into the existing multiple cloning site. The sequences for the 6X histidine tag, TEV spacer, and TEV protease recognition site (for his-tag removal) is shown in the center of the map.

### **Section 2.2.1 Rev (WT, N60, and N70) Step by Step Purification Protocol**

Plasmid: YP001 (Rev-TEV) with Amp<sup>+</sup> in T7 expression system

Cell line for expression: BL21(DE3)

1. Induce at OD<sub>600</sub>=0.6 with 1mM IPTG O/N
2. Spin at 5000 RPM for 30min in a swing bucket rotor and collect cell pellet
3. Dissolve cell pellet in sonication buffer (8M Urea, 100mM NaCl, 10mM Imidazole, 10mM Tris, 5mM BME at pH 7.2)
4. Sonicate 30s x 8 (50% duty cycle)
5. Spin at 17000 rpm for 30min in 50 mL centrifuge tube (polypropylene) and collect the supernatant
6. Load the supernatant onto the pre-equilibrated Ni column (sonication buffer) and wash with buffer until UV absorbance reaches baseline
7. Elute the Rev protein with Ni Elute buffer (8M Urea, 100mM NaCl, 1M Imidazole, 10mM Tris, 5mM BME at pH 7.2).
8. Load the protein solution onto the pre-equilibrated SP-Sepharose column (8M Urea , 100mM NaCl, 10mM Tris, 5mM BME at pH 7.2), wash with SP equilibration buffer until UV absorbance reaches baseline
9. Elute the Rev protein with SP elution buffer (5M Guanidine HCl, 1M NaCl, 10mM Tris, 5mM BME at pH 7.2) over 10 CV at a FR (flow rate) of 3 mL/min.

10. Dilute to [protein] = 60  $\mu$ M against TEV proteolysis buffer (1 M guanidine-HCl, 50 mM Tris- HCl, 5 mM beta-mercaptoethanol, pH 8.0)
11. Add TEV protease as 1:10 in molar ratio to Rev:TEV for O/N for proteolysis
12. Add 5 M guanidine to dissolve any precipitate
13. Load the protein solution onto pre-equilibrated (1 M guanidine-HCl, 50 mM Tris- HCl, 5 mM beta-mercaptoethanol, pH 8.0) Ni-NTA column and collect flow through.
14. Wash column with 5M Guanidine HCl, 1M NaCl, 100mM NaCl, 10mM Tris, 5mM BME at pH 7.2 and collect uncut protein.
15. Concentrate the flow through with centiprep 3k down to around 0.6 mg/ml; measure the concentration of the Rev, and calculate the total amount of Rev.
16. Perform HPLC to remove nucleic acid contamination.
  - a. Acidify Rev (in 5M guanidine) using 0.1% TFA (50% TFA stock)
  - b. Load acidified Rev onto pre-equilibrated C18 column at 5% B (acetonitrile, 0.05% TFA)
  - c. The column is washed with ~5 CVs of 5% B and subjected to a gradient of 5-70 %B over 10 CV at a FR of 5 mL/min
  - d. Rev elutes at about 50% B
  - e. Measure 280 nm/260 nm ratio for nucleic acid contamination
  - f. Analyze mass by ESI-MS
  - g. 1, 2, and 5 mg aliquots are lyophilized and stored at -20°C

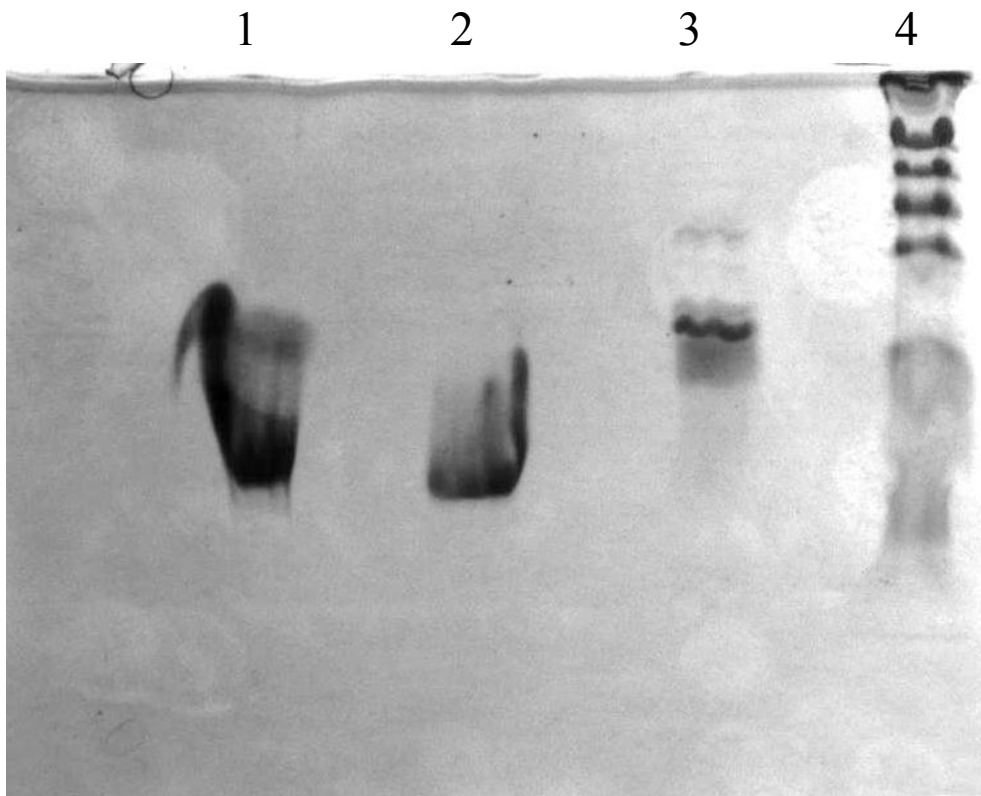


**Figure 15 SDS-PAGE of purified and TEV cut RevN60, RevN70, and RevWT.** Lanes: (1) RevN60, MW = 7.4 kDa, (2) RevN70, MW = 8.5 kDa, (3) RevWT, MW = 13.2 kDa, (4) Protein Markers, 10 kDa and 17 kDa markers are labeled. \*Due to the basicity of Rev ( $pI = 9$ ) and guanidine (denaturant), Rev constructs run aberrant on SDS-PAGE. All protein masses have been verified via ESI-MS.

### Section 2.3 Chimeric tRNA Constructs

A major obstacle to performing structural studies of proteins bound to their RNA target is obtaining the pure, milligram quantities of nucleic acid required to perform X-ray crystallography trials or NMR (Nuclear Magnetic Resonance) experiments. Synthetic RNA is very costly and the current method of using T7 polymerase creates heterogeneous transcripts leaving limited amounts of the desired product. Moreover, while numerous different constructs of the RRE may need to be sampled before finding a viable molecule for NMR or crystallization, one needs to find a cost-effective means to achieve this goal. In 2007, *Ponchon* and *Dardel* were able to design chimeric tRNA molecules which contained RNA sequences of interest. The target sequences were cloned into the anticodon region of human lysyl-tRNA, leaving the acceptor stem, T $\psi$ C, and D-loop intact. The gene (DNA sequence) for the tRNA is designed such that any hair-pin RNA sequence of interest (~370 nts. maximum) may be inserted into the anti-codon stem. The gene containing a robust promoter (bacterial *lpp*-lipoprotein promoter) was then sub-cloned into a commercial, expression vector and transformed into *E.coli* for over-expression (Figure 16). These constructs were then separated from cellular RNA and purified using ion-exchange and/or affinity chromatography to ~95% purity [84]. Over-expression of numerous hair-pin RNA sequences was achieved, ranging in size from 30 to ~370 nucleotides in length using the tRNA as a scaffold. One of the constructs expressed and purified contained the “kissing loop” region of HIV RNA and gel-shift analysis demonstrated the molecule migrated as a dimer, further supporting this as a

viable technology for the production of RNA. The investigators also found that the chimeric tRNA was resistant to cellular ribonuclease activity leaving the molecule intact for purification and subsequent structural and molecular biology investigations [84,85,86]. This technology has proven to be extremely useful for obtaining sufficient quantities of recombinant RNA.

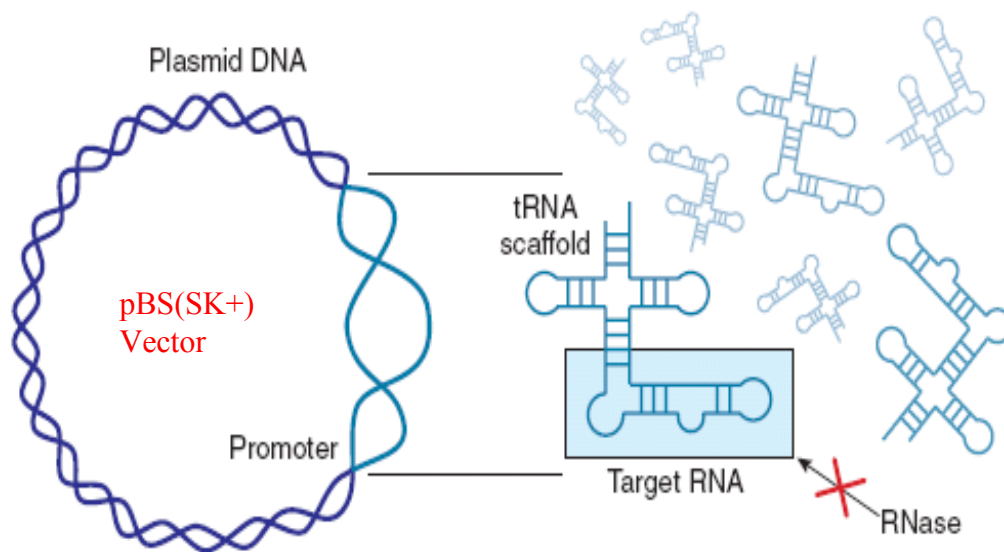


**Figure 16 Schematic for expression of chimeric tRNA from pBS(SK+) containing target RNA sequences.** All chimeric tRNAs are expressed in the pBS(SK+) vector. The RNA is under the control of the constitutive *lpp* (bacterial). The advantage of using a tRNA scaffold is the resistance of the RNA to cellular ribonucleases.

### **Section 2.3.1 Rationale for Design of RRE-containing Chimeric tRNAs**

HIV Rev is a RNA binding protein which recognizes with specificity a 351-nucleotide sequence contained within the HIV genome [15,20,48,87,88]. The RRE is characterized by a series of hairpin and stem-loop structures which have shown to be important for initial recognition by Rev and subsequent assembly along the RRE (Figure 7). However, the contribution of these stem-loop structures flanking stem loop-IIB to Rev's function and subsequent export of HIV RNA from the nucleus remains elusive. This work will feature a modified stem loop-IIB fragment (sIIB) and stem loop-IIa, IIB, and IIC (IIB) of the RRE expressed in natural tRNAs. The molecules were used in size-exclusion chromatography, analytical ultracentrifugation, and small angle X-ray scattering experiments to study the Rev:RRE RNA interaction(s). The following sections will describe the rationale for designing the molecules as well as gene sequences and predicted secondary structures for each structure.

#### **Section 2.3.1 sIIB-RRE (Insertion) Sequence**

The choice for the RRE fragment(s) for expression via the chimeric tRNA technology was based upon propensity for assembly and size of the RNA insert. I needed to find a sequence which was based upon the RRE, formed a discrete complex upon interaction with Rev, and short enough to ensure sufficient expression as longer hairpin inserts do not express as well. Initially, our goal was to crystallize the Rev/RRE complex. Previous experiments performed in 1994 showed that a sequence resembling stem loop-IIB (RWZ1) bound a monomer of Rev and may not support ternary

interactions to study the assembly of Rev [72] (Figure 17). The modified stem loop-IIB sequence supported the formation of a higher order, discrete Rev/RRE complexes with high specificity at a protein/RNA molar ratio of 16:1 making it ideal target for crystallization and solution biophysical measurements. RWZ2 (named sIIB in this work) contained a UC-bulge flanking the nonWatson-Crick base-paired bubble with an extended duplex region opposite the hairpin [72].

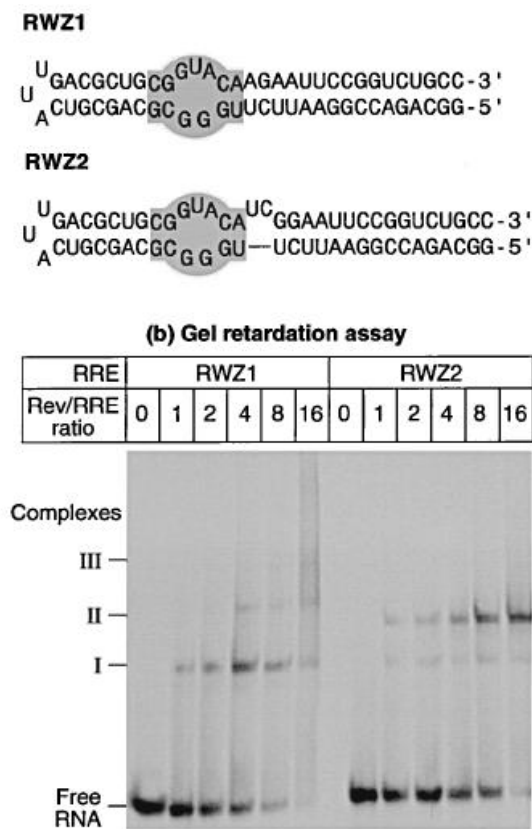


**Figure 17 Gel shift experiment comparing Rev binding to RWZ1 and RWZ2 (sIIB).** The experiment used two RRE sequences related to the high-affinity Rev binding site, stem loop-IIB. The introduction of a UC bulge flanking the unpaired base region (RWZ2) demonstrates the increased cooperativity of Rev binding over binding to RWZ1. This is evident by the formation of a higher-order species at identical Rev:RNA ratios. [72]

## Section 2.3.2 Design of sIIB-containing -tRNA<sup>Lys</sup>, -tRNA<sup>Phe</sup>, and tRNA<sup>MetI</sup>, sIIB-

### Section 2.3.2.1 tRNA<sup>Lys</sup>

sIIB-tRNA<sup>Lys</sup> employs the human lysyl tRNA as the scaffold for the expression of the sIIB (RWZ2) (Figure 18). The human lysyl tRNA scaffold was chosen due to its previous success in expressing RNA hairpin sequences of similar size, and the crystallizability of human lysyl tRNA [85,89].

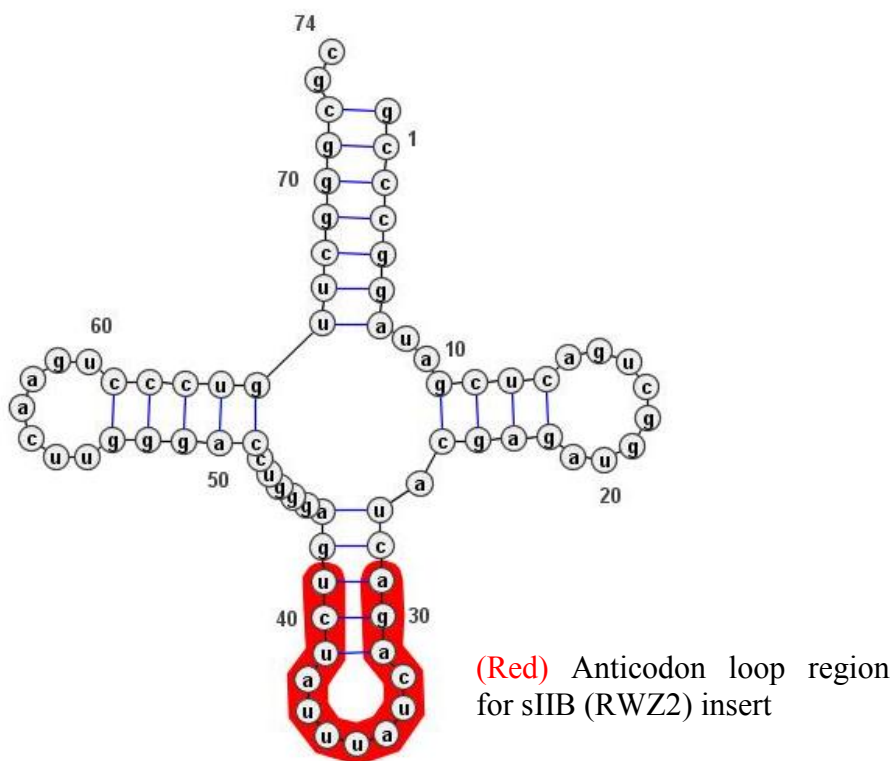


**Figure 18 Lysyl tRNA (Human).** Energy minimized (MFold) 2-dimensional representation of human lysyl tRNA (Using Varna online software <http://en.biosoft.net/rna/VARNA.html>). The anticodon residues which are removed for the RWZ2 sequence are in red.

## Gene sequence for sIIB-tRNA<sup>Lys</sup>

The gene sequences for all of the chimeric tRNAs were adapted from a previously published template [85]. From 5'→3', the DNA sequence includes the *Xho*II restriction site, *Lpp* promoter, *Eco*RI restriction site, tRNA scaffold, *Eag* restriction site, sIIB sequence, *Eag* restriction site, tRNA scaffold, *Pst*I restriction site, *rrn*C terminator, and *Hind*III restriction site, respectively. Below is the annotated gene sequence for sIIB-tRNA<sup>Lys</sup>.

### A.

5' *ctcgag* *gtcgcccatcaaaaaatattctcaacataaaaaactttgtgtaatacttgtaacgct* *gaattc*

*Xho*II

*Lpp* promoter

*Eco*RI

*gcccggatagctcagtcggtagagcag* *eggccg* *ccggaattcttgggcgcagcgtcattgac*

Human Lysyl tRNA Scaffold

*Eag*

sIIB Insert

*gctgcggtacatcggaattccgg* *eggccg* *cggtccagggtcaagtcctgttcgggcgcca*3'

sIIB Insert

*Eag*

Human Lysyl tRNA Scaffold

*ctgcag* *atccttagcgaaagctaaggattttttt* *aagctt* 3'

*Pst*I

*rrn*C terminator

*Hind*III



### Section 2.3.2.2 sIIB-tRNA<sup>Phe</sup>

sIIB-tRNA<sup>Phe</sup> employs the Yeast phenylalanyl tRNA as the scaffold for the expression of the sIIB (RWZ2) (Figure 20). This phenylalanyl tRNA was never reported to have been used as a scaffold for expressing RNA hairpin sequences. It was chosen due to its crystallizability and the idea that these same crystal contacts may be important for crystallizing sIIB-tRNA<sup>Phe</sup> in complex with Rev and Rev variants [90].

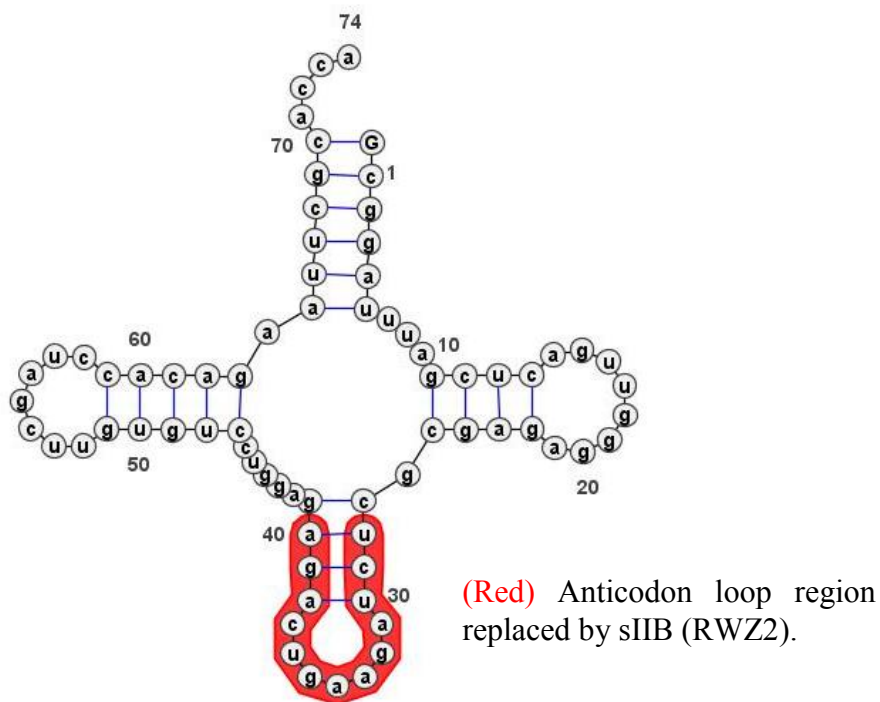


**Figure 20 Phenylalanyl tRNA (Yeast).** Yeast Phenylalanyl tRNA (Represented by Varna online software <http://en.biosoft.net/rna/VARNA.html>). The anticodon loop and insert site are highlighted in red.

## Gene sequence for sIIB-tRNA<sup>Phe</sup>

The gene sequences for all of the chimeric tRNAs were adapted from a previously published DNA gene template for expressing chimeric tRNAs [85]. From 5'→3', the DNA sequence includes the *Xho*I restriction site, *Lpp* promoter, *Eco*RI restriction site, tRNA scaffold, *Eag* restriction site, sIIB sequence, *Eag* restriction site, tRNA scaffold, *Pst*I restriction site, *rrnC* terminator, and *Hind*III restriction site, respectively. Below is the annotated gene sequence for sIIB-tRNA<sup>Phe</sup>.

### A.

5' *ctcgag* *gtcgcccatcaaaaaatattctcaacataaaaaactttgtgtaatacttgaacgct* *gaattc*

*Xho*I

*lpp promoter*

*Eco*RI

*gcgatttagctcagttgggagagcgc* *ccggaattcttgggcgcagcguattgac*

Phenylalanyl tRNA Scaffold

sIIB Insert

*gctgcggtacatcggaattccggtcgcc* *gaggtcctgtgttcgatccacagaattcgacca3'*

sIIB Insert

Phenylalanyl tRNA Scaffold

*ctcgag* *atccttagcgaagctaaggattttttt* *aagctt* 3'

*Pst*I

*rrnC terminator*

*Hind*III

B.

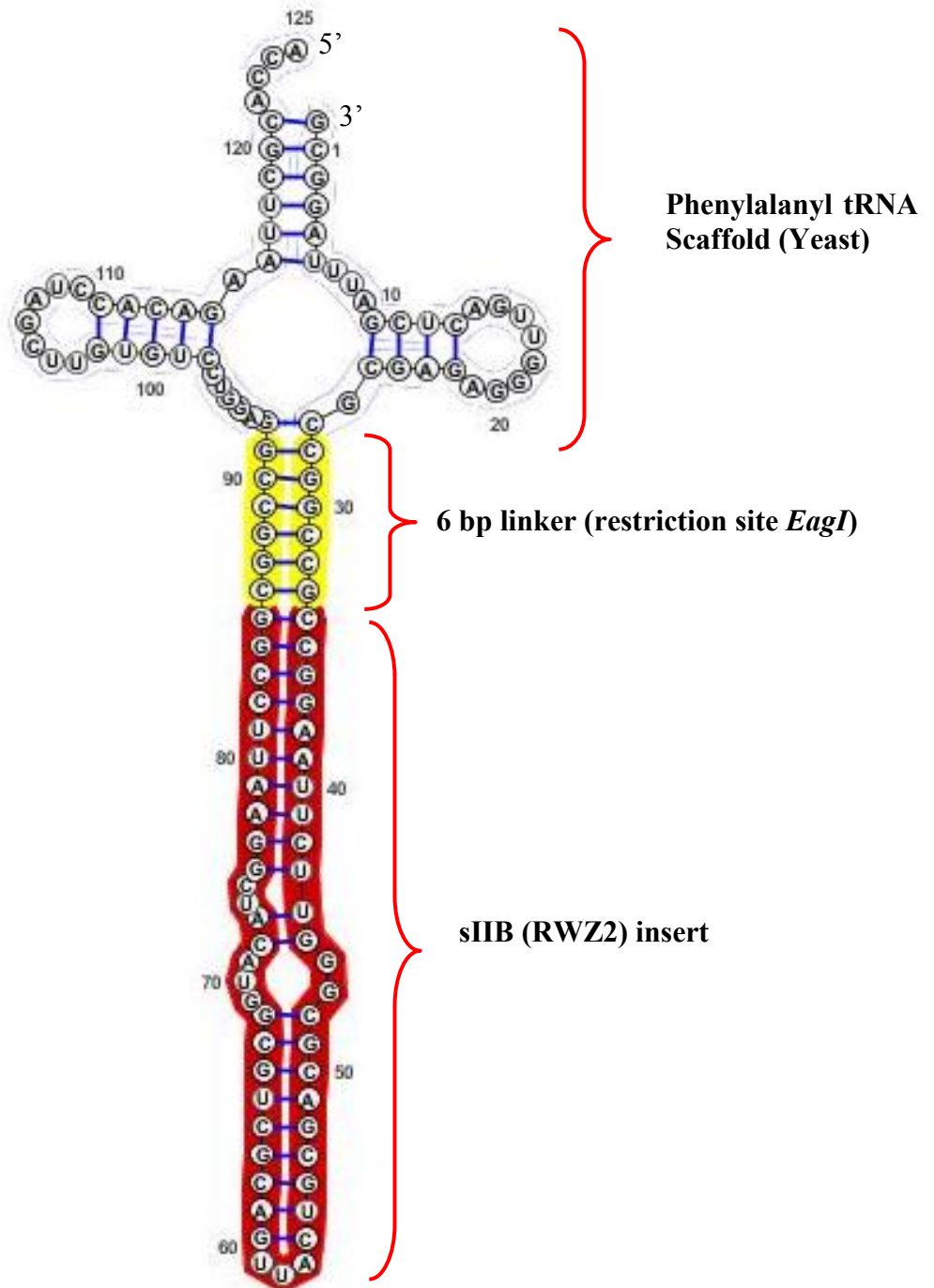


**Figure 21 Phenylalanyl tRNA (Yeast).** (A) Annotated gene sequence for sIIB-tRNA<sup>Phe</sup>, (B) Energy minimized (MFold) 2-dimensional representation of sIIB-tRNA<sup>Phe</sup> (Using Varna online software). The structure is color coded and labeled as scaffold, linker, and sIIB insert.

### Section 2.3.2.3 sIIB-tRNA<sup>MetI</sup>

sIIB-tRNA<sup>MetI</sup> employs the initiator methionyl tRNA from *E.coli* as the scaffold for the expression of the sIIB (RWZ2) (Figure 22). This scaffold was chosen due to its crystallizability and the idea that these same crystal contacts may enable the crystallization sIIB-tRNA<sup>Phe</sup> in complex with Rev and Rev variants [91].

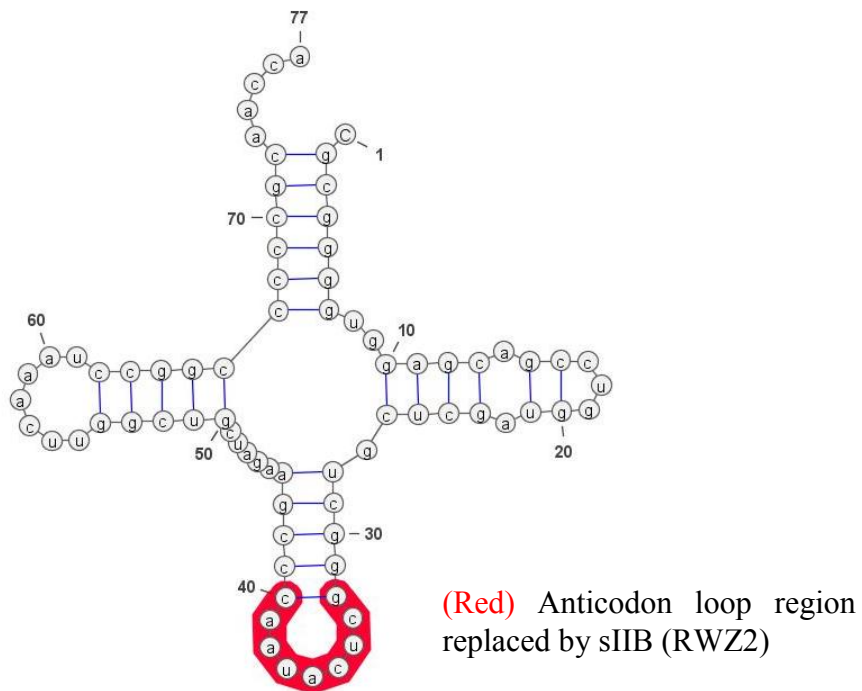


**Figure 22 Initiator methionyl tRNA (*E.coli*).** Initiator methionyl tRNA (Represented by Varna online software <http://en.biosoft.net/rna/VARNA.html>). The anticodon loop and insert site are highlighted in red.

Gene sequence for sIIB-tRNA<sup>MetI</sup>

A.

5' *ctcgag gtcgccccatcaaaaaaaaaatattctcaacataaaaaactttgtgtaataacttgtaacgct gaattc*

*XhoI*

*Lpp promoter*

*EcoRI*

*cgcggggtggagcagcctgtagctcgt eggccg ccggaattcttgggcgcagcgtcattgac*

Initiator methionyl tRNA Scaffold *Eag*

**sIIB Insert**

*gctgcggtacatcggaattccgg eggccg aaggtcgtcggttcaaatecgccccgcaacca3'*

**sIIB Insert**

*Eag*

Initiator methionyl tRNA Scaffold

*ctcgag atccttagcgaagtaaggattttttt aagctt 3'*

*PstI*

*rrnC terminator*

*HindIII*

B.

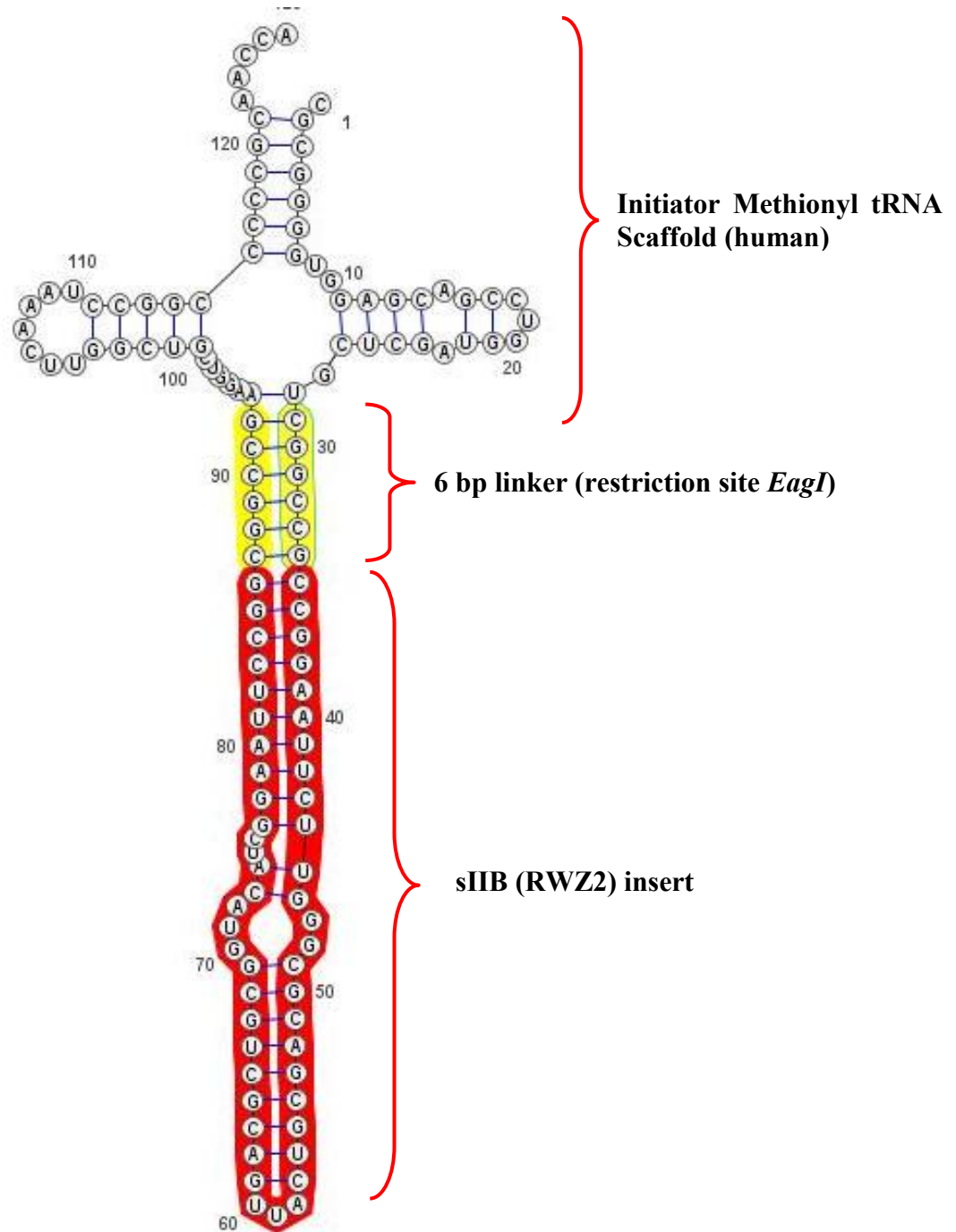


**Figure 23 Initiator methionyl tRNA (*E. coli*)** (A) Annotated gene sequence for sIIB-tRNA<sup>Met</sup>, (B) Energy minimized (Mfold) 2-dimensional representation of sIIB-tRNA<sup>Met</sup> (Using Varna online software). The structure is color coded and labeled as scaffold, linker, and sIIB insert.

#### **Section 2.3.2.4 IIB-tRNA<sup>Phe</sup>**

IIB- tRNA<sup>Phe</sup> employs the Yeast phenylalanyl tRNA scaffold to express a larger portion of the Rev Response Element. Since the assembly of Rev on the RRE is not well understood, it was necessary to first express smaller portions of the RRE (sIIB fragment) then progress to larger RNA inserts containing additional hairpin sequences near the high-affinity site, Stem Loop-IIB. The IIB fragment contains Stem Loop-IIB as well as Stem Loop-IIa and Stem Loop-IIc which allows for the understanding of the contribution of these sequences to Rev RRE binding and assembly in the context of the full-length Rev Response Element (Figure 24). The sections below will cover the IIB-tRNA<sup>Phe</sup> gene sequence, position of the IIB sequence within the RRE, as well as the expression and purification of IIB-tRNA<sup>Phe</sup>.



Gene Sequence for IIB-tRNA<sup>Phe</sup>

5' *ctcgag* *gtcgcccatcaaaaaatattctcaacataaaaaactttgtgtaataacttgtaacgct* *gaattc*  
*XhoI* *lpp* promoter *EcoRI*

*gcggatttagctcagttgggagagcgc* *c*  
Scaffold Linker

*gcactatgggcgcagcgtcaatgacgtctgacggtacaggccagacaattattgtctgatatagtc*  
IIB insert

*g* *gaggtcctgtgttcgatccacagaattcgacca*  
Linker Scaffold

*ctgcag* *atccttagcgaagctaaggattttttt* *aagctt* 3'  
*PstI* Terminator *HindIII*

**Figure 25 Annotated gene sequence for IIB-tRNA<sup>Phe</sup> construct.** Colored coded and labeled DNA sequence for IIB-tRNA<sup>Phe</sup> included restriction sites for subcloning, promoter, scaffold, linker, IIB insert, and termination sequence.

## Chimeric tRNA Design

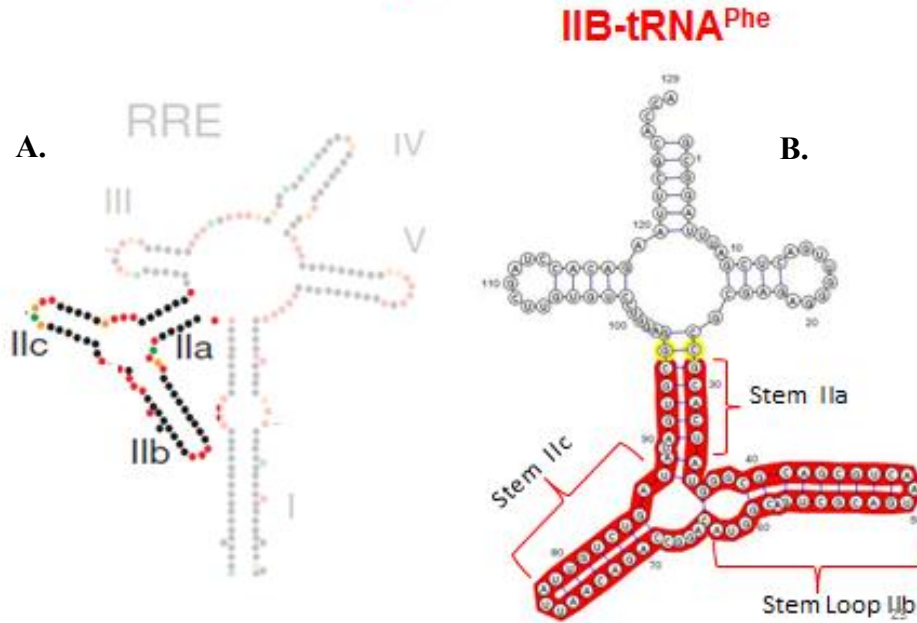


**Figure 26** Position of the RRE contained within IIB sequence (A) Position of IIB fragment within the Rev Response Element. (B) IIB fragment within the phenylalanyl tRNA scaffold.

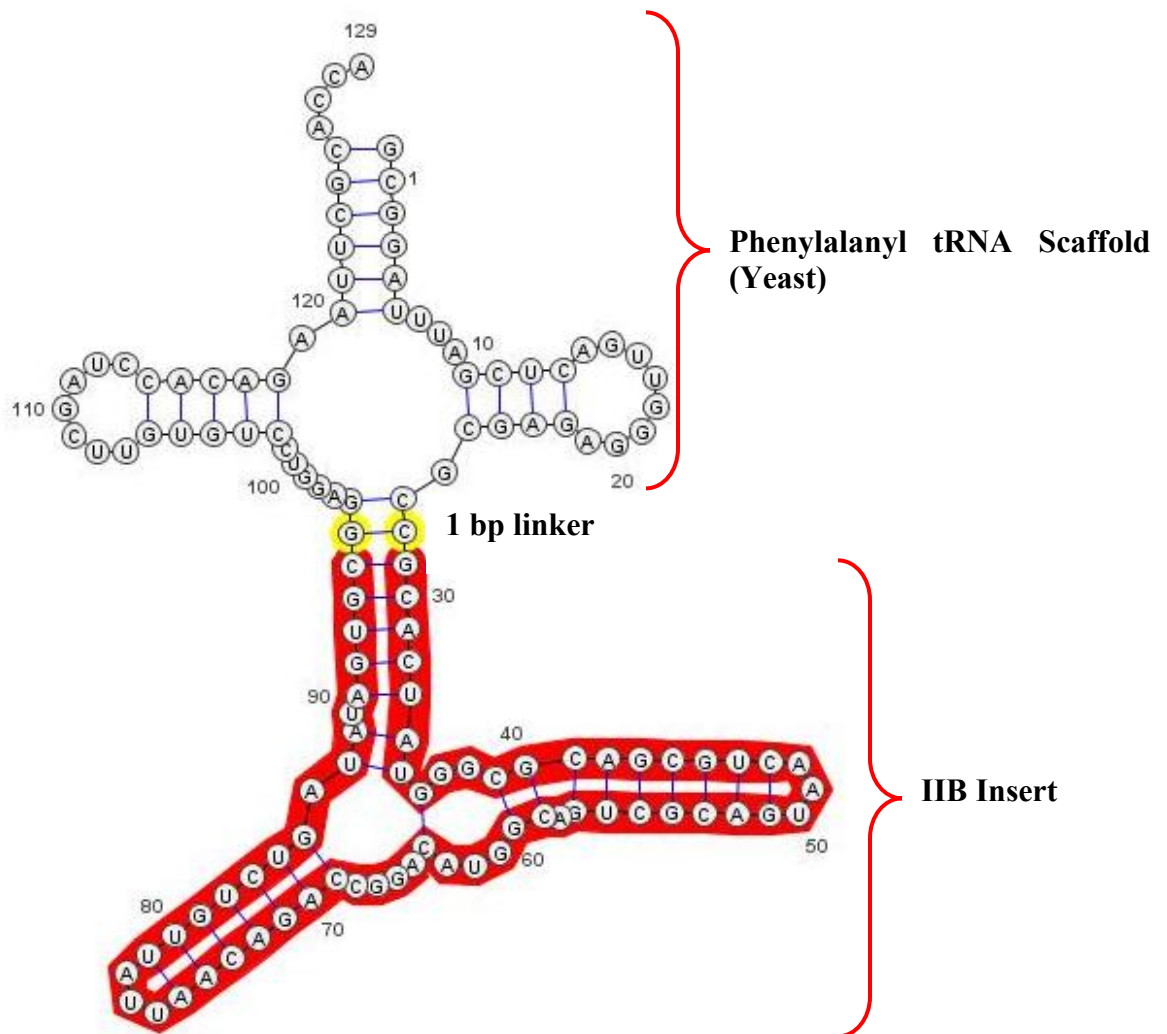


**Figure 27 sIIB-tRNA<sup>Phe</sup>. Energy minimized (MFold) 2-dimensional representation of IIB-tRNA<sup>Phe</sup> (<http://en.biosoft.net/rna/VARNA.html>). The structure is color coded and labeled as scaffold, linker, and sIIB insert.**

## Section 2.4 Expression and Purification of RRE-containing Chimeric tRNAs

The use of chimeric tRNAs containing target RNA sequences is a recent development that potentially allows for the production of milligram quantities of RNA [84,85]. The technology is based on the replacement of the anticodon loop region of the tRNA with a desired RNA hairpin sequence. Expression is under the constitutive *lpp* promoter (*E.coli*, lipoprotein) and a *rrnC* termination sequence. The 5' to 3' organization of the chimeric tRNA gene with RNA insert is as follows: 5' XhoI → *lpp* promoter EcoRI → tRNA Scaffold → RNA insert → tRNA Scaffold → *PstI* → *rrnC* terminator *HindIII* 3'. The *XhoI* and *HindIII* restriction sites allow for subcloning into a desired vector, and restriction sites flanking the tRNA scaffold sequences allow for the removal and placement of a new RNA hairpin insert. Initially, I used the (human) lysyl tRNA scaffold which had been previously characterized by NMR, showed good expression (milligram quantities) and had an established purification protocol. The gene for sIIB-tRNA<sup>Lys</sup> insert was ordered from DNA 2.0® contained within plasmid PJ201. A trial expression in the PJ201 shuttle vector in multiple *E.coli* cell lines proved to be ineffective. The sIIB-tRNA<sup>Lys</sup> gene was subsequently subcloned into the pBlueScript (SK+) (Figure 30). The vector was then transformed into several cell lines and tested for expression. The *E. coli* cell lines were BL21(DE3), JM101, HMS174(DE3), HMS174, and XL1-Blue. The only cell line which showed expression was BL21(DE3) (Figure 28). Cell RNA extracts were analyzed by Native PAGE (12%). The sIIB-tRNA<sup>Lys</sup> is not resolved from 5S rRNA due to the relatively high (12%) acrylamide.

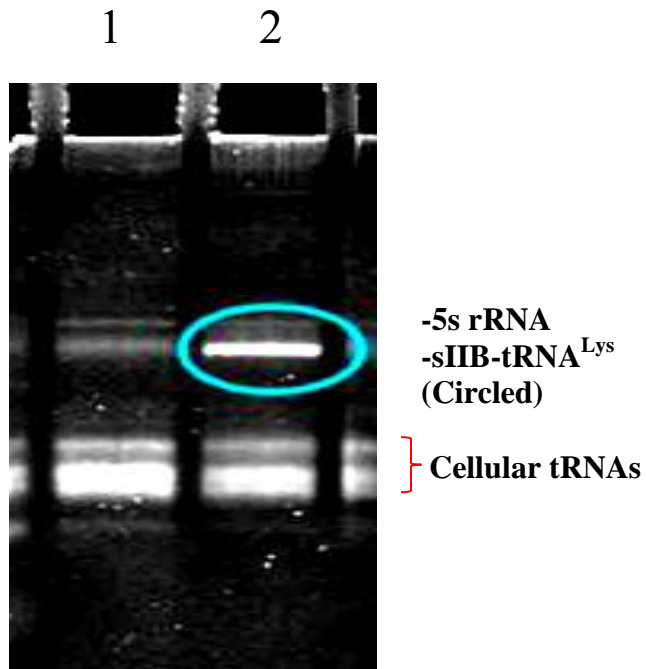


**Figure 28 Expression of sIIB-tRNA<sup>Lys</sup>.** The sIIB-tRNA<sup>Lys</sup> was subcloned into the pBS(SK+) and expressed in *E. coli* cell line BL21(DE3). Native PAGE (12%) (Lane 1) crude RNA extract from cells containing pBS(SK+) without sIIB-tRNA<sup>Lys</sup> insert transformed into BL21(DE3). (Lane 2) crude RNA extract from cells containing pBS(SK+) with sIIB-tRNA<sup>Lys</sup> insert transformed into BL21(DE3). The sIIB-tRNA<sup>Lys</sup> is not resolved from 5S rRNA due to the high % of acrylamide. The two species resolve with Native PAGE (7%).

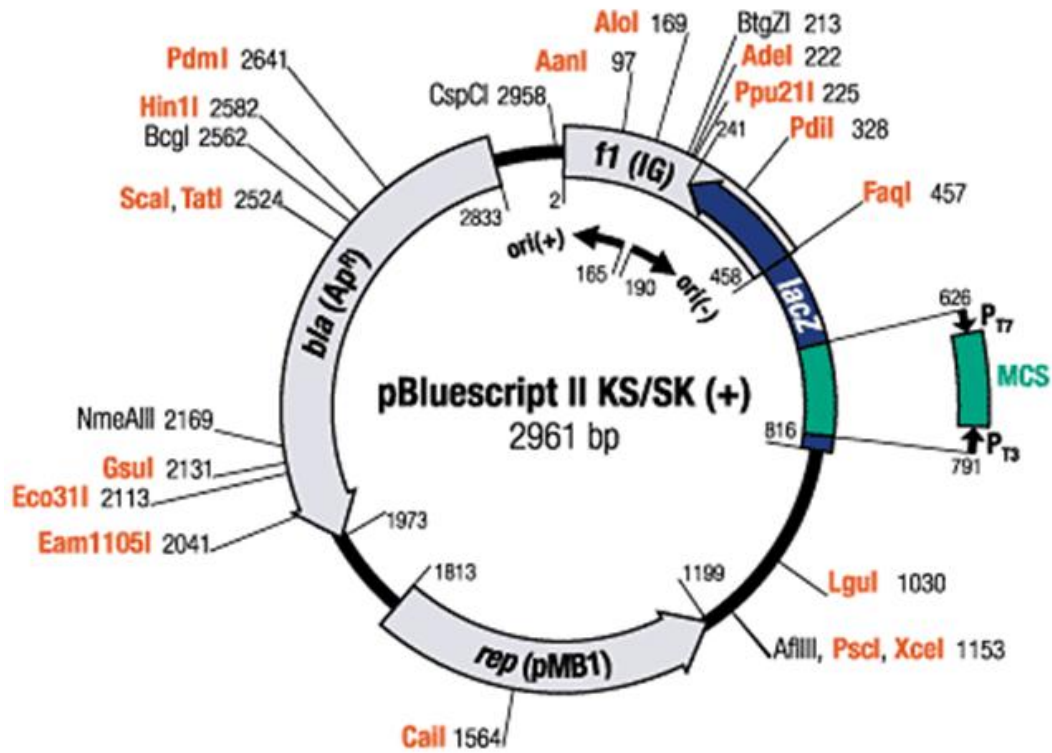


**Figure 29 pBS(SK+) vector.** Vector used for expression of all chimeric tRNA constructs. The vector is 2961 bp in length containing gene encoding for ampicillin resistance.

<http://www.fermentas.com/en/support/technical-reference/phage-plasmid-dna/pbluescriptII>

### **Section 2.4.1 Protocol for Chimeric tRNA Expression and Purification**

Below is the protocol for expression and purification of sIIB-tRNA<sup>Lys</sup>, sIIB-tRNA<sup>MetI</sup>, sIIB-tRNA<sup>Phe</sup>, and IIB-tRNA<sup>Phe</sup>. The purification of the chimeric tRNAs is divided into two chromatography stages. Stage 1 is the crude (Q-Sepharose-FPLC) separation of cellular RNA and excess phenol from the expressed chimeric tRNAs. Stage 2 involves high-resolution (MonoQ-HPLC) enrichment of the chimeric tRNA and separation from cellular tRNAs and 5S rRNA.

#### **Purification Protocol for sIIB-tRNA<sup>Phe</sup> (Version for Publication):**

The sIIB-tRNA<sup>Phe</sup> gene was designed in-house, ordered from DNA 2.0, and subsequently subcloned into the pBS(SK+) vector. The sIIB-tRNA<sup>Phe</sup> plasmid was expressed under a constitutive *E. coli* promoter (*lpp*-lipoprotein promoter) in *E. coli* strain BL21DE3. Cells were grown O/N @ 37°C in 2XYT media supplemented with 50 µg/mL of ampicillin then harvested and pelletized by centrifugation at 5,000 rpm in swing bucket rotor for 30 min at 4°C. Following centrifugation, cell pellets were dissolved in 50 mL of Buffer C (10 mM magnesium acetate, 1 mM Tris-HCl, pH 7.4) and 1X volume of Tris-saturated phenol using 50 mL polypropylene centrifugation tubes followed by agitation for 1 hr. Following agitation, the phenol solution was centrifuged @ 10K RPM for 1 hr at RT. The aqueous layer (upper layer) was carefully removed and 0.1X volume of 5 M NaCl is added. 2X volumes of 95% EtOH was then added and solution was stored at -20°C for O/N precipitation. Precipitated nucleic acid was pelletized by centrifugation at 10K RPM for 1 hr. Pelletized nucleic acid was suspended

in 50 mL of Buffer A (40 mM Tris-HCl, pH 7.4) and subjected to low-resolution anion-exchange chromatography (Q-Sepharose 16/10, GE Life Sciences, 20 mL CV) for crude separation and removal of contaminating phenol. The samples are loaded in Buffer A followed by 5 CV of column washing until UV baseline is obtained. The %B was then adjusted to 35% for 3 CV. The separation gradient was from 35%-80% Buffer B (1M NaCl, 40 mM Tris, pH 7.4) over 4 hr at a flow rate of 3 mL/min. The sIIB- tRNA<sup>Phe</sup> was contained in the second elution peak. Peak fractions were analyzed via Native PAGE (7%) with standards and pooled fractions containing sIIB- tRNA<sup>Phe</sup> were pooled and diluted 2-fold with Buffer A for high-resolution separation using a HPLC-MonoQ HR 16/10 (GE Life Sciences). Following the loading of the RNA, the column is washed with ~5 CV of Buffer A. The % Buffer B was then adjusted to 40% until conductance was stable. A gradient from 400 mM-750 mM NaCl was used to separate cellular tRNA, 5S rRNA, and sIIB- tRNA<sup>Phe</sup>. sIIB- tRNA<sup>Phe</sup> was analyzed for purity via Native-PAGE (7%) prior to experiments. The sIIB-tRNA<sup>Phe</sup> migrates in between the upper band which corresponds to 5S rRNA and cellular tRNA.

### **Step by step protocol For Expression and Purification of Chimeric tRNA:**

Buffer A: 40 mM Tris, pH 7.4

Buffer B: 40 mM Tris, pH 7.4, 1M NaCl

Buffer C: 10 mM Magnesium Acetate, 1 mM Tris, pH 7.4

1. Plate freshly transformed BL21(DE3) with pBS(SK+) vector (containing chimeric tRNA insert) onto 50 µg/ml ampicillin supplemented agar plates

2. Grow plates O/N at 37°C
3. Transfer single colony to 50 ml Luria Broth media supplemented with 50 µg/ml ampicillin
4. Grow 50 ml culture O/N at 37°C on shaker
5. Transfer 50 ml culture to 2L 2xYT media supplemented with 50 µg/ml Ampicillin for O/N incubate 2L culture O/N at 37°C
6. Pelletize cells by centrifuging at 4500RPM for 30 minutes in the high-speed centrifuge @ RT.
7. Resuspend pellet in 50 mL of buffer C.
8. Add one volume of Tris-buffered phenol in 50 mL polypropylene centrifuge tubes and gently agitate for 1h at RT on gel rocker station.
9. Centrifuge at 10K RPM for 1hr and collect aqueous phase (minimize phenol uptake).
10. Add 0.1 volume of 5M NaCl and 2X volumes of 95% EtOH.
11. Precipitate O/N at -20°C in 250 mL Erlenmeyer flask
12. Centrifuge precipitated solution at 10K RPM for 1hr, carefully pour off supernatant, and allow to air-dry for 30 minutes
13. Resuspend pellet in 50ml of buffer A

Stage 1 Purification: Q-sepharose column (GE Healthcare, 16/10 Q FF, 20 mL column volume)

1. Equilibrate Q-sepharose column (GE Healthcare, 16/10 Q FF) with buffer A using the GE<sup>®</sup> Healthcare AKTA Prime
2. Load sample onto column at 3.5 mls/min.
3. Switch to buffer A until baseline absorbance is reached
4. Switch to buffer B and adjust to 35% (buffer B)
5. Run gradient from 35%-80% (Buffer B) over 4hrs at 3.0 mL/min for cellular tRNA and chimeric tRNA separation. Collect 10 mL fractions.
6. Pool 2<sup>nd</sup> peak for MonoQ (HPLC) purification

Stage 2: MonoQ (Pharmacia 16/10, HPLC)-Akta Purifier

1. Dilute pooled fractions from Q-Sepharose column with one volume of buffer A
2. Equilibrate MonoQ 16/10 (20 mL) column with 5 column volumes of buffer A
3. Load sample (3 mgs maximum) onto column using Line A at 5 ml/min
4. Wash column until stable baseline is reached with buffer A
5. Adjust % buffer B to 40%
6. Use( tRNA gradient) Method and set parameters as follows:
  - a. FR = 2.5mls/min
  - b. Starting buffer B concentration: 40%
  - c. Gradient: 40-75%, 25 column volumes (500mls)
  - d. Collect 6ml fractions in 18 cm. tubes
  - e. Chimeric tRNA should elute at (~65-70 mS/cm) for all chimeric tRNAs

7. Following Native PAGE (7%) analysis, pool fractions from large peak for 2<sup>nd</sup> MonoQ purification
8. Repeat same protocol for 2<sup>nd</sup> MonoQ purification (This is designed to remove any contaminants left by initial MonoQ column). Fractions should be diluted 2-fold to reduce [NaCl] with Buffer A before loading onto MonoQ. Total load should be 3 mg of RNA.
9. Run fractions across large peak on 7% PAGE to check for purity, pool fractions and concentrate with Sartorius® (5k cut-off) concentrators as needed for experiments.

#### **Section 2.4.2 Protocol for (Chimeric) tRNA:Rev Complex Gel Shift, and Size-Exclusion Chromatography**

This section will provide the protocol and buffer conditions used for gel shift and size-exclusion chromatography experiments on Rev:Chimeric tRNA complexes. Results of the experiments will be covered in Chapter 3.

#### **Protocol for ShodexKW803 and Gel Experiments: Chimeric tRNA:Rev Complexes**

Buffer A: 200 mM NaCl, 40 mM Tris, pH 7.2, 2 mM  $\beta$ -mercaptoethanol, (100  $\mu$ M Mg<sup>2+</sup>)

Order of addition in making Rev:RNA complexes: Buffer A  $\rightarrow$  tRNA  $\rightarrow$  Rev

-TV=200 $\mu$ l

1. Measure stock concentrations of chimeric tRNA and Rev
2. Calculate volume needed to make 5  $\mu$ M chimeric tRNA in 200  $\mu$ l
3. Calculate volume needed to make desired molar ratio of Rev
4. Determine volume of buffer A needed for 200  $\mu$ l
5. Add calculated volume of buffer to each tube (tRNA:Rev ratio)
6. Add calculated volume of tRNA for 5  $\mu$ M
7. Add calculated volume of Rev for desired molar ratio
8. O/N dialyze complexes in buffer A using Thermo-Scientific Slide-A-lyzer® mini dialysis units
9. Measure volume of each complex and adjust each to 200  $\mu$ l (Use Corning-500 $\mu$ l-3k cut-off concentrators)
10. Following O/N dialysis and volume adjustment to 200  $\mu$ l, remove 30  $\mu$ l and mix with 670  $\mu$ l (1/23 dilution) of dialysate for UV/Vis spectroscopy using 260, 285, and 290nm
11. Remove 10  $\mu$ l of O/N dialyzed complex and use for Native PAGE (7% acrylamide) analysis

12. Keep remaining sample for ShodexKW803 and native gel shift experiments

**Protocol for performing ShodexKW803 Experiments:**

Running Buffer A: 200 mM NaCl, 40 mM Tris, pH 7.2, 2 mM  $\beta$ -mercaptoethanol, (100  $\mu$ M Mg<sup>2+</sup>)

1. Equilibrate ShodexKW803 column O/N with Buffer A at 0.1 ml/min
2. Use 1 ml syringe and aspirate 160  $\mu$ l of complex
3. Wash injection loop (100  $\mu$ l) with ~300  $\mu$ l of buffer A
4. Inject 160 $\mu$ l of sample into 100 $\mu$ l injection loop, run at 0.35 ml/min, and collect 0.5 ml fractions if desired. Use 260, 285, and 290nm for detection.

**Protocol for performing Native PAGE Gel Shift Experiments (7% acrylamide)**

1. Add 6  $\mu$ l ddH<sub>2</sub>O  $\rightarrow$  10  $\mu$ l sample  $\rightarrow$  2  $\mu$ l 10x TBE  $\rightarrow$  2  $\mu$ l 10x dye (bromophenol blue)=20  $\mu$ l TV  
- Use the 10  $\mu$ l aliquot of complex saved following O/N dialysis
2. Equilibrate gel at 150V for 1hr.

-Recipe for 7% Native PAGE

TV = 100 mls

1. Mix 10 mL of 10X TBE, 17.5 mL (40% acrylamide), 72.5 mL of ddH<sub>2</sub>O, 350 µl TEMED, and 450 µl of ammonium persulfate (APS)
3. Load wells with 20 µl of sample and run at 250V until bromophenol has migrated ½ way down length of gel
4. Stain gel with 0.5 µg/ml of Ethidium bromide for ~30 minutes

### **Section 2.4.3 Expression and Purification of sIIB-tRNA<sup>Lys</sup>, sIIB-tRNA<sup>MetI</sup>, sIIB-tRNA<sup>Phe</sup>, and IIB-tRNA<sup>Phe</sup>**

This section will cover the expression and purification of sIIB-tRNA<sup>Lys</sup>, sIIB-tRNA<sup>MetI</sup>, sIIB-tRNA<sup>Phe</sup>, and IIB-tRNA<sup>Phe</sup>. All chimeric tRNAs are expressed and purified using the protocols described in the above Section 2.4.1. Figures will show chromatograms for Q-Sepharose (low resolution) and MonoQ (HPLC) as well as native-PAGE of fractions from each of the chromatograms. The RNAs are initially subjected to a low-resolution Q-Sepharose column to remove residual phenol from the preparation, and to crudely separate the chimeric tRNAs from cellular tRNAs and 5S rRNA. Following crude separation, the chimeric RNAs are further enriched with a high-resolution HPLC MonoQ column.

#### **Expression and Purification of sIIB-tRNA<sup>Lys</sup>**

sIIB-tRNA<sup>Lys</sup> was the initial chimeric tRNA with the sIIB (RWZ2) fragment expressed. It was expressed in BL21(DE3) in the vector pBS(SK+). The figure below

shows elution of sIIB-tRNA<sup>Lys</sup> from the low-resolution Q-Sepharose (GE) column. Elution fractions were subjected to 7% native-PAGE for analysis. The peaks are labeled in red, blue, and green and correspond to cellular tRNA, sIIB-tRNA<sup>Lys</sup>, and 5S rRNA, respectively. The yield for a 2L culture is ~10 mgs. Fractions corresponding to sIIB-tRNA<sup>Lys</sup> were pooled and subjected to the MonoQ column for further enrichment.

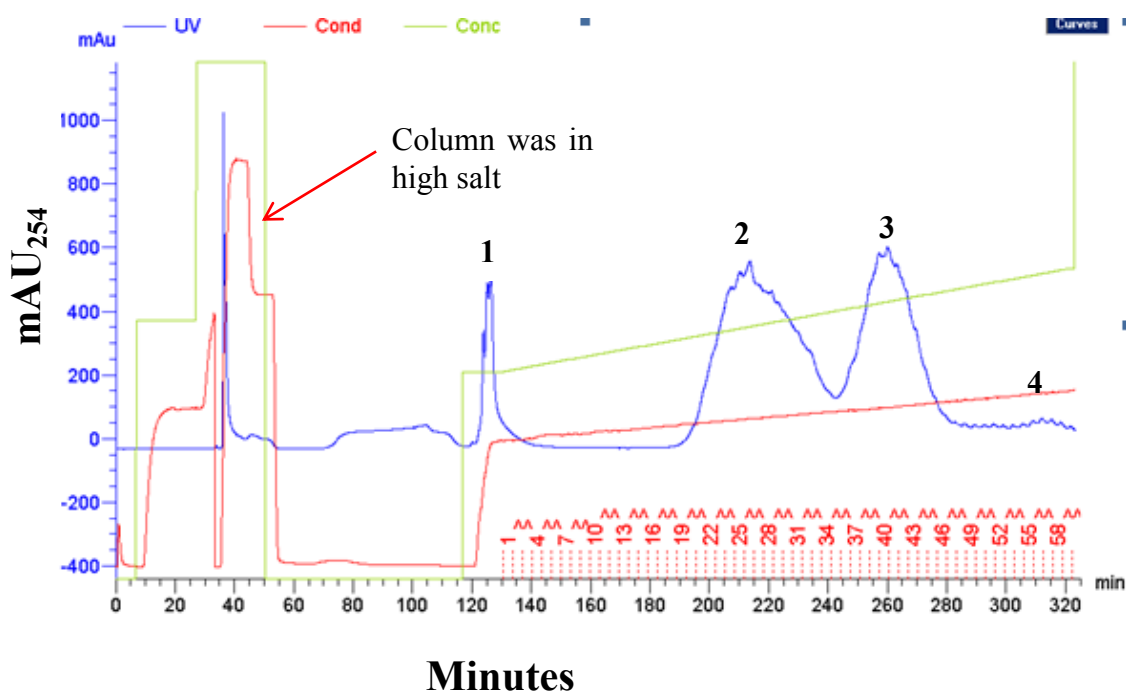


**Figure 30 Q-Sepharose chromatogram showing purification of sIIB-tRNA<sup>Lys</sup>.** Elution profile of sIIB-tRNA<sup>Lys</sup>. Elution peaks represent (1) residual phenol from preparation, (2) cellular tRNA, (3) sIIB-tRNA<sup>Lys</sup> (4) 5S rRNA and higher molecular weight RNAs. The gel in Figure 31 represents fractions from labeled peaks. Only 254 nm absorbance is shown.

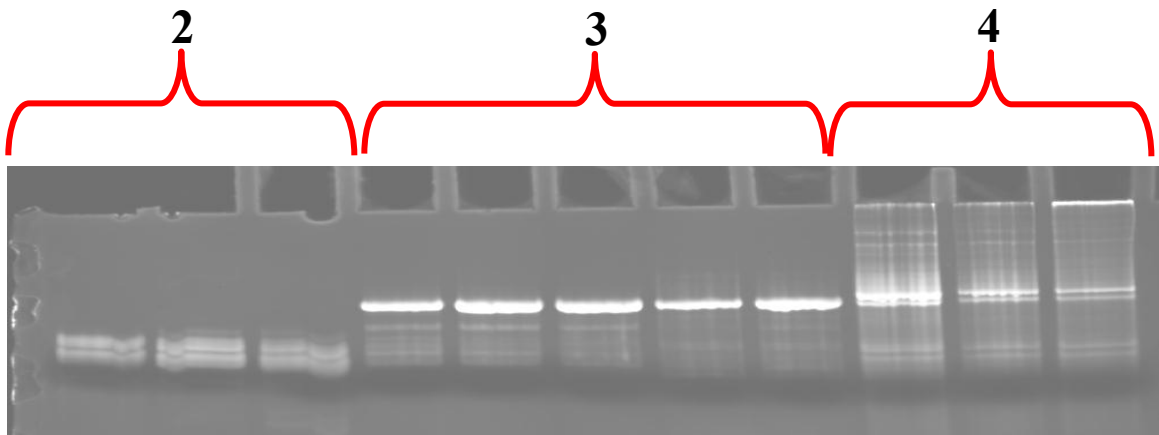


**Figure 31 Native PAGE (12%) of Q-Sepharose fractions of sIIB-tRNA<sup>Lys</sup> elution profile.** Fractions represent (2) cellular tRNA, (3) sIIB-tRNA<sup>Lys</sup> (4) 5S rNA and higher molecular weight RNAs.

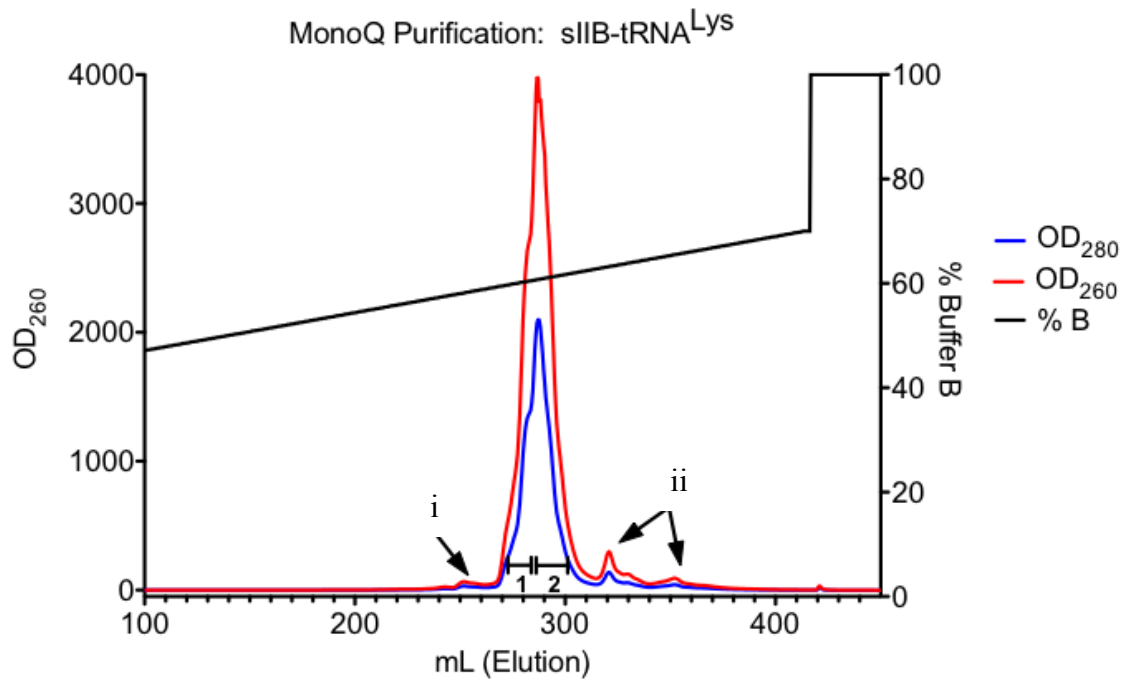


**Figure 32** Elution profile of MonoQ 16/10 purification of sIIB-tRNA<sup>Lys</sup> with 260nm (Red) and 280nm (Blue) absorbances, and % Buffer B (Black) (1M NaCl). The peaks are labeled (i) cellular tRNA, (1 and 2) sIIB-tRNA<sup>Lys</sup> fractions on 7% native PAGE analysis, and (ii) 5S rRNA and higher molecular weight species.

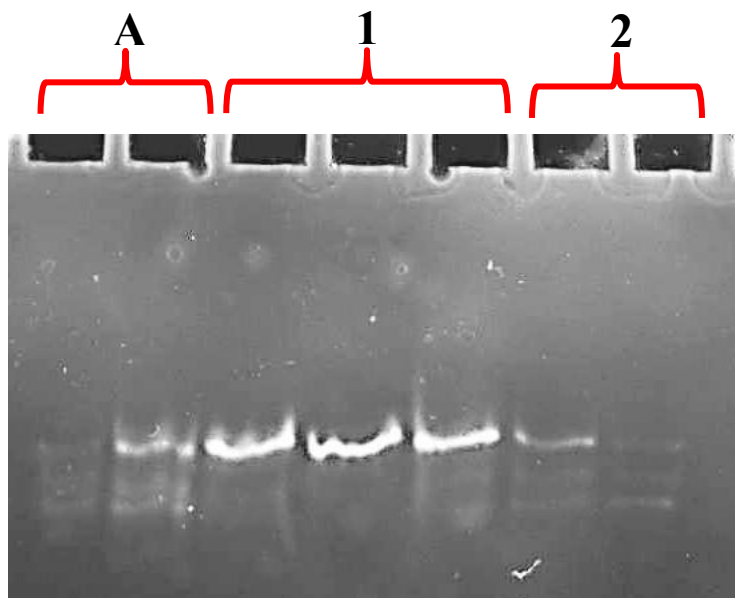


**Figure 33 Native PAGE (7%) of fractions from Figure 32.** Fractions represent (A) cellular tRNA, (1) denoted portion of peak, (2) denoted portion of peak.

## Expression and Purification of sIIB-tRNA<sup>Phe</sup>

sIIB-tRNA<sup>Phe</sup> is expressed in BL21(DE3) cell line in the vector pBS(SK+). The yield for a 2L in 2xYT medium is ~15 mgs. The chimeric tRNA<sup>Phe</sup> showed the largest yield of all of the tRNA scaffolds used for RRE RNA expression. The yield for a 2L prep is ~15 mg. Figure 34 represents the expression of IIB- tRNA<sup>Phe</sup> and the HPLC (MonoQ) purified product as well as HPLC (MonoQ) purified sIIB- tRNA<sup>Phe</sup>

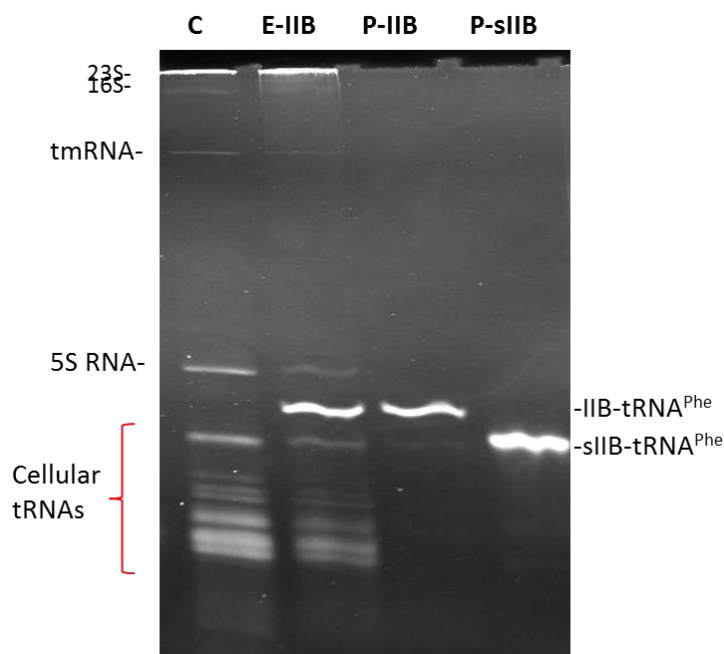


**Figure 34 7% Native-PAGE of IIB-tRNA<sup>Phe</sup> and sIIB- tRNA<sup>Phe</sup> showing relative positions of *E.coli* 23S rRNA, 16S rRNA, tmRNA, 5S rRNA, and cellular tRNAs. Lane: (C), BL21(DE3) with no plasmid; (E-IIB), expression of IIB-tRNA<sup>Phe</sup>; (P-IIB), purified IIB-tRNA<sup>Phe</sup>; (P-sIIB), purified sIIB- tRNA<sup>Phe</sup>.**

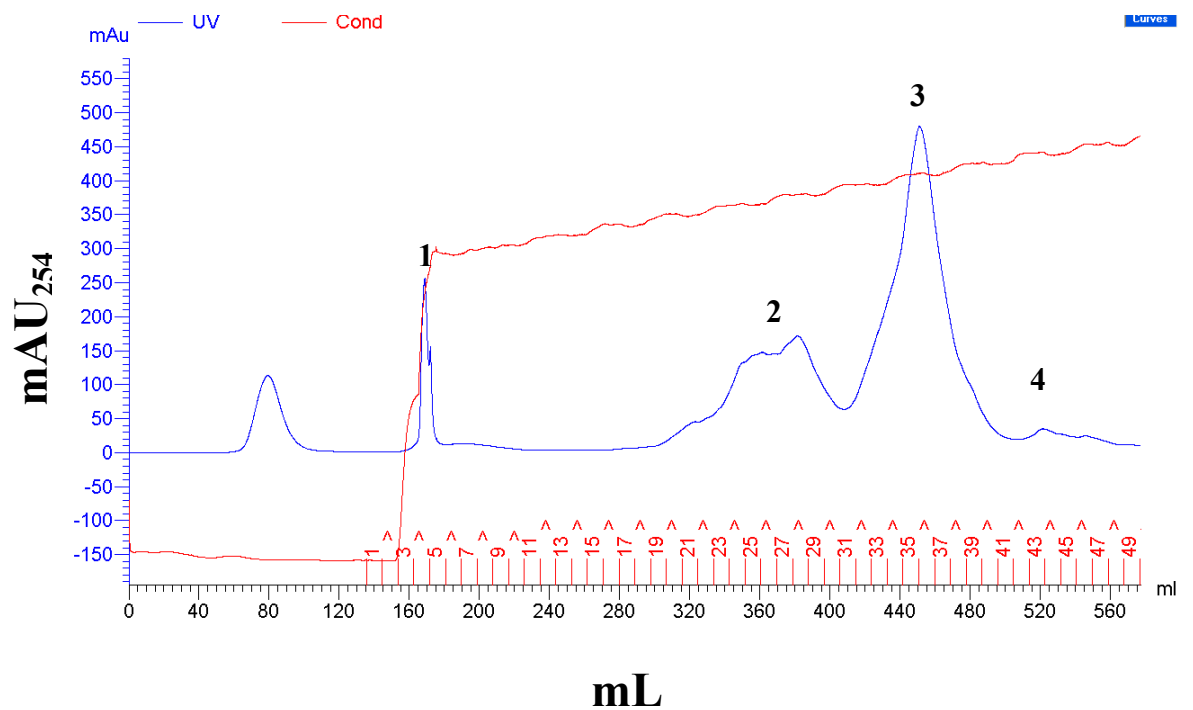


**Figure 35 Elution profile of Q-Sepharose purification of sIIB-tRNA<sup>Phe</sup>.** Elution peaks represent (1) residual phenol from preparation, (2) cellular tRNA, (3) sIIB-tRNA<sup>Lys</sup> (4) 5S rRNA and higher molecular weight RNAs. Only 254nm absorbance (Blue) and conductance (Red) is shown

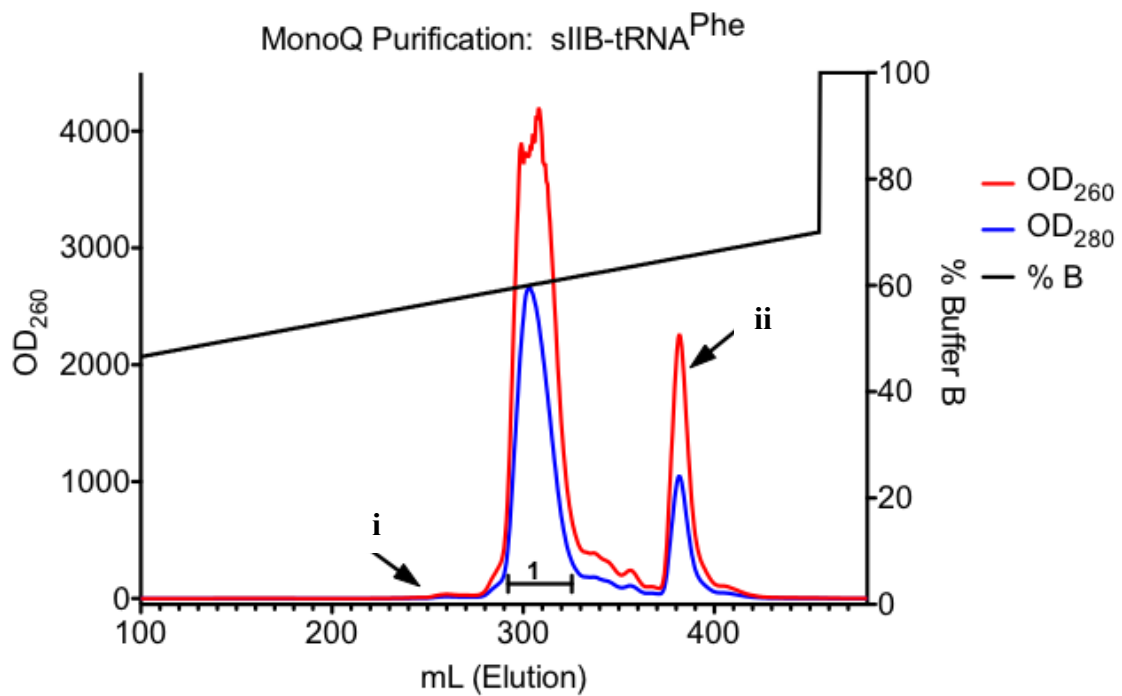


**Figure 36** Elution profile of MonoQ 16/10 purification of sIIB-tRNA<sup>Phe</sup> with 260nm (Red) and 280nm (Blue) absorbances, and % Buffer B (Black) (1M NaCl). The peaks are labeled (i) cellular tRNA, (1) sIIB-tRNA<sup>Phe</sup> fractions on 7% native PAGE, and (ii) 5S rRNA and higher molecular weight species.

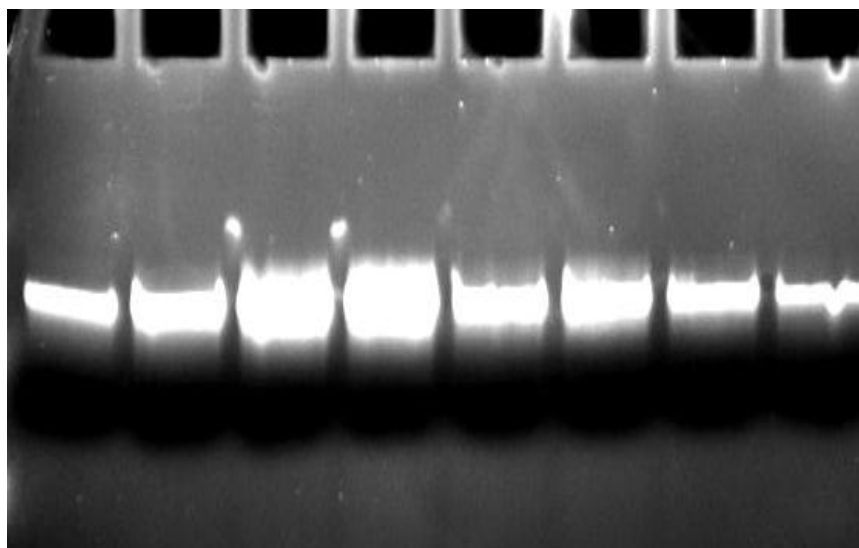


**Figure 37 Native PAGE (7%) of fractions across peak (1).** Lanes represent fractions across peak (1) sIIB-tRNA<sup>Phe</sup> elution peak labeled (1) in previous figure.

## Purification of sIIB-tRNA<sup>MetI</sup>

sIIB-tRNA<sup>MetI</sup> was expressed in BL21(DE3) in the vector pBS(SK+). Figures 38 and 39 below shows elution of sIIB-tRNA<sup>MetI</sup> from the MonoQ (16/10) ion-exchange column, and fractions analyzed by native-PAGE (7%), respectively. The yield for a 2L culture is ~5 mgs.

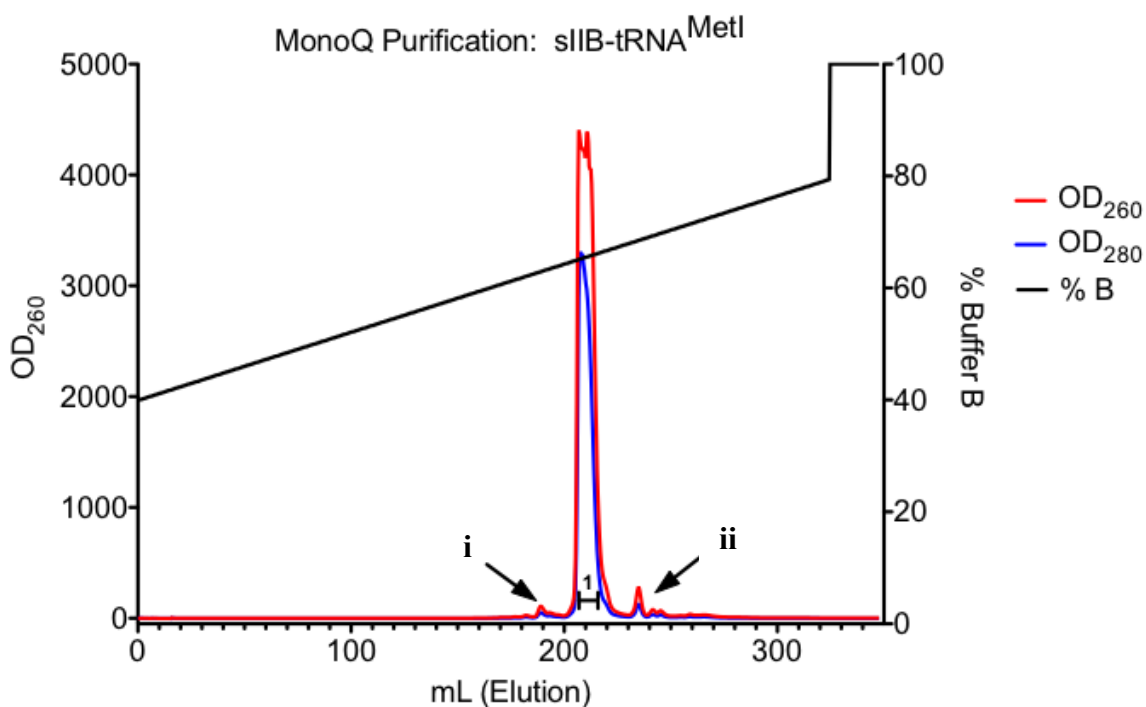


**Figure 38** Elution profile from MonoQ 16/10 purification of sIIB-tRNA<sup>MetI</sup>. The peaks are labeled (i) cellular tRNA, (1) sIIB-tRNA<sup>Phe</sup> fractions on 7% native PAGE (Figure 39), and (ii) 5S rRNA and higher molecular weight species.

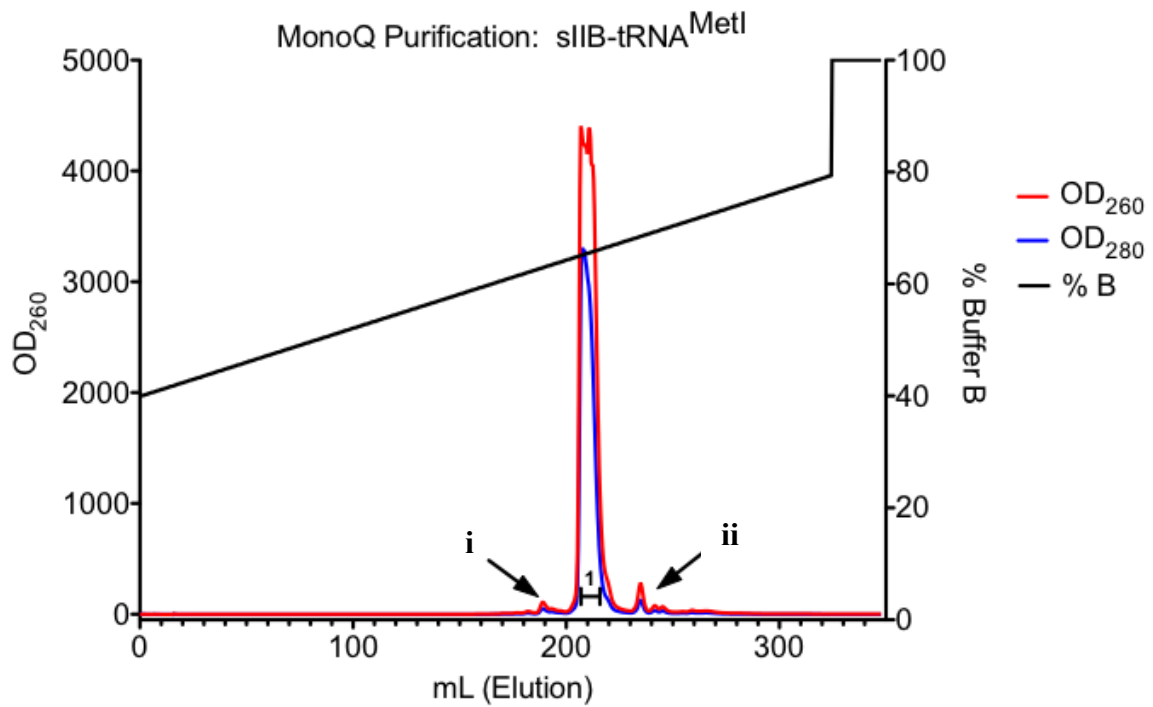


**Figure 39** Elution profile from MonoQ 16/10 purification of sIIB-tRNA<sup>MetI</sup>. The peaks are labeled (i) cellular tRNA, (1) sIIB-tRNA<sup>Phe</sup> fractions on 7% native PAGE (Figure 39), and (ii) 5S rRNA and higher molecular weight species.

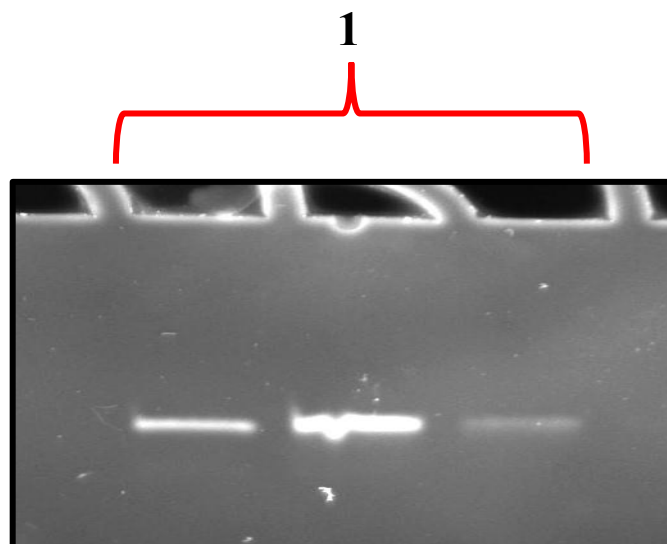


**Figure 39 Native PAGE (7%) of fractions from Figure 38.** Lanes represent fractions from peak sIIB-tRNA<sup>MetI</sup> elution peak labeled (1).

#### **Expression and Purification of IIB-tRNA<sup>Phe</sup>**

IIB-tRNA<sup>Phe</sup> is expressed in BL21(DE3) cell line in the vector pBS(SK+). The yield for a 2L in 2xYT medium is ~10 mgs. Figures 40, 41, 42, and 43 show Q-Sepharose represents the expression of IIB- tRNA<sup>Phe</sup> and the HPLC purified product as well as HPLC purified sIIB- tRNA<sup>Phe</sup>.

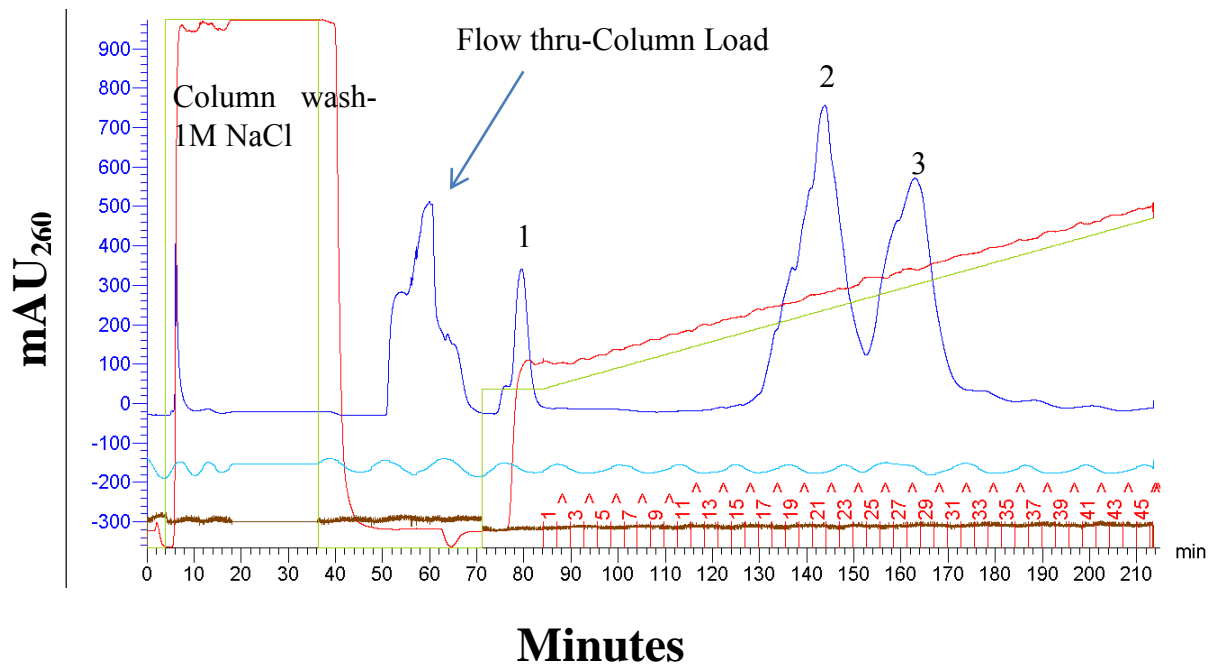


**Figure 40** Elution profile from Q-Sepharose purification of IIB-tRNA<sup>Phe</sup>. Elution peaks represent (1) residual phenol from preparation, (2) cellular tRNA, (3) sIIB-tRNA<sup>Lys</sup> (4) 5S rRNA and higher molecular weight RNAs. Only 260nm absorbance (Blue) and conductance (Red) is shown. Native PAGE (7%) of fractions shown in Figure 2.32.

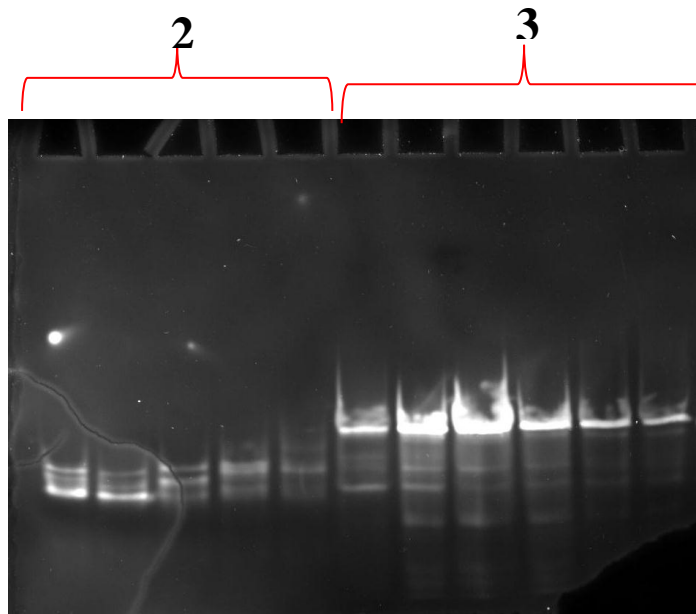


**Figure 41 Native PAGE (7%) representing fractions from Q-Sepharose elution for purification of IIB-tRNA<sup>Phe</sup>.** Lanes labeled (2) represent fractions corresponding to cellular tRNAs, and lanes labeled (3) represent fractions containing IIB-tRNA<sup>Phe</sup>. Refer to Figure 40 for elution profile.

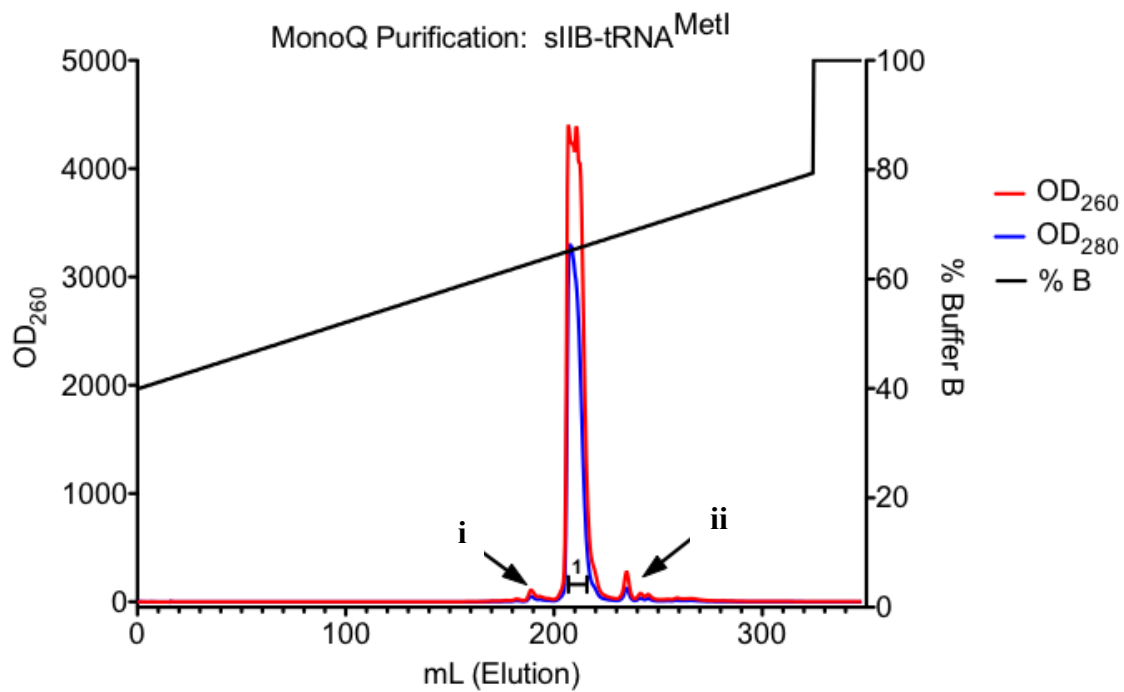


**Figure 42 Elution profile from MonoQ 16/10 purification of IIB-tRNA<sup>Phe</sup>.** The peaks are labeled (i) cellular tRNA, (1) IIB-tRNA<sup>Phe</sup> fractions on 7% native PAGE (Figure 2.30), and (ii) 5S rRNA and higher molecular weight species.

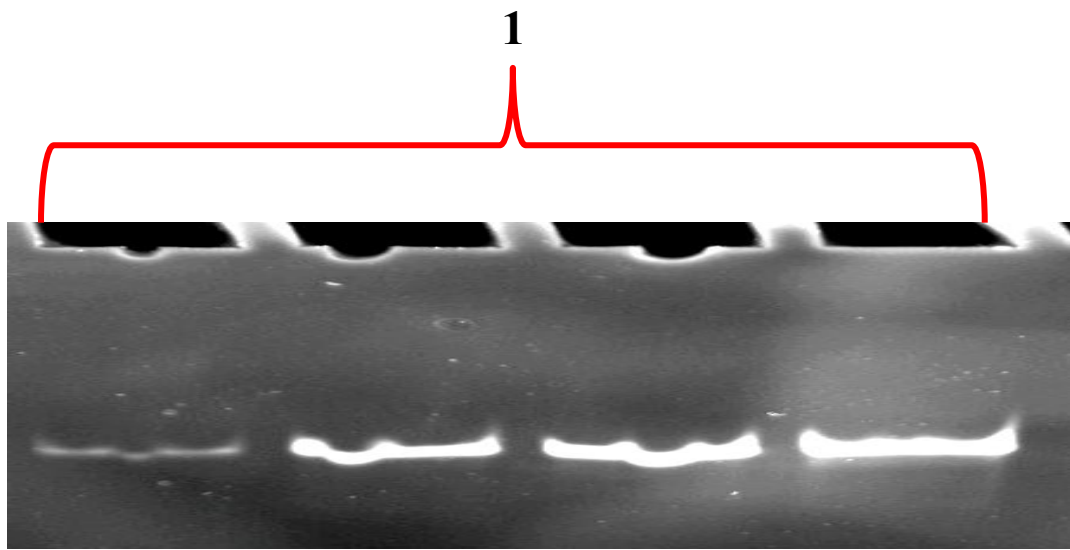


**Figure 43** 7% Native-PAGE of MonoQ purified IIB-tRNA<sup>Phe</sup>. Lanes represent purified IIB-tRNA<sup>Phe</sup> fractions across the peak labeled (1) in Figure 42.

### CHAPTER 3: REV-MEDIATED DIMERIZATION OF RRE RNA

Two separate crystal structures of the Rev dimer have been solved [69,70]. One structure features details of the A:A dimerization interface (Residues L18 and Ile55) and the other features details of the B:B interface (residues L12 and L60). However, the details of the mechanism by which Rev interacts with RRE RNA remain elusive. Gel shift data with Rev bound to sIIB-tRNA<sup>MetI</sup> shows the formation of a discrete Rev:RNA species. SEC, AUC, and SAXS experiments on Rev:sIIB-tRNA<sup>Phe</sup> complexes allowed for the construction of a model by which Rev mediates a dimer of RRE RNA. Using data collected via SEC, AUC-SV, and SAXS experiments, models of the sIIB-tRNA<sup>Phe</sup> monomer as well as a Rev-mediated dimer of sIIB-tRNA<sup>Phe</sup> were constructed. The accuracy of the sIIB-tRNA<sup>Phe</sup> monomer was evidenced by the agreement of the experimental and calculated elution volumes and the fit of the model of the 3D reconstruction using SAXS data.

#### Section 3.1 Gel Shift Analysis: Rev forms a discrete complex with sIIB-tRNA<sup>MetI</sup>

Gel shift experiments were performed on Rev:sIIB-tRNA<sup>MetI</sup> complexes. Stoichiometric amounts of Rev were prepared with sIIB-tRNA<sup>MetI</sup> for separation on 7% native PAGE (Figure 44). The samples were prepared from a Rev stock containing guanidine-HCl, and following dilution of the stock with the RNA, each complex contained ~400 mM guanidine, whose effect on binding of Rev to RNA is unknown. The buffer condition was 200 mM NaCl, 50 mM Tris, 2 mM beta-mercaptoethanol, pH 7.2. The Rev:RNA molar ratios sampled on the gel were 0.25:1, 0.5:1, 0.75:1, 1:1, 1.25:1,

1.50:1, 1.75:1, 2.0:1, 2.5:1, 3.0:1, and 3.5:1. Figure 45 shows the titration series of Rev:sIIB-tRNA<sup>MetI</sup> complexes. As the ratio of Rev:sIIB-tRNA<sup>MetI</sup> increased, the free RNA was depleted with the formation of two more slowly migrating bands, which likely correspond to Rev:RRE complexes. The disparity in migration position of each band may be explained by the number of Revs that bridge the Rev-mediated sIIB-tRNA<sup>Phe</sup> dimer. Alternatively, the upper band may represent a Rev-mediated RNA dimer with the lower band showing multiple Revs bound to a single sIIB-tRNA<sup>Phe</sup>. Interestingly, at a 3:1 molar ratio of Rev:sIIB-tRNA<sup>MetI</sup> there is the formation of single band representing a single Rev:RNA species. At a higher ratios, a complex that did not enter the gel matrix was produced, which may be a Rev/RNA aggregate. Identifying conditions that support formation of a discrete Rev:RNA species was one of our objectives, since such a complex might be expected to crystallize more readily than heterogeneous mixtures. The following sections describe in detail solution biophysical experiments with Rev:sIIB-tRNA<sup>Phe</sup> complexes to determine the nature of the Rev:RRE complex.

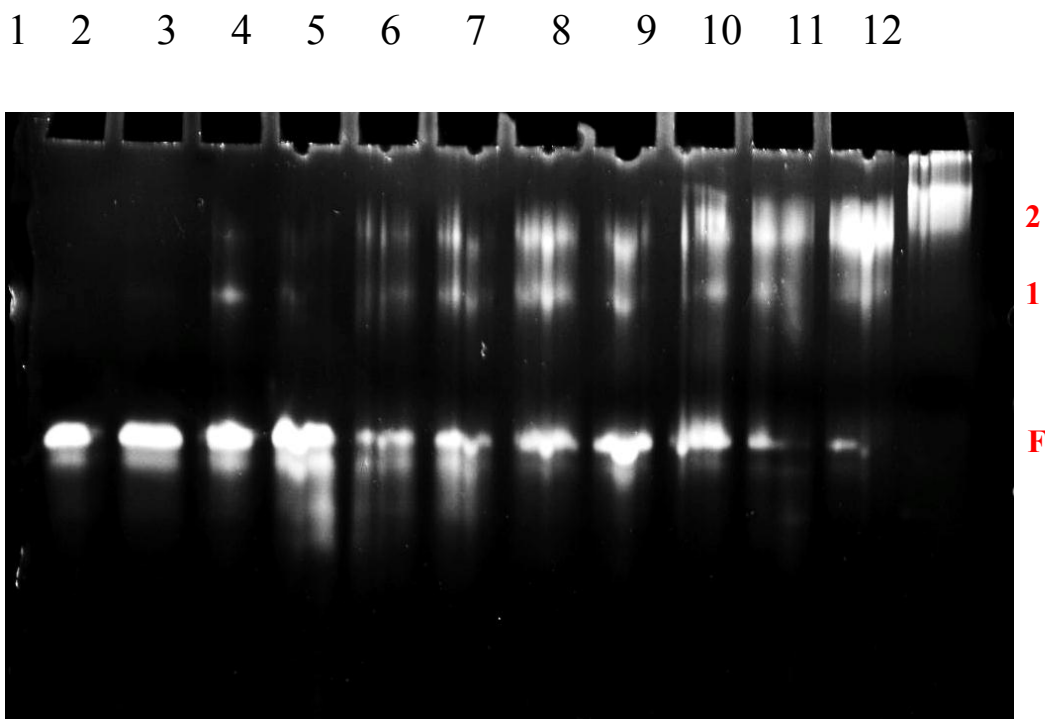


**Figure 44 Gel shift of Rev:sIIB<sup>MetI</sup> complexes.** Lanes: (1) sIIB-tRNA<sup>MetI</sup> (48 picomoles), (2) 0.25 Meq of Rev (12 picomoles), (3) 0.5 Meq, (4) 0.75 Meq, (5) 1.0 Meq, (6) 1.25 Meq, (7) 1.5 Meq, (8) 1.75 Meq, (9) 2.0 Meq, (10) 2.5 Meq, (11) 3.0 Meq, (12) 3.5 Meq. Lanes 1-11 show the formation of higher-order Rev:RNA complexes with increasing molar equivalents of Rev added. **(F)** Free RNA, **(1)** tRNA-sIIB with one Rev bound, **(2)** tRNA-sIIB with two Revs bound. Lane 11 shows a discrete Rev:sIIB-tRNA<sup>MetI</sup>. In lane 12, a majority of the Rev:RNA complex does not enter the gel matrix.

### Section 3.2 Biophysical Measurements on Rev:sIIB-tRNA<sup>Phe</sup> Complexes

This section describes solution biophysical experiments performed on mixtures of sIIB-tRNA<sup>Phe</sup> with Rev (or RevN70) to determine the size and stoichiometry of the complexes formed. The central and most extensive experiments undertaken were a series of size-exclusion chromatography (SEC) analyses of sIIB-tRNA<sup>Phe</sup> alone and complexed with Rev (and RevN70). These experiments explored several different methods of sample

preparation and a variety of final buffer conditions, as well as using Rev molecules labeled in different ways to help assess the protein:RNA relative stoichiometry. Under a set of optimized conditions, analytical ultracentrifugation (AUC) of Rev:sIIB-tRNA<sup>Phe</sup> assemblies was undertaken to identify the absolute number of sIIB-tRNA<sup>Phe</sup> monomers in the complex. Together, the SEC and AUC results indicate that Rev mediates a dimer of sIIB-tRNA<sup>Phe</sup> in solution. Calculated sedimentation properties and column elution positions based on atomic models of sIIB-tRNA<sup>Phe</sup> and its complex with Rev are consistent with the experimental results. Small angle X-ray scattering (SAXS) analysis was used to confirm that our model for the sIIB-tRNA<sup>Phe</sup> monomer matches experiment at low resolution, and preliminary data on the Rev:sIIB-tRNA<sup>Phe</sup> complex are consistent with a dimer of sIIB-tRNA<sup>Phe</sup> that differs somewhat from our current models for the complex. The experimental set-up for each technique was detailed in Chapter 2: Materials and Methods.

### **Section 3.2.1 SEC of sIIB-tRNA<sup>Phe</sup> Monomer and Rev:sIIB-tRNA<sup>Phe</sup> Complexes**

Size-exclusion chromatography (SEC) separates biological macromolecules based upon their hydrodynamic radii, which depend on the volume (or mass) and shape of the species. Accordingly, the technique is useful for determining the oligomeric states of protein-protein, RNA-protein, or DNA-protein assemblies. This section describes SEC experiments performed on sIIB-tRNA<sup>Phe</sup> complexed with Rev, RevN70, and a cysteine-labeled Rev species to determine the size and approximate shape of sIIB-tRNA<sup>Phe</sup> and the Rev:sIIB-tRNA<sup>Phe</sup> complex, as well as the Rev:RNA stoichiometry of the complex. All

complexes were prepared as described in the protocol in Chapter 2: Materials and Methods.

Gel filtration experiments were carried out using a Shodex KW803 column calibrated with Blue Dextran (2 MDa), Aldolase (161 kDa), tRNA<sup>Phe</sup> (25 kDa), Lysozyme (14.5 kDa), and Tyrosine (181.19 Da) (Figure 45). The excluded volume was determined to be 5.9 mL (Blue Dextran), and the included volume is 12.7 mL (Tyrosine). The calibration performed in our laboratory closely matches the calibration curve published by the manufacturer for use with this column.

Following calibration of the Shodex KW803 column, Rev was mixed with the phenylalanyl tRNA (Yeast) at different Rev:RNA molar ratios and RNA concentrations as a control to determine if Rev interacts with the tRNA scaffold at these concentrations. The running buffer composition was 200 mM NaCl, 100  $\mu$ M MgCl, 50 mM Tris, 2 mM beta-mercaptoethanol, pH 7.2. At 0.5  $\mu$ M tRNA<sup>Phe</sup>, Rev did not bind the tRNA at any tested molar ratios (Figure 46): the elution of the tRNA<sup>Phe</sup> monomer at 9.1 ml is unperturbed, and no RNA elutes at an earlier position. Curiously, at increasing Rev:tRNA<sup>Phe</sup> molar ratios, the  $A_{260}$  decreased monotonically. This may be due to the RNA interacting with Rev which is nonspecifically bound to the column matrix. At [tRNA<sup>Phe</sup>] = 5  $\mu$ M, Rev formed multiple higher-order species at all Rev:tRNA<sup>Phe</sup> ratios, indicative of nonspecific binding to the scaffold (Figure 47). At a 1:1 Rev:RNA, peaks at 6.5 and 8.0 mL appeared and became more apparent as the Rev:RNA molar ratio increased. The elution peak at 8.0 mL may represent increasing numbers of Rev bound

to a single RNA. The trailing 6.5 mL peak may represent Rev:RNA aggregates containing more than one RNA. Conversely, at a  $[sIIB-tRNA^{Phe}] = 0.5 \mu M$  the Rev:sIIB-tRNA<sup>Phe</sup> species eluted as a discrete species at 6.9 mL (Figure 49). The 6.9 mL species represented a large complex which elutes as a 600 kDa spherical RNA. The remainder of this section describes the behavior of Rev:sIIB-tRNA<sup>Phe</sup> complexes on the Shodex KW803 column.

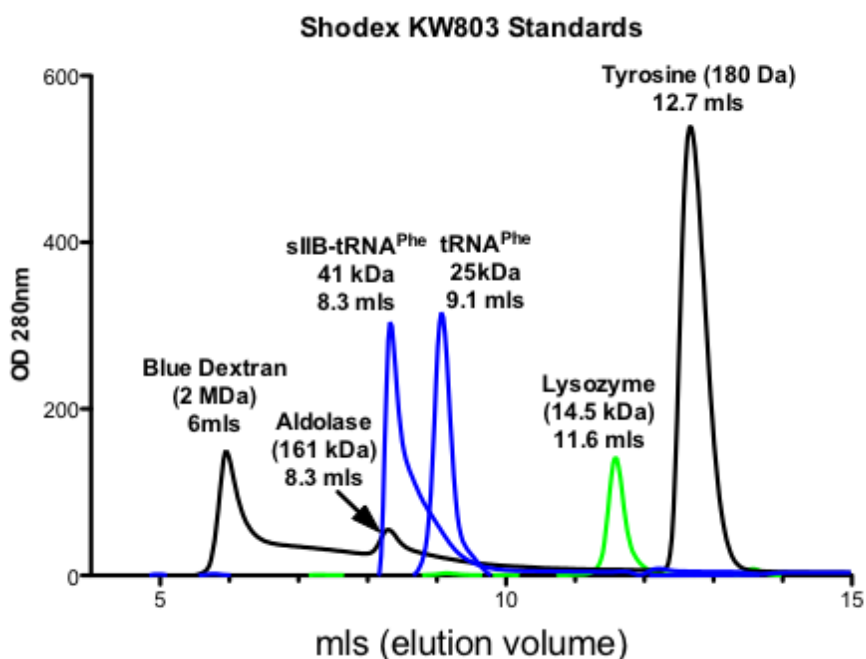


**Figure 45 Standards for Shodex KW803 size-exclusion column.** The excluded volume for the column is 6 mL. The Blue Dextran (2 MDa) and Aldolase (161 kDa) markers were loaded together and eluted at 6 mL and 8.3 mL, respectively. sIIB-tRNA<sup>Phe</sup> and tRNA<sup>Phe</sup> elute at 8.3 mL and 9.1 mL, respectively. Lysozyme eluted at 11.6 mL. Tyrosine eluted at 12.7 mL and represents the included volume of the column.

SEC: tRNA<sup>Phe</sup> (baker's Yeast):Rev Complexes

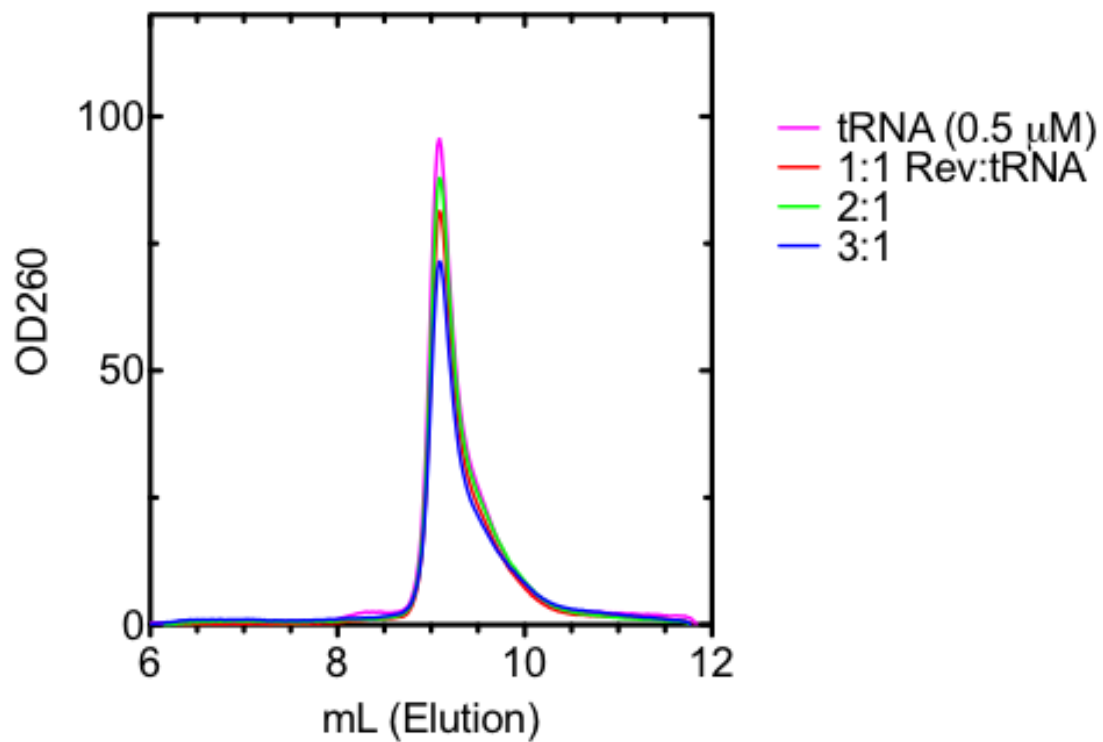


**Figure 46 SEC elution profiles of Rev:tRNA<sup>Phe</sup>.** At [tRNA<sup>Phe</sup>] = 0.5 μM, Rev did not bind to the tRNA<sup>Phe</sup> at Rev:RNA ratios of 1:1, 1:2, 1:3, or 1:4.

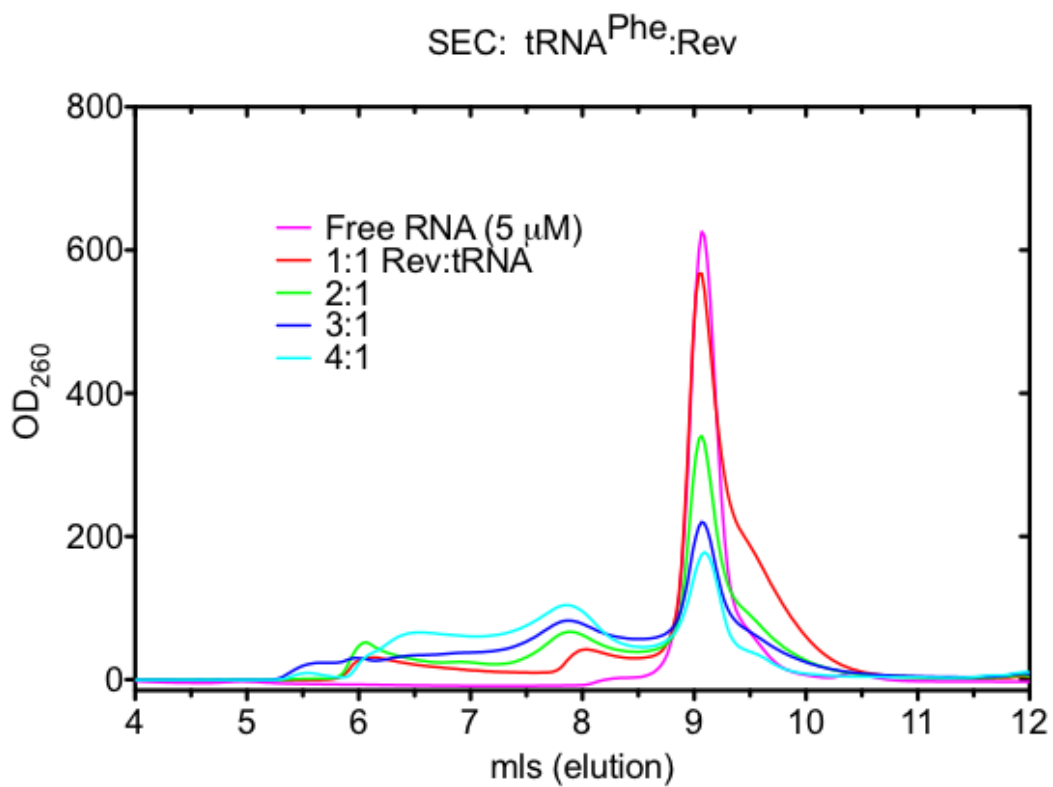


**Figure 47 SEC elution profiles of Rev:tRNA<sup>Phe</sup>.** At a [tRNA<sup>Phe</sup>] = 5  $\mu$ M, Rev formed multiple higher-order complexes with tRNA<sup>Phe</sup>. This indicated nonspecific binding of Rev to scaffold RNA.

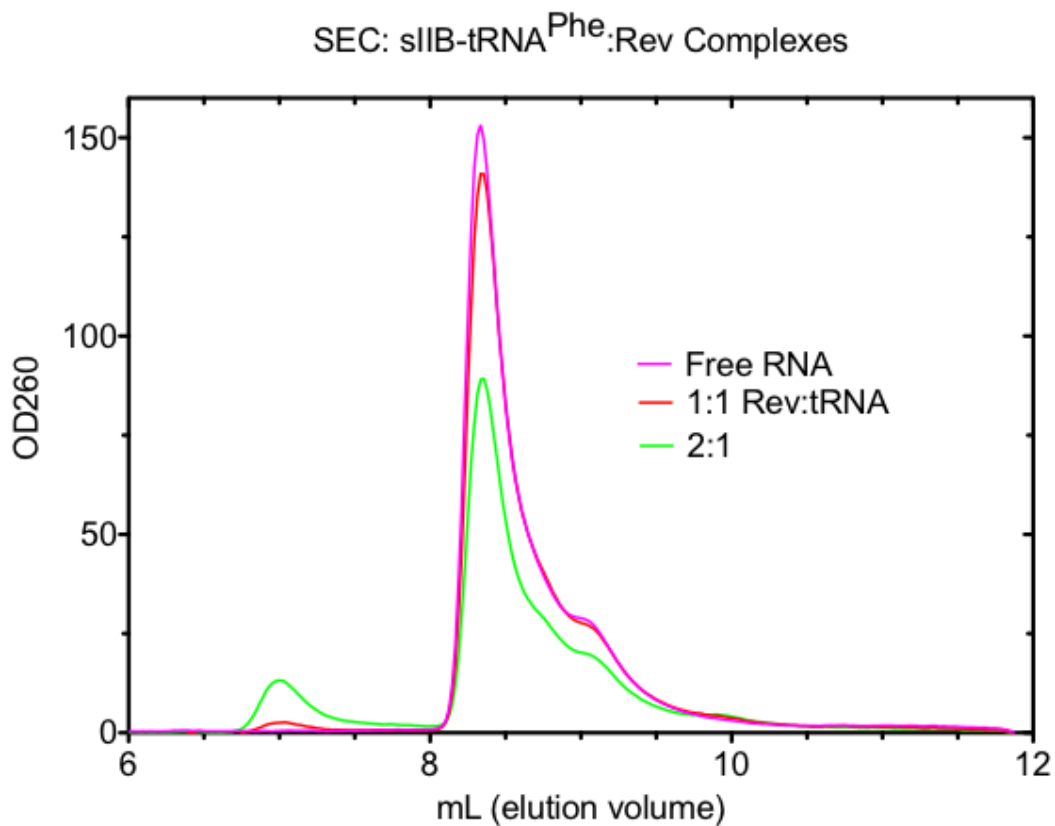


**Figure 48 SEC elution profiles of Rev:sIIB-tRNA<sup>Phe</sup>.** At [sIIB-tRNA<sup>Phe</sup>] = 0.5  $\mu$ M, Rev formed a discrete species with sIIB-tRNA<sup>Phe</sup> which eluted at 6.9 mL. The sIIB-tRNA<sup>Phe</sup> monomer eluted at 8.23 mL.

### Section 3.2.1.1 SEC of Purified sIIB-tRNA<sup>Phe</sup>

The sIIB-tRNA<sup>Phe</sup> monomer has a molecular weight of 40.31 kDa but its elution volume is 8.23 mL ( $\pm$  0.017 mL) which is equivalent to the elution position a spherical RNA with a mass of 183 kDa (Figure 49). The remarkable contrast in the elution volumes indicate that the RNA is eluting as an oligomer or as a monomer with a highly elongated shape. Section 3.2.3 shows atomic models of sIIB-tRNA<sup>Phe</sup>.

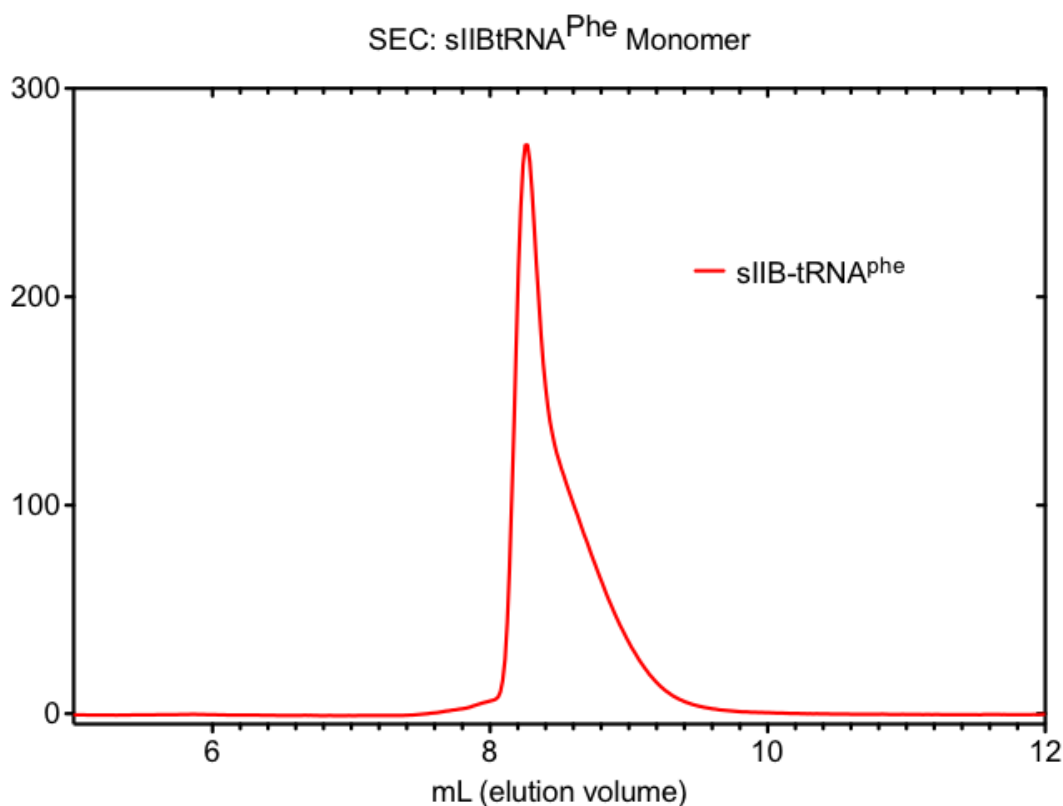


**Figure 49** Shodex KW803 elution profile of purified sIIB-tRNA<sup>Phe</sup>, [RNA] = 5  $\mu$ M. sIIB-tRNA<sup>Phe</sup> elutes at 8.23 mL, equivalent to a spherical RNA with a mass of 183 kDa.

### Section 3.2.1.2 SEC of Rev:sIIB-tRNA<sup>Phe</sup> Complexes

The Rev:sIIB-tRNA<sup>Phe</sup> complex elutes from the Shodex KW803 column as discrete species at 6.9 mL ( $\pm$  0.023 mL) at all Rev:sIIB-tRNA<sup>Phe</sup> ratios at both [RNA] = 0.5  $\mu$ M and 5.0  $\mu$ M. The position of the Rev:sIIB-tRNA<sup>Phe</sup> complex at 6.9 mL is equivalent to the elution position of a spherical protein of 400 kDa or a spherical RNA with a mass of 600 kDa. The molecular weight markers are given in Figure 45. As the molar ratio of Rev:sIIB-tRNA<sup>Phe</sup> was increased there was more observable complex with less unbound, monomeric sIIB- tRNA<sup>Phe</sup> (Figure 50). At a Rev:RNA ratio of 4:1, all of the sIIB-tRNA<sup>Phe</sup> was complexed with Rev forming a Rev:RNA species (Figure 51).

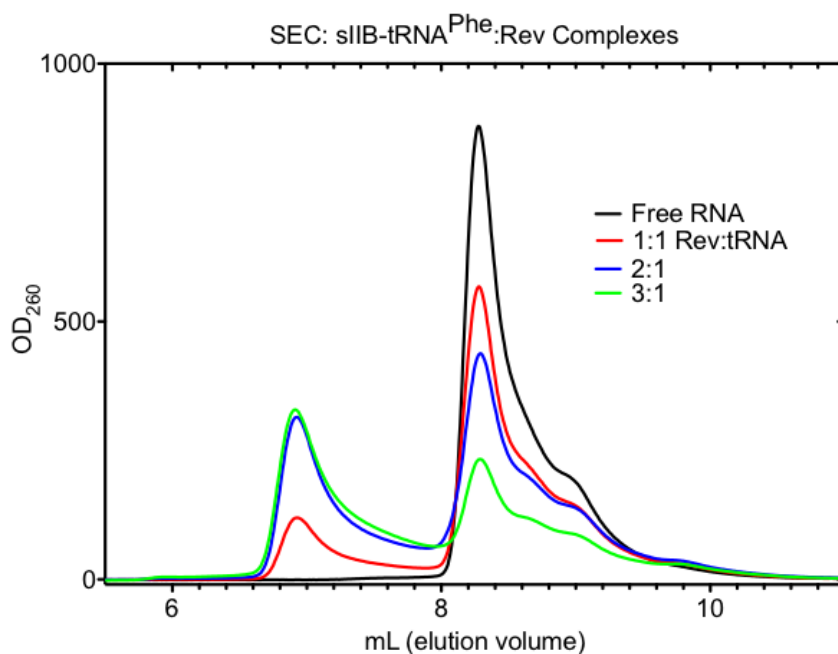


**Figure 50 Shodex KW803 elution profiles of Rev:sIIB-tRNA<sup>Phe</sup>, [RNA] = 5  $\mu$ M.** Increasing the molar equivalents of Rev results in more of the Rev:sIIB-tRNA<sup>Phe</sup> complex as observed at the elution position of 6.9 mL.

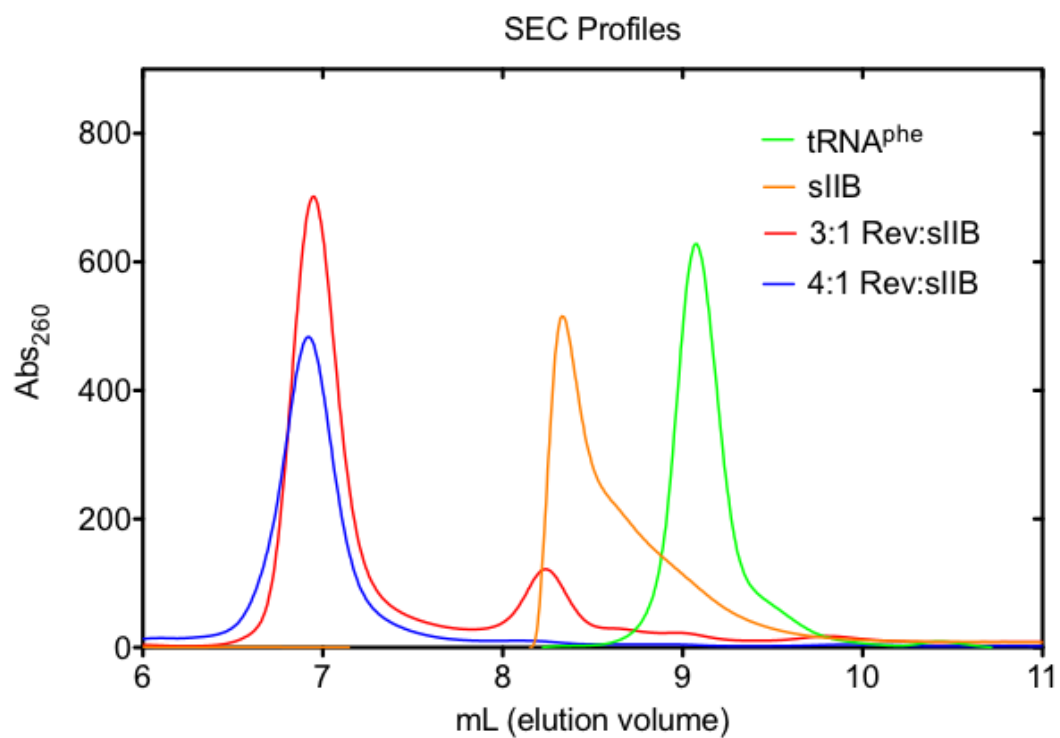


**Figure 51 SEC Elution profiles complexed sIIB-tRNA<sup>Phe</sup>, [RNA] = 5  $\mu$ M.** At a Rev:sIIB-tRNA<sup>Phe</sup> of 4:1 all of the RNA is complexed with Rev elution at 6.9 mL (red). Elution position of a 3:1, Rev:RNA complex (red). Elution position (8.23 mL) of sIIB-tRNA<sup>Phe</sup> monomer (orange). Elution position (9.1 mL) of phenylalanyl tRNA (Yeast) (green).

### Section 3.2.1.3 SEC of RevN70:sIIB-tRNA<sup>Phe</sup> Complexes

C-terminal residues of Rev have are important for RRE binding. Rev:RRE gel shift experiments demonstrated that the removal of C-terminal residues perturb binding to the RRE which may explain the aberrant binding behavior of RevN70 [67]. The C-terminal truncation of Rev complexed with RRE RNA migrated faster than full-length Rev:RRE complexes indicating a smaller Rev:RNA complex. This property of a C-terminal truncation of Rev was confirmed in the SEC data collected on RevN70:sIIB-tRNA<sup>Phe</sup> complexes. The RevN70 did bind to sIIB-tRNA<sup>Phe</sup>, however, the complexes eluted very differently than Rev:sIIB-tRNA<sup>Phe</sup> complexes. The data show that the Rev:sIIB-tRNA<sup>Phe</sup> complexes eluted at 6.9 mL, much earlier than the RevN70:sIIB-tRNA<sup>Phe</sup> which eluted at 8.1 mL (Figure 52). The error of  $\pm 0.017$  shows that the elution position of the RevN70:sIIB-tRNA<sup>Phe</sup> is significantly different from that of the sIIB-tRNA<sup>Phe</sup> monomer which elutes at 8.28 mL. This may be due to RevN70 being unable to self-assemble or the protein is unable to mediate an oligomer of RNA as is proposed in this work. The role of the C-terminus in RRE binding and assembly is not well understood.

\

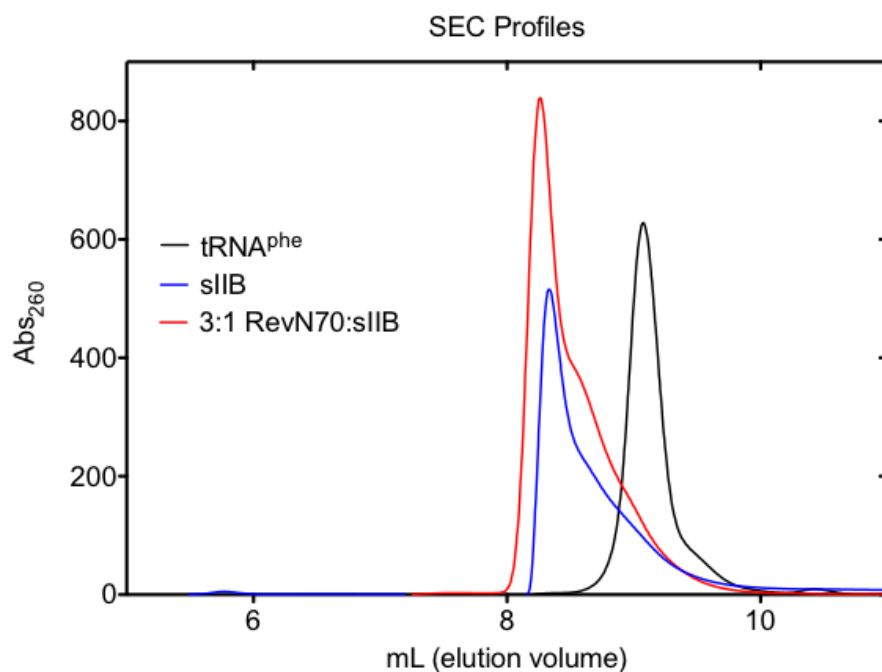


**Figure 52 SEC Elution RevN70 complexed sIIB-tRNA<sup>Phe</sup>, [RNA] = 5 μM.** Removal of C-terminal residues (71-116) disrupts the assembly of Rev onto RRE RNA as evidenced by the elution of the RevN70:sIIB-tRNA<sup>Phe</sup> complex (red) at 8.13 mL. The sIIB-tRNA<sup>Phe</sup> monomer elutes at 8.23 mL (blue) with tRNAPhe eluting at 9.1 mL (black).

#### Section 3.2.1.4 SEC of Rev<sup>Fluo</sup>:sIIB-tRNA<sup>Phe</sup> Complexes

In order to confirm that the Rev:sIIB-tRNA<sup>Phe</sup> complex contained Rev the protein was labeled with iodoacetamido-fluorescein at cysteines 87 and 91 (Rev<sup>Fluo</sup>). Mass spectrometry was performed on Rev<sup>Fluo</sup>. It was determined that 50% was labeled at a single cysteine and 50% labeled at both cysteines. Rev<sup>Fluo</sup>-sIIB-tRNA<sup>Phe</sup> complexes were mixed at 1:1, 2:1, and 3:1 molar ratios and resolved on the Shodex column with UV detection at 260 nm, 280 nm, and 495 nm (Figure 53). In Figure 57, only the A<sub>260</sub> is shown. The elution peak at 6.9 mL was the only peak which contained absorbance at 495 nm indicating the presence of Rev (Figure 54). The elution position of the sIIB-tRNA<sup>Phe</sup> monomer at 8.3 mL did not contain any 495 nm absorbance with the [RNA] = 5 μM (Figure 58). The 495 nm/260 nm ratios across the 6.9 ml peak at Rev:RNA ratios of 2:1 and 3:1 indicates a stoichiometry of ~1.5:1 Rev:RNA (Figure 55). This stoichiometry measurement may be distorted, however, because modification of the cysteine residues affected the amount of complex produced (although not the elution position of the complex). The labeled complexes may be disassembling more readily as they elute through the column compared to the unlabeled complex. To determine if the peak observed at 6.98 mL position represented a discrete Rev:RNA species was not the result of complex disassembly, 1 μM Rev was added to the running buffer (Figure 56). The running buffer composition was 200 mM NaCl, 100 μM MgCl<sub>2</sub>, 2 mM β-mercaptoethanol, 50 mM Tris, 1 μM Rev, pH 7.2. The peak observed at 6.98 mL suggested the formation of a Rev:sIIB-tRNA<sup>Phe</sup> complex with no “free” monomer.

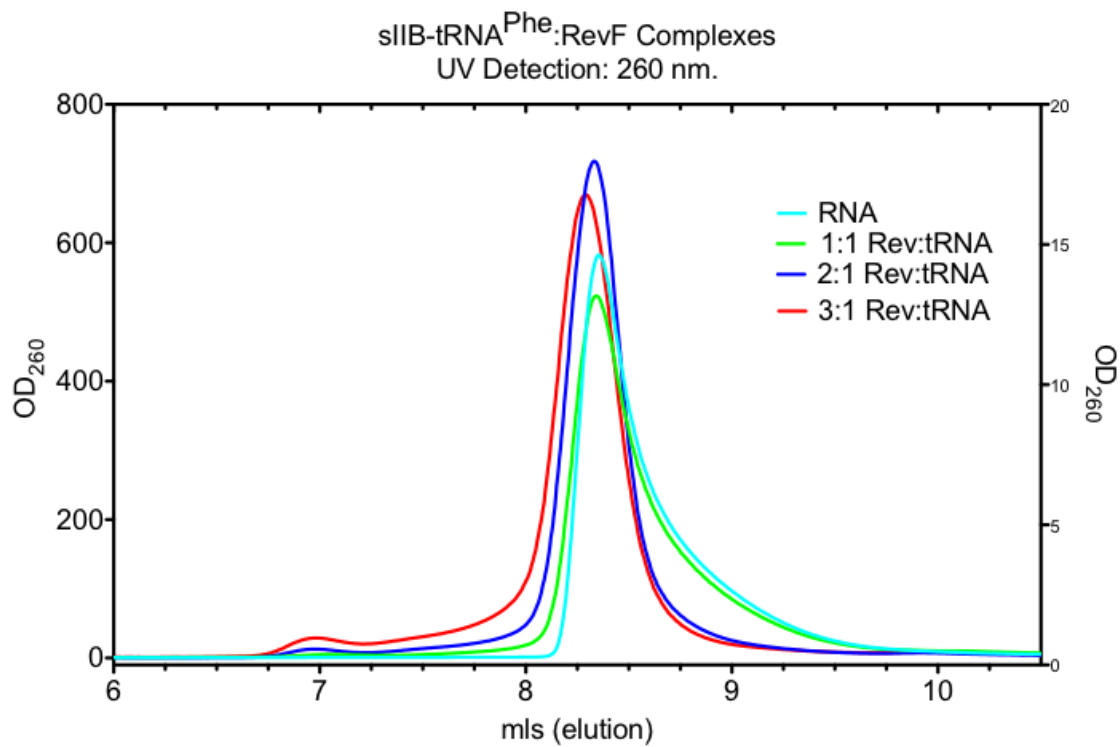


**Figure 53 SEC Elution profiles of Rev<sup>Fluor</sup>:sIIB-tRNA<sup>Phe</sup>.** The modification of cysteines (residues 87 and 91) with fluorescein perturbed the formation of Rev:RNA complexes observed at 6.9 mL.

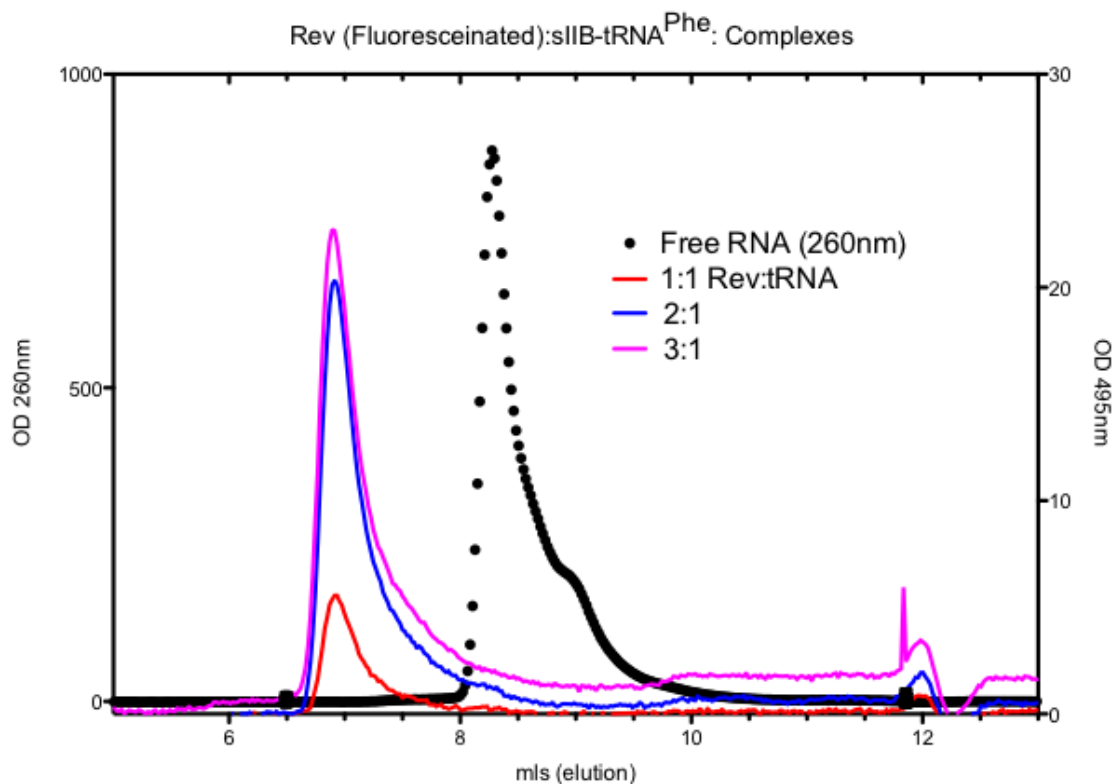


**Figure 54 SEC Elution profiles of Rev<sup>Fluo</sup>:sIIB-tRNA<sup>Phe</sup> showing 495 nm absorbance of complexes and 260 nm absorbance of the sIIB-tRNA<sup>Phe</sup> Monomer, [RNA] = 5  $\mu$ M. As evidenced by UV absorbance at 495 nm, all of the fluorescein-labeled Rev is contained in the Rev:sIIB-tRNA<sup>Phe</sup> complex observed at 6.9 mL. The sIIB-tRNA<sup>Phe</sup> monomer elutes at 8.23 mL.**

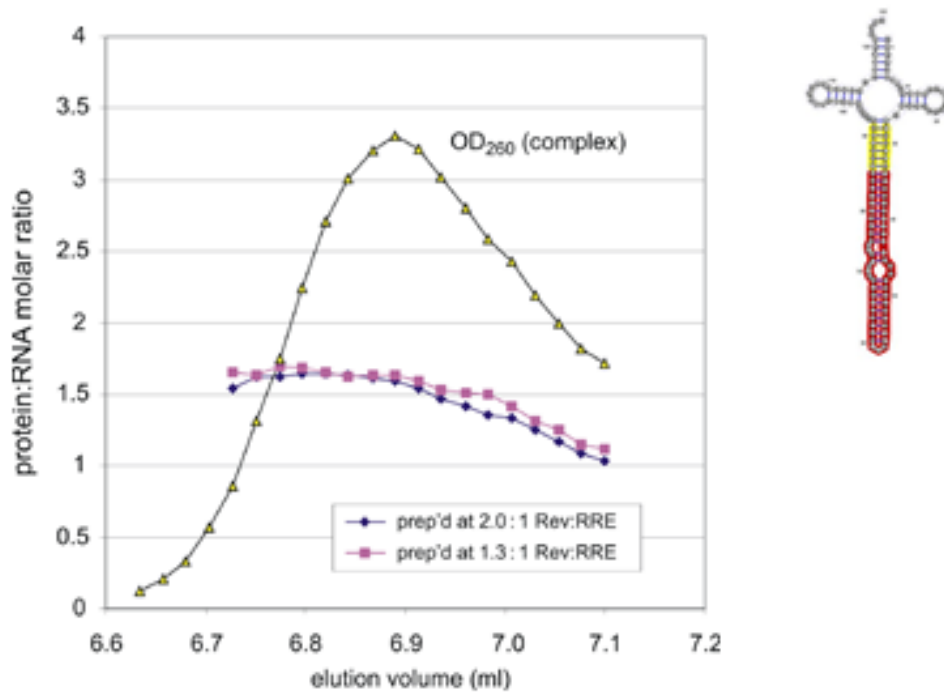


**Figure 55** 495 nm absorbance across the Rev<sup>Fluor</sup>:sIIB-tRNA<sup>Phe</sup> complex peak (6.9 mL). The 495 nM absorbance across the complex peak may indicate that the complexes are disassembling as they elute through the column. Integration of the 495 nm/260 nm absorbances reveal that the stoichiometry of the 2:1 and 3:1, Rev:RNA, complexes is ~1.5:1 or 3:2, Rev:RNA. This is indicative of a Rev-mediated dimer.

The hydrodynamic properties of the RNA change drastically following binding to Rev as evidenced by the elution position of the Rev:sIIB-tRNA<sup>Phe</sup> complex at 6.98 mL and has a large hydrodynamic radius. Interestingly, the elution position at 6.9 ml does not change at different Rev:RNA molar ratios suggesting that while additional Rev may help to cooperatively bridge a RNA dimer, the overall size of the complex varies little. The SEC data collected on Rev<sup>Fluo</sup>:sIIB-tRNA<sup>Phe</sup> complexes prove that the protein is present only in the complex peak eluting at 6.98 ml at [RNA] = 5 μM. It is likely that Rev initially binds the RNA as a dimer followed by the second RNA binding to the free ARM sequence of the second monomer. Alternatively, Rev may bind as a monomer to sIIB-tRNA<sup>Phe</sup> followed the cooperative dimerization of Rev to mediate the RNA dimer or higher order oligomer. In contrast, removing C-terminal residues 71-116 from Rev (RevN70) does not prevent binding to the RNA but does not support the higher order assembly observed for wild-type Rev:sIIB-tRNA<sup>Phe</sup>. The RevN70:sIIB-tRNA<sup>Phe</sup> complex eluted at 8.1 mL whereas the sIIB-tRNA<sup>Phe</sup> elutes at 8.23 mL.

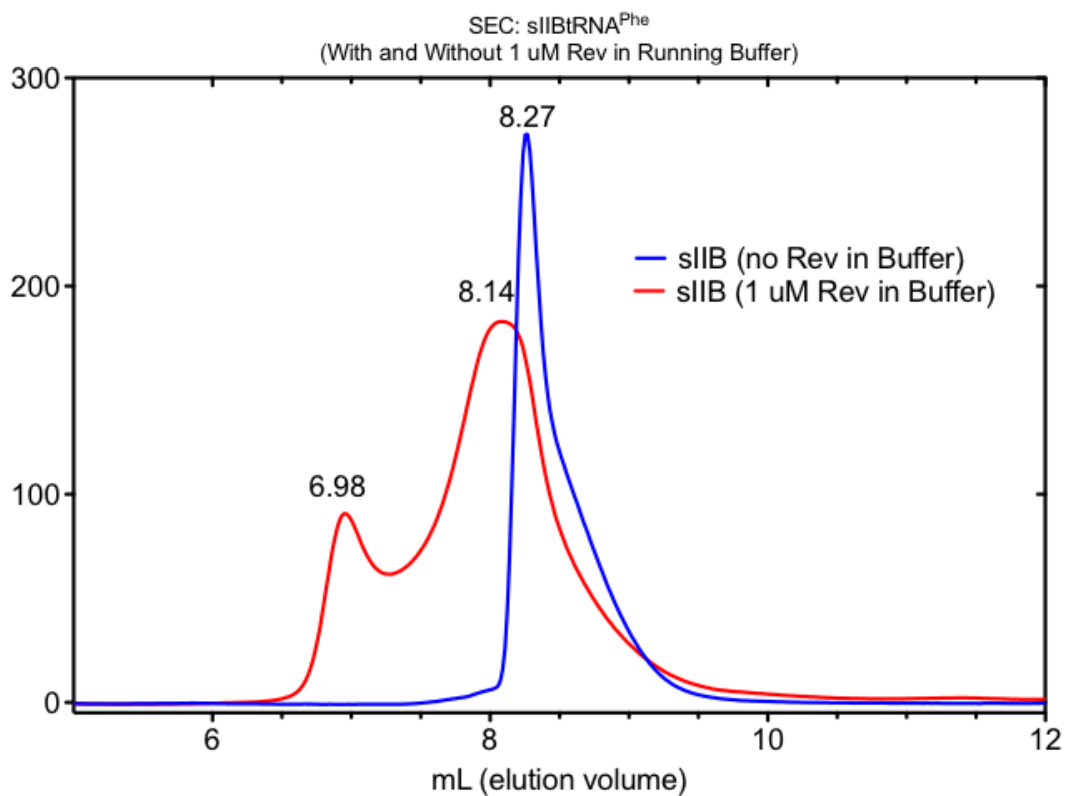


**Figure 56 SEC Elution profiles of sIIB-tRNA<sup>Phe</sup> monomer in the presence of 1  $\mu$ M Rev in elution buffer (Red) compared with sIIB-tRNA<sup>Phe</sup> monomer under normal buffer conditions (Blue), [RNA] = 5  $\mu$ M. The elution of the sIIB-tRNA<sup>Phe</sup> monomer in the presence of 1  $\mu$ M Rev in the elution buffer shows the binding of monomeric or dimeric Rev binding to the RNA at 8.14 mL and the formation of a Rev:sIIB-tRNA<sup>Phe</sup> complex eluting at 6.9 mL.**

### Section 3.2.2 Analytical Ultracentrifugation: sIIB-tRNA<sup>Phe</sup> and Rev:sIIB-tRNA<sup>Phe</sup> Complexes

Analytical ultra-centrifugation (AUC) reports on the shape, mass, and size-distribution of macromolecules in solution. One advantage of this technique is being able to observe the oligomeric state of macromolecular assemblies under native solvent conditions. During a sedimentation velocity AUC experiment, a macromolecular solution is subjected to a centrifugal field, and the rate at which the macromolecules sediment is detected optically to determine the S-value, which can be used (in the Svedberg equation) to extract information about the volume and shape of the species if its density is known.

$$S = \frac{u}{\omega^2 r} = \frac{M(1 - \bar{v}\rho)}{N_A f} = \frac{MD(1 - \bar{v}\rho)}{RT} \quad \text{Equation 1}$$

The variables of the Svedberg equation are  $u$ , which is the observed radial velocity of the macromolecule,  $\omega$ , the angular velocity of the rotor,  $\omega r$ , the centrifugal field,  $M$ , the molar mass,  $\bar{v}$ , the partial specific volume of the molecule,  $\rho$ , the density of the solvent,  $N_A$ , Avogadro's number,  $f$ , the frictional coefficient,  $D$ , the diffusion coefficient, and  $R$ , the universal gas constant.

Analytical ultracentrifugation (AUC) was used to determine the size, shape, and hydrodynamic properties of monomeric sIIB RNA and of the Rev:RNA complexes. To observe the effect of  $[\text{Mg}^{2+}]$  on the sedimentation rate of the sIIB-tRNA<sup>Phe</sup> monomer, the

RNA was prepared at 100  $\mu\text{M}$  (or 5 mM)  $\text{MgCl}_2$  in 200 mM NaCl, 40 mM Tris, pH 7.2, and 2 mM  $\beta$ -mercaptoethanol. The experiments were carried out on XL-A Analytical Ultracentrifuge (Beckman-Coulter®) at room temperature in a An-60Ti rotor with 2-channel centerpiece cells.

The sIIB-tRNA<sup>Phe</sup> sediments at 4.8S at  $[\text{Mg}^{2+}] = 100 \mu\text{M}$  and 5 mM (Figure 57). Following the determination of the sedimentation rates, SEDFIT was used to determine the possible composition(s) of the 4.8S species (Figure 58). Equation 1 shows that the observed sedimentation rate  $s$  depends on the values of  $M$ ,  $\bar{v}$ , and  $f$ , so we calculate the  $f$  that would result for different possible species whose mass and  $\bar{v}$  we can estimate, given that protein partial specific volume is  $\sim 0.73$  and RNA partial specific volume is  $\sim 0.53$ - $0.55$  [92,93,94]. The calculated value of  $f$  tells us about the shape that the species would need to adopt to sediment at the observed value of  $S$ .

Fixed parameters for the SEDFIT calculation representing the monomer are molar mass ( $M$ ) = 40.31 kDa and solvent density ( $\rho$ ) = 1.008 g/ml. For partial specific volume  $\bar{v} = 0.53$  (or 0.55), the calculated frictional ratio for the monomer was  $f/f_0 = 1.69$  (or 1.60). Therefore, if the species in the centrifuge is an RNA monomer, it must be very non-spherical, since these frictional ratios would correspond to prolate ellipsoids of axial ratio  $a/b = 8.34$  (or 7.07). If, on the other hand, we assume that sIIB-tRNA<sup>Phe</sup> is dimeric, then for a mass of 80.62 kDa and  $\bar{v} = 0.53$ , the frictional ratio  $f/f_0$  must be 2.68, which would correspond to an axial ratio  $a/b = 28.47$ . This axial ratio is unrealistic, so the assumption of dimerization is shown to be unreasonable, and we conclude that the 4.8S

species is monomeric sIIB-tRNA<sup>Phe</sup>, which must adopt a shape that deviates considerably from that of a sphere. Combining these findings with conclusions from SEC data are consistent with the RNA being cylindrical and oblong in shape. Subsequently, Rev:sIIB-tRNA<sup>Phe</sup> mixtures were analyzed by AUC. Complexes were prepared at 5  $\mu$ M RNA at Rev:RNA molar ratios of 1:1, 2:1, and 3:1. The mixtures were dialyzed overnight into 200 mM NaCl, 100  $\mu$ M MgCl<sub>2</sub>, 50 mM Tris, 2 mM  $\beta$ -mercaptoethanol, pH 7.2. Two species were detected: the 4.8S species, which likely corresponds to the sIIB-tRNA<sup>Phe</sup> monomer, and a second species that sediments more rapidly at 9.8S, which we infer corresponds to a Rev:RNA complex (Figure 58). Both of these species were observed at 1:1, 2:1, and 3:1 Rev:RNA ratios. To determine the compositions consistent with the 9.8S species, we calculated frictional ratios ( $f/f_0$ ) for complexes containing different numbers of RNA and Rev monomers. Complexes containing a single sIIB-tRNA<sup>Phe</sup> give  $f/f_0$  values (and corresponding axial ratios) that are not physically realistic unless bound to more than a dozen equivalents of Rev. Since more than half the RNA sediments as complex at a 3:1 Rev:RNA ratio, we conclude that the complex must contain more than one copy of sIIB-tRNA<sup>Phe</sup>. Complexes containing two RNAs and from zero to ten equivalents of Rev produce results that are consistent with 9.8S and are physically possible. The top portion of (Table 1) gives molecular weights for two RNAs with increasing equivalents of Rev (2, 4, 6, and 8 Revs). The bottom part of the table gives calculations for  $\bar{v}$ , hydrodynamic radius, hydration radius, density, frictional ratios, and

axial ratios. From these calculations, it is reasonable to conclude that the 9.8S species is a Rev-mediated sIIB-tRNA<sup>Phe</sup> dimer, however, the Rev stoichiometry is not clear.

# of tRNA	# of Rev	#tRNA*MW* $\bar{v}$	#Rev*MW* $\bar{v}$	MW of Complex		$\bar{v}$ Result	MW tRNA	MW Rev
2	2	42.7286	19.232304	107.14	53.57	0.578317	40.31	13.26
2	4	42.7286	38.464608	133.66	66.83	0.607461	<u>RNA <math>\bar{v}</math></u>	<u>Rev <math>\bar{v}</math></u>
2	6	42.7286	57.696912	160.18	80.09	0.626954	0.53	0.7252
2	8	42.7286	76.929216	186.7	93.35	0.64091		
2	10	42.7286	96.16152	213.22	106.61	0.651393		
2	12	42.7286	115.393824	239.74	119.87	0.659558		
2	14	42.7286	134.626128	266.26	133.13	0.666096		
2	16	42.7286	153.858432	292.78	146.39	0.67145		
2	18	42.7286	173.090736	319.3	159.65	0.675914		
2	20	42.7286	192.32304	345.82	172.91	0.679694		
# of tRNA	# Num of Rev	$\bar{v}$ Result	rh	rO	D	f/f0	a/b prolate	a/b oblate
2	2	0.578317192	3.99	2.91	5.38E-07	1.37	4.42	4.16
		0.607460781	3.72	2.96	5.77E-07	1.26	2.9	2.8
		0.626954127	3.51	2.99	6.11E-07	1.18	1.82	1.79
		0.640909566	3.38	3.01	6.35E-07	1.12	0	0
		0.65139349	3.28	3.03	6.52E-07	1.09	0	0
		0.659557954	3.21	3.04	6.69E-07	1.05	0	0
		0.666096026	3.14	3.05	6.83E-07	1.03	0	0
		0.671449662	3.09	3.06	6.93E-07	1.01	0	0
		0.675913987	3.05	3.06	7.05E-07	0.99	0	0
		0.679693598	3.01	3.07	7.13E-07	0.98	0	0
2	4	0.578317192	4.98	3.13	4.31E-07	1.59	7.86	7.11
		0.607460781	4.63	3.18	4.64E-07	1.46	5.77	5.33
		0.626954127	4.38	3.21	4.89E-07	1.36	4.47	4.2
		0.640909566	4.21	3.24	5.09E-07	1.3	3.62	3.44
		0.65139349	4.09	3.26	5.24E-07	1.26	3.03	2.92
		0.659557954	4	3.27	5.37E-07	1.22	2.57	2.49
		0.666096026	3.91	3.28	5.49E-07	1.19	2.16	2.11
		0.671449662	3.85	3.29	5.57E-07	1.17	1.86	1.83
		0.675913987	3.79	3.3	5.66E-07	1.15	1.52	1.5
		0.679693598	3.75	3.3	5.73E-07	1.13	1.18	1.18
2	6	0.578317192	5.97	3.32	3.60E-07	1.8	11.6	10.29
		0.607460781	5.54	3.38	3.88E-07	1.64	8.85	7.96
		0.626954127	5.25	3.41	4.08E-07	1.54	7.21	6.56
		0.640909566	5.05	3.44	4.25E-07	1.47	6.11	5.62
		0.65139349	4.91	3.46	4.37E-07	1.42	5.37	4.99
		0.659557954	4.78	3.47	4.49E-07	1.38	4.76	4.46
		0.666096026	4.8	3.48	4.47E-07	1.38	4.82	4.51
		0.671449662	4.61	3.49	4.65E-07	1.32	3.99	3.77
		0.675913987	4.54	3.5	4.72E-07	1.3	3.67	3.49
		0.679693598	4.49	3.51	4.78E-07	1.28	3.42	3.27
2	8	0.578317192	6.95	3.5	3.09E-07	1.99	15.56	13.69
		0.607460781	6.46	3.55	3.32E-07	1.82	12.24	10.84

$\bar{v}$  = partial specific volume

rh = hydrodynamic radius

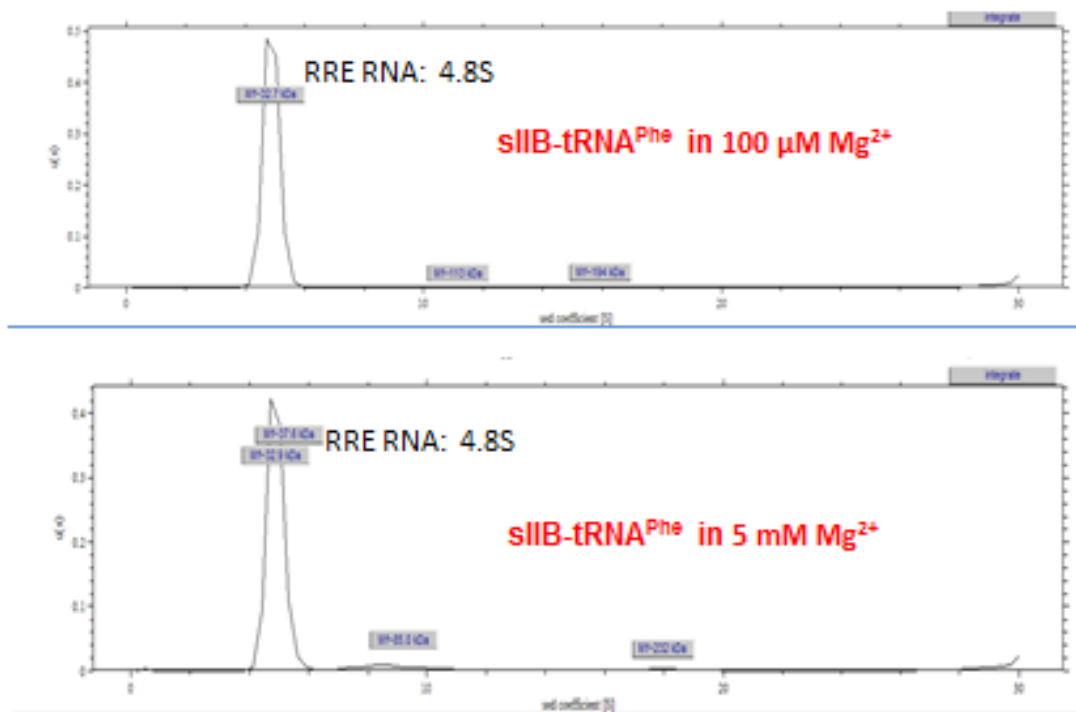
rO = radius of molecule

D = solvent density

f/f0 = frictional ratio

a/b = axial ratio

**Table 1** Calculated analytical ultracentrifugation parameters for Rev:sIIB-tRNA<sup>Phe</sup> Complexes using SEDFIT



42

**Figure 57 S-values extracted from SV-AUC data for the sIIB-tRNA<sup>Phe</sup> monomer in 100 μM and 5 mM MgCl<sub>2</sub>.** The monomeric sIIB-tRNA<sup>Phe</sup> sedimented with a value of 4.8S in 200 mM NaCl, 50 mM Tris, 2 mM beta-mercaptoethanol, pH 7.2 at [Mg<sup>2+</sup>] = 100 μM and 5 mM.

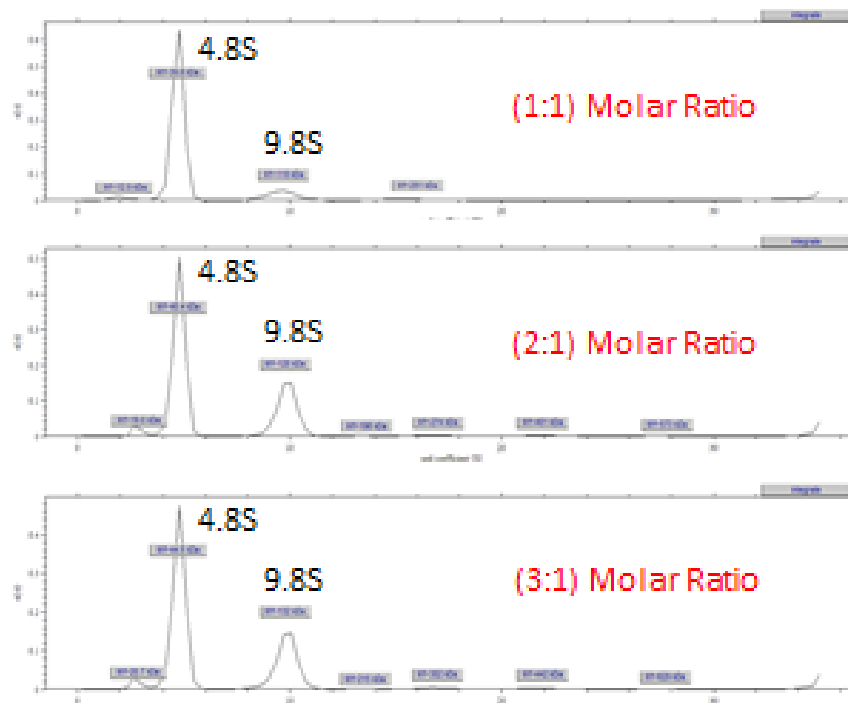


**Figure 58 S-values extracted from SV-AUC data for Rev/sIIB-tRNA<sup>Phe</sup> mixtures.** Monomeric or unbound sIIB-tRNA<sup>Phe</sup> sedimented at a value of 4.8S. The Rev: sIIB-tRNA<sup>Phe</sup> sedimented with a value of 9.8S.

### Section 3.2.3 Modeling of the sIIB-tRNA<sup>Phe</sup> Monomer

Estimating the masses and partial specific volumes of Rev:RNA complexes of different stoichiometries enable us to define a range of compositions that are consistent with the experimental  $S$  value from AUC (see previous section), but with information about the frictional ratio ( $f/f_0$ ) of the complex, which depends on shape, we could extract definitive compositions from the AUC data. Information about the shape of the complex is contained in the elution volume of the complex from a calibrated SEC column, which yields the hydrodynamic radius ( $r_h$ ). A given frictional ratio or hydrodynamic radius is consistent with many possible structures: these values do not uniquely define a shape. But the structure of a macromolecule (or assembly) does uniquely determine a frictional ratio and hydrodynamic radius, which can be computed from the atomic coordinates [95]. Indeed, the sedimentation coefficient calculated from the yeast tRNA<sup>Phe</sup> structure closely matches the experimental  $S$  value [96], and the hydrodynamic radius calculated in the same manner closely predicts the elution volume of yeast tRNA<sup>Phe</sup> from our calibrated SEC column. Because sIIB-tRNA<sup>Phe</sup> is composed of RNA elements of known structure, we built an atomic model for sIIB-tRNA<sup>Phe</sup> from which we could calculate hydrodynamic parameters.

The model for sIIB-tRNA<sup>Phe</sup> was constructed using Pymol from three RNA segments whose structures had been solved and deposited in the Protein Data Bank. The model consisted of the crystal structure for the phenylalanyl tRNA (Yeast) serving as the scaffold, and two segments of identical A-form RNA, and the NMR structure of the 34-

nucleotide stem loop-IIB RRE fragment representing the sIIB insert (PDB 1ETF) [21,90]. An A-form RNA extension was least squares superimposed onto the A-form bases of the anticodon stem using backbone phosphates of four sets of consecutive base pairs (8 atoms controlling the superposition) and excess residues of the anticodon loop were removed. The stem loop-IIB NMR structure was then introduced at the distal end of the A-form extension by a similar super-position (Figures 59 and 60), ensuring that the spacing of the tRNA element and the RRE stem loop correspond to the sequence of sIIB-tRNA<sup>Phe</sup>. Because the junctures between the segments were built by superposition of A-form RNA, the shape of the resulting model arises from the assumptions about the chimeric RNA elements and contains little user bias. No energy minimization of the final structure was performed.

Using this model for sIIB-tRNA<sup>Phe</sup>, the sedimentation coefficient calculated by Hydropro [95] is 4.77S and the elution volume was 8.28 ml. This is in excellent agreement with the 4.8S and 8.3 mL values of the sIIB-tRNA<sup>Phe</sup> monomer from the experimental data (Table 1). This data suggested that sIIB-tRNA<sup>Phe</sup> behaved as a monomer for the biophysical measurements.

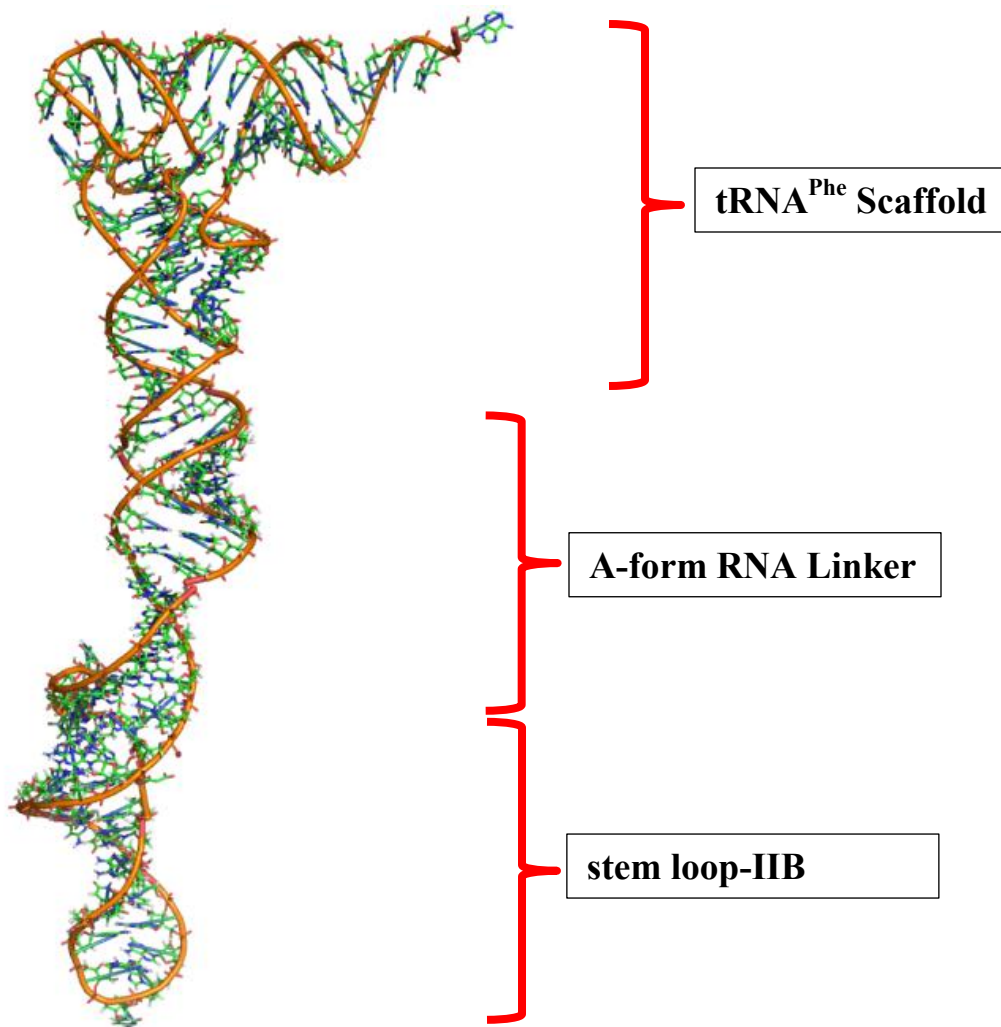


**Figure 59 Model of sIIB-tRNA<sup>Phe</sup> monomer.** The sIIB-tRNA<sup>Phe</sup> model is composed of the tRNA<sup>Phe</sup> (scaffold), A-form RNA (connecting scaffold to sIIB insert), and the stem loop-IIB structure.

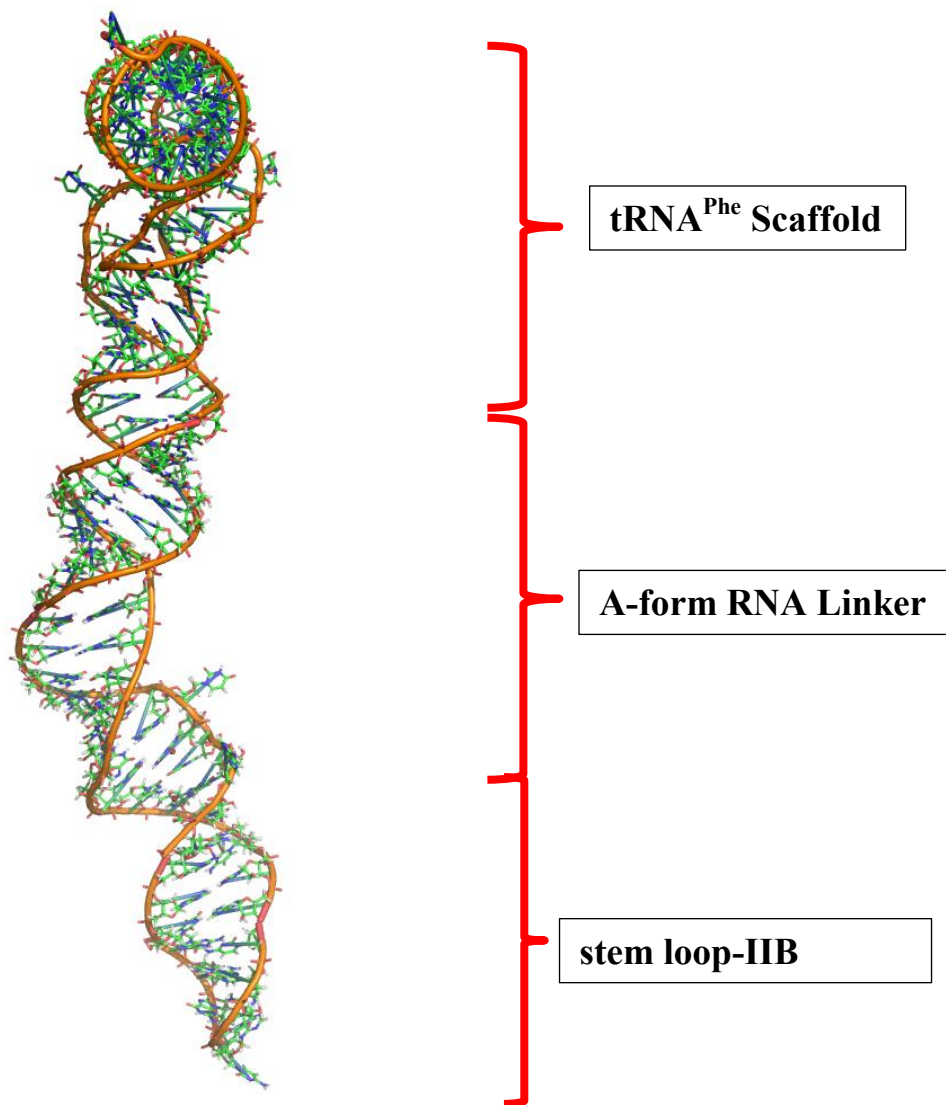


**Figure 60 Model of sIIB-tRNA<sup>Phe</sup> monomer rotated 90° from previous representation (Figure 59).** The sIIB-tRNA<sup>Phe</sup> model is composed of the tRNA<sup>Phe</sup> (scaffold) with anticodon residues removed, A-form RNA (connecting scaffold to sIIB insert), and stem loop-IIB.

### Section 3.2.4 Modeling the Rev-mediated sIIB-tRNA<sup>Phe</sup> Dimer

The sedimentation properties and behavior of macromolecular assemblies on size exclusion chromatography can be particularly informative about shape when the particles deviate strongly from spherical geometry. Particles with  $f/f_0 = 1.2$  deviate only modestly from spherical geometry, and so they sediment or elute from SEC columns much like a sphere of the same density that has been hydrated with 0.3 g of water per g of macromolecule. However, particles that deviate considerably from spherical geometry give large measured (and calculated) frictional ratios and elute from SEC columns much earlier than a sphere of the same volume. Given that the sIIB-tRNA<sup>Phe</sup> monomer is itself highly oblong, we reasoned that its complex with Rev might also be quite non-spherical, and that this could explain the SEC elution volume for the Rev:sIIB-tRNA<sup>Phe</sup> complex (6.98 ml, equivalent to an RNA sphere of 640 kDa). No experimental structure for the Rev:RRE is available, so we developed models for Rev:sIIB-tRNA<sup>Phe</sup> by superposing our model for the sIIB-tRNA<sup>Phe</sup> monomer onto crystal structures of Rev dimers.

We developed two models for the Rev-mediated dimer of sIIB-tRNA<sup>Phe</sup> (Tables 2 and 3). One model used the crystal structure of the Rev dimer (PDB ID 2X7L) with each monomer interacting via the A:A (Rev:Rev) interface [69] (Figure 61 and 62). The second model utilized the Rev dimer structure (PDB ID 3LPH) where the monomers interact via the B:B (Rev:Rev) interface (Figures 63 and 64). The model for sIIB-tRNA<sup>Phe</sup> was built using the NMR structure of an RRE fragment bound to the ARM peptide from Rev (PDB 1ETF), so we superposed one copy of sIIB-tRNA<sup>Phe</sup> onto each

Rev monomer in a dimer by superimposing the ARM peptide C $\alpha$  atoms. The spacing between the RNA monomers in the two models is very different due to the relative positions of the ARM regions in the A:A and B:B dimers. As calculated by Hydropro, the elution volume of the sIIB-tRNA<sup>Phe</sup> dimer model (Rev<sub>2</sub>:sIIB-tRNA<sup>Phe</sup><sub>2</sub>, Table 1) using the Rev dimer from DiMattia (PDB ID 2X7L) is 7.09 ml. This value is in close agreement with the experimentally measured elution volume of the Rev:sIIB-tRNA complex at 6.98 ml (Table 2). The sIIB-tRNA<sup>Phe</sup> dimer model constructed using the Rev dimer associated by the B:B interface elutes at 7.30 ml as calculated by Hydropro (Figure 67 and 68) (Table 1). This is in contrast to the experimentally determined position of 6.9 ml. The disparity between the two models indicates that it is likely that the initial dimer binding to stem loop-IIB on RRE RNA is dictated by the residues interacting by the A:A interface, and the subsequent monomer binds via the B:B interface.

The calculated sedimentation coefficient for the Rev<sub>2</sub>:sIIB-tRNA<sup>Phe</sup><sub>2</sub> (A:A) model was 7.09S, and the calculated S-value of the Rev<sub>2</sub>-sIIB<sub>2</sub> (B:B) was 7.68S (Table 2). The experimentally measured value for the complex was 9.8S (Table 3). This disparity in sedimentation rates between calculated data from the models and experimental data could be explained by the fact that the stoichiometry of the Rev:sIIB-tRNA<sup>Phe</sup> remains unknown and the partial specific volume ( $\bar{v}$ ) would be dependent on the number of Rev's mediating the RNA dimer. Small changes in the partial specific volume of the Rev:RNA complex would represent large changes on the S-value.

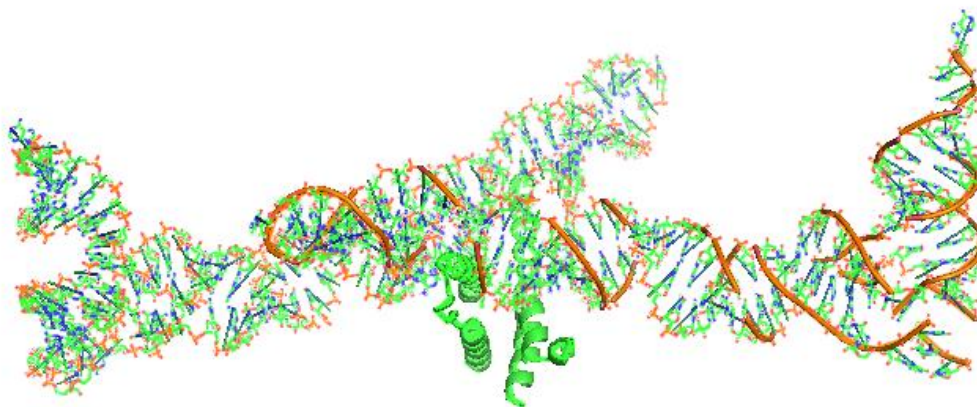


**Figure 61 Model of a Rev<sub>2</sub>: sIIB-tRNA<sup>Phe</sup><sub>2</sub>.** The Rev-mediated dimer model of sIIB-tRNA<sup>Phe</sup> using crystal structure of the A:A Rev dimer interface (PDB ID 3LPH)

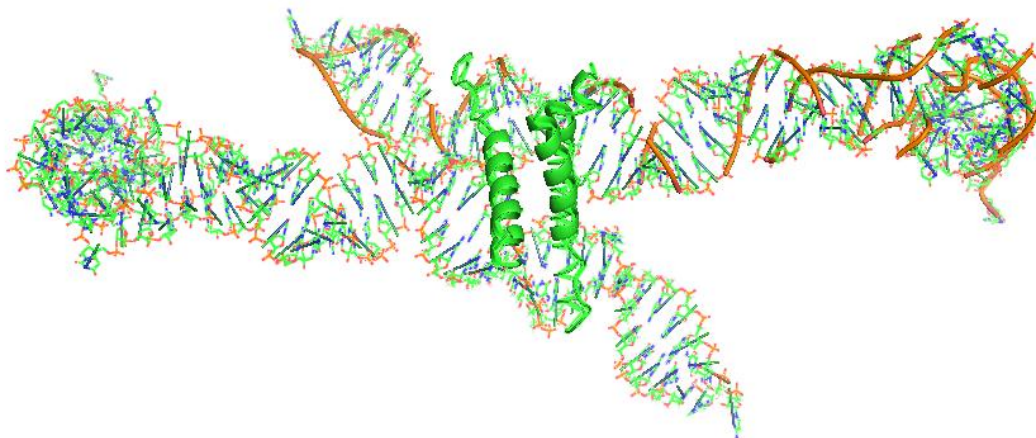


**Figure 62 Model of a Rev<sub>2</sub>: sIIB-tRNA<sup>Phe</sup><sub>2</sub>.** The Rev-mediated dimer model of sIIB-tRNA<sup>Phe</sup> using crystal structure of the A:A Rev dimer interface (PDB ID 3LPH) rotated to show the spacing between the sIIB-tRNA<sup>Phe</sup> monomers.



**Figure 63 Model of a Rev<sub>2</sub>: sIIB-tRNA<sup>Phe</sup><sub>2</sub>.** The Rev-mediated dimer model of sIIB-tRNA<sup>Phe</sup> using crystal structure of the B:B Rev dimer interface (PDB ID 2X7L) rotated to show the spacing between the sIIB-tRNA<sup>Phe</sup> Monomers.



**Figure 64 Model of a Rev<sub>2</sub>: sIIB-tRNA<sup>Phe</sup><sub>2</sub>.** The Rev-mediated dimer model of sIIB-tRNA<sup>Phe</sup> using crystal structure of the B:B Rev dimer interface (PDB ID 2X7L).

<b>Model</b>	<b>#</b>	<b>MW (kDa)</b>	<b>Elution (ml)</b>	<b>MW<sub>app</sub> (kDa)</b>	<b>sed (S)</b>	<b>R<sub>g</sub> (Å)</b>
tRNA <sup>Phe</sup>		25	9.3	64	3.90	23.9
sIIB-tRNA <sup>Phe</sup>	1	40	8.28	174	4.77	42.2
Rev <sub>1</sub> -sIIB <sub>1</sub>	2	53	8.12	204	5.04	42.5
Rev <sub>2</sub> -sIIB <sub>1</sub>	3	66	8.06	217	5.70	42.0
<b>Rev<sub>2</sub>-sIIB<sub>2</sub> (A:A)</b>	<b>4</b>	<b>107</b>	<b>7.05</b>	<b>600</b>	<b>7.09</b>	<b>62.1</b>
Rev <sub>2</sub> -sIIB <sub>2</sub> (B:B)	5	107	7.30	463	7.68	53.7
Rev <sub>2</sub> -sIIB <sub>4</sub>	6	137	7.04	600	8.21	59.4

**Table 2 Measured hydrodynamic properties of tRNA, sIIB-tRNA<sup>Phe</sup>, and its complexes with Rev and RevN70**

<b>Species</b>	<b>MW (kDa)</b>	<b>Elution (ml)</b>	<b>MW<sub>App</sub> (kDa)</b>	<b>sed (S)</b>	<b>R<sub>g</sub> (Å)</b>
tRNA <sup>Phe</sup>	25	9.09	78	n.d.	24.3
sIIB-tRNA <sup>Phe</sup>	40	8.36	161	4.8	43±1
sIIB + Rev	?,a	6.98	640	9.8	–
	?,a	8.23	183	n.d.	n.d.
sIIB + RevN70	?,b	8.23	183	n.d.	n.d.
? unknown but (a) Rev = 13kDa, (b) RevN70 = 8.5 kDa					

**Table 3 Calculated hydrodynamic properties of models for sIIB-tRNA<sup>Phe</sup> with Rev**

### Section 3.2.5 SAXS: tRNA<sup>Phe</sup> and sIIB-tRNA<sup>Phe</sup>

Small Angle X-Ray Scattering (SAXS) is a low-resolution technique ( $\sim 10\text{\AA}$  resolution) used to determine shapes of macromolecules or molecular complexes under a variety of solution conditions [97,98,99]. The experiment consists of exposing a sample to a highly focused beam of X-rays and recording the scattered intensity at a range of scattering angles. The scattering curve is plotted as Intensity (I) vs. scattering angle ( $q = (4\pi/\lambda)\sin(\theta)$  or  $s = \sin(\theta)/\lambda$ ) and provides information which can be used to obtain parameters such as the molecular weight (MW), radius of gyration ( $R_g$ ), and the “foldedness” of the molecule [97,99,100,101].

Information about the particle in solution can be gleaned from SAXS data in several ways. The Guinier plot, or natural log of scattering intensity versus angle squared, is linear in the region closest to the beam stop, the intercept is proportional to the square of the scattering mass, and the slope of the line is equal to the radius of gyration divided by three. The Guinier region provides qualitative information on the aggregation state of the molecules in solution: a nonlinear dependence of  $\ln(I)$  vs.  $q^2$  in the Guinier region may indicate that the molecule is aggregating, or that inter-particle correlations are attenuating the scatter. A linear dependence indicates that the buffer conditions are ideal for data collection. If Guinier region indicates aggregation, solution conditions such as ionic strength, divalent ion concentration, or macromolecule concentration are adjusted to improve the Guinier region and provide ideal scattering profiles.

The Kratky plot, or scattered intensity times scattering vector squared versus angle ( $I \cdot s^2$  vs.  $s$ ), provide information on the overall global structure of the molecule and its compactness or “foldedness”. Globular proteins follow Porod’s law and the Kratky curve is bell-shaped. Unfolded macromolecules lack the bell-shaped peak and have a plateau in the larger  $q$ -region.

While the former analyses are based directly on the experimental data, additional insights can be obtained by Fourier transformation of the scattering data  $I(q)$  to yield the distance distribution function  $P(r)$ , a histogram of interatomic distance vectors that reflects the spatial distribution of distances inside the molecule in one dimension. This distribution can be analyzed to provide a second measure of the particle radius of gyration ( $R_g$ ). Calculating a  $P(r)$  curve from intensity data requires an estimate of the maximum dimension of the particle ( $D_{\max}$ ), and in favorable cases the actual  $D_{\max}$  can be inferred by examining  $P(r)$  curves calculated for a series of guesses for the maximum dimension.

#### **Section 3.2.4.1 SAXS Analysis: tRNA<sup>Phe</sup>**

Initially, SAXS experiments were performed on the natural yeast tRNA<sup>Phe</sup>. The tRNA<sup>Phe</sup> was ordered from Sigma® and prepared by dialyzing into 200 mM NaCl, 50 mM Tris, 5 mM MgCl<sub>2</sub>, pH 7.2. Following dialysis, the RNA was concentrated to 5 mg/ml for experiments. Data was collected on a Rigaku BioSAXS-1000 camera on a Rigaku FRD generator using CuK <sub>$\alpha$</sub>  radiation at UTMB-Galveston.

A theoretical scattering curve was generated from the crystal structure (PDB 1TN1) using CRY SOL [97,102,103]. The experimental and theoretical scattering data were compared as Log (I) vs.  $s$  and Kratky plots (Figures 65 and 66). The Kratky plot, which amplifies the mid- $q$  region, demonstrated that the global architecture of the crystal structure and the tRNA<sup>Phe</sup> in solution match closely. There was no aggregation of the RNA as evidenced by the slope of the line in the Guinier region (Figure 67). The experimental radius of gyration of 26.3 Å closely matches the calculated radius of gyration (24 Å) [96]. The best experimental estimate for  $D_{\max}$  was 74 Å (Figure 68), which closely matches the longest interatomic distance in the crystal structure. Using the scattering data, *ab initio* reconstructions of the molecular shape were performed with the program DAMMIN [97,99,104]. Multiple reconstructions were averaged together to generate the final bead model. The crystal structure of the tRNA<sup>Phe</sup> was in agreement with the bead model density as demonstrated by figures 69 and 70. This SAXS analysis shows that the technique can produce reliable and accurate low-resolution structural information on RNA in solution and stimulated us to undertake SAXS analysis of the sIIB-tRNA<sup>Phe</sup> monomer (Section 3.2.4.2).

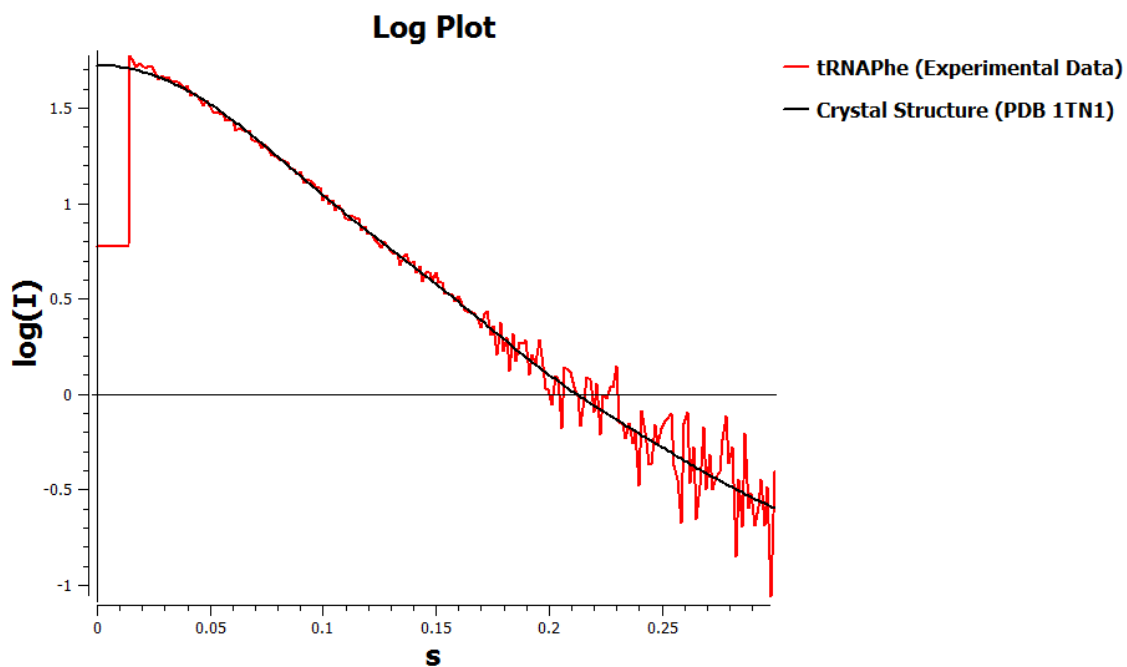


**Figure 65** Log(I) vs.  $s$  plot(s) from SAXS data on tRNA<sup>Phe</sup>. Overlay of experimental and theoretical Log(I) vs.  $s$  plots of tRNA<sup>Phe</sup>. The theoretical scattering curve was generated using CRY SOL from the crystal structure of the phenylalanyl tRNA (Yeast) (PDB ITN1).

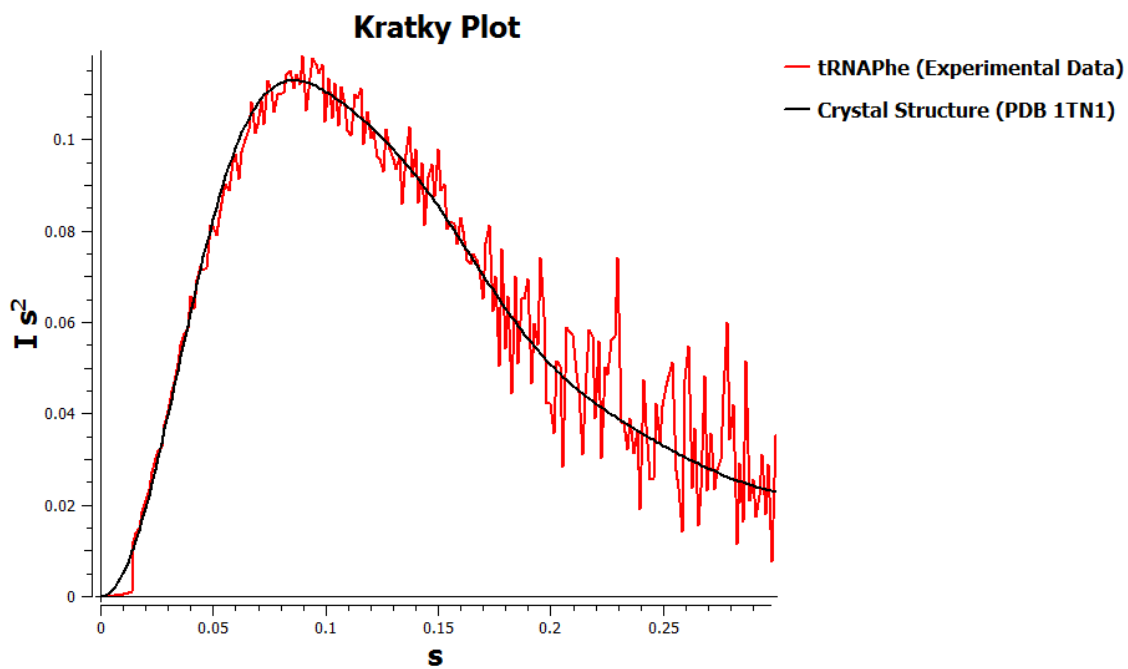


**Figure 66 Kratky Plot ( $I \cdot s^2$  vs.  $s$ ).** Overlay of experimental and theoretical Kratky plots ( $I \cdot s^2$  vs.  $s$ ) of tRNA<sup>Phe</sup>. The theoretical curve was generated using CRY SOL from the crystal structure of the phenylalanyl tRNA (Yeast) (PDB 1TN1).

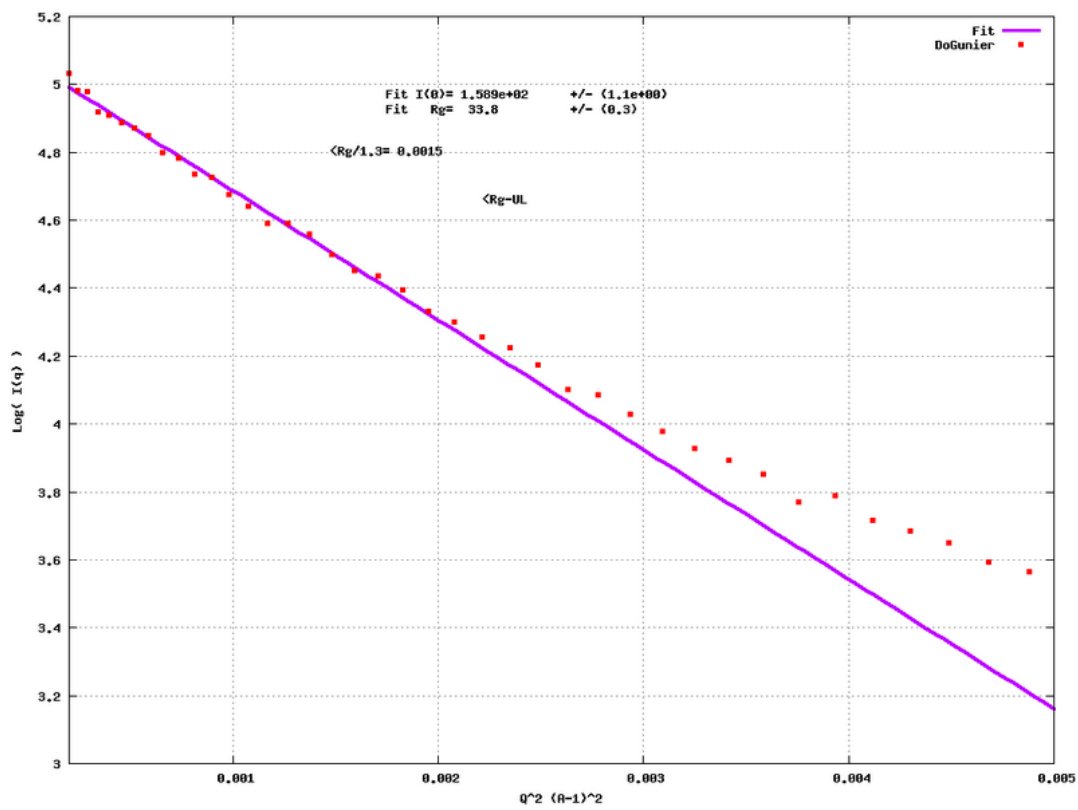


**Figure 67 Guinier Plot for tRNA<sup>Phe</sup>.** The Guinier plot revealed that there was no significant aggregation in the RNA sample.

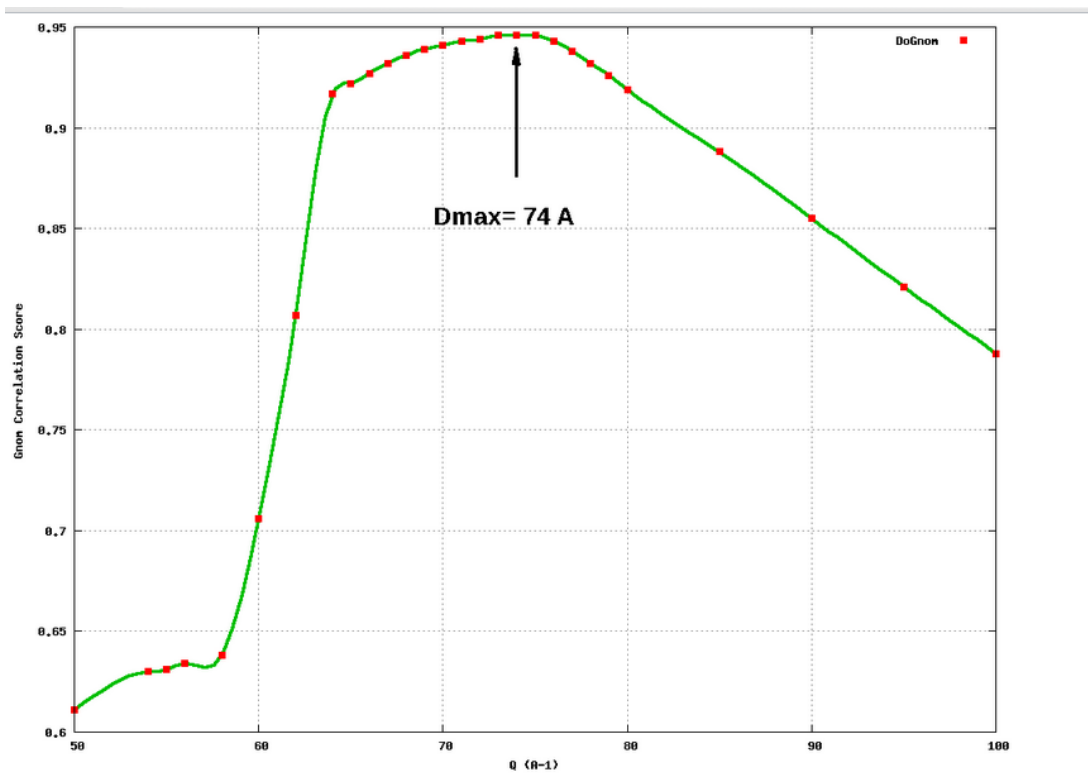


**Figure 68**  $D_{Max}$  determination for tRNA<sup>Phe</sup>. The maximum dimension for tRNA<sup>Phe</sup> as determined from the experimental scattering profile was 74Å.

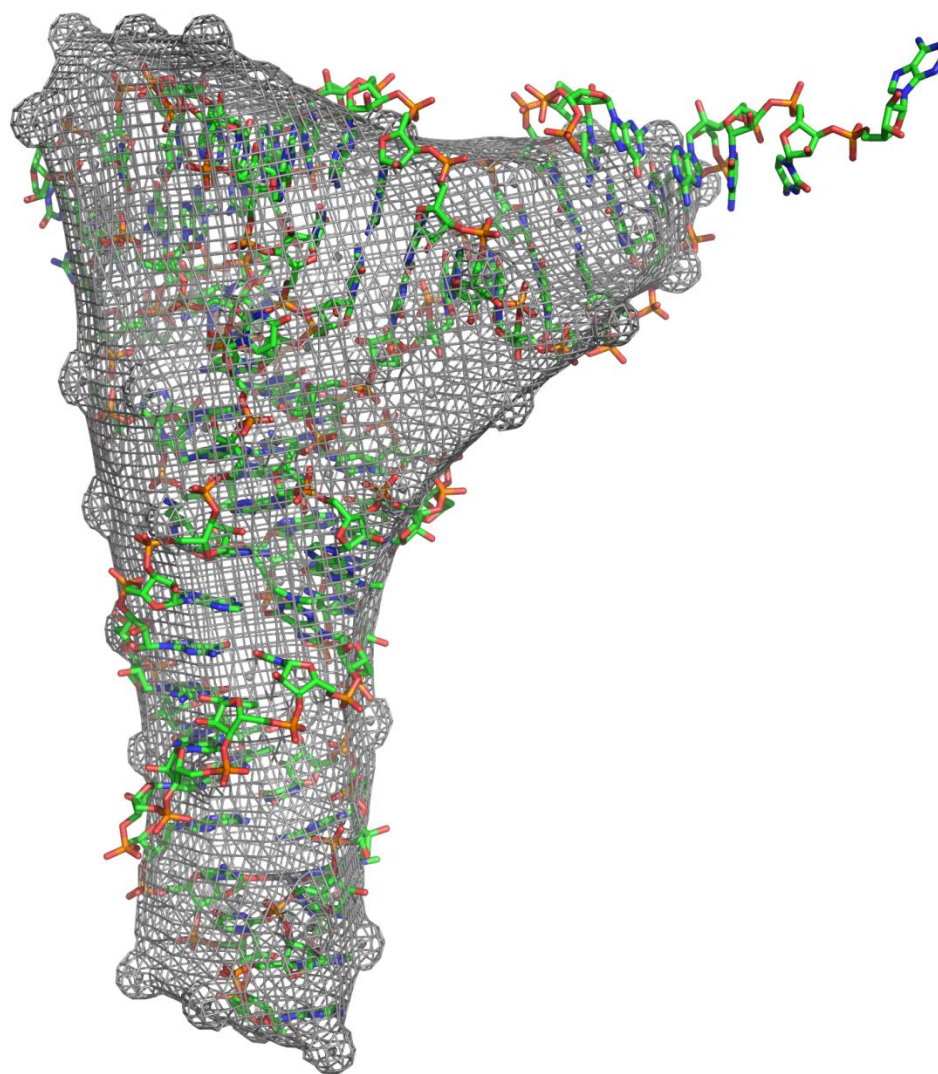


**Figure 69** Bead model of tRNA<sup>Phe</sup> derived from SAXS data compared with the crystal structure. The tRNA<sup>Phe</sup> was manually manoeuvred into the bead model density which demonstrated the accuracy of the generated bead model

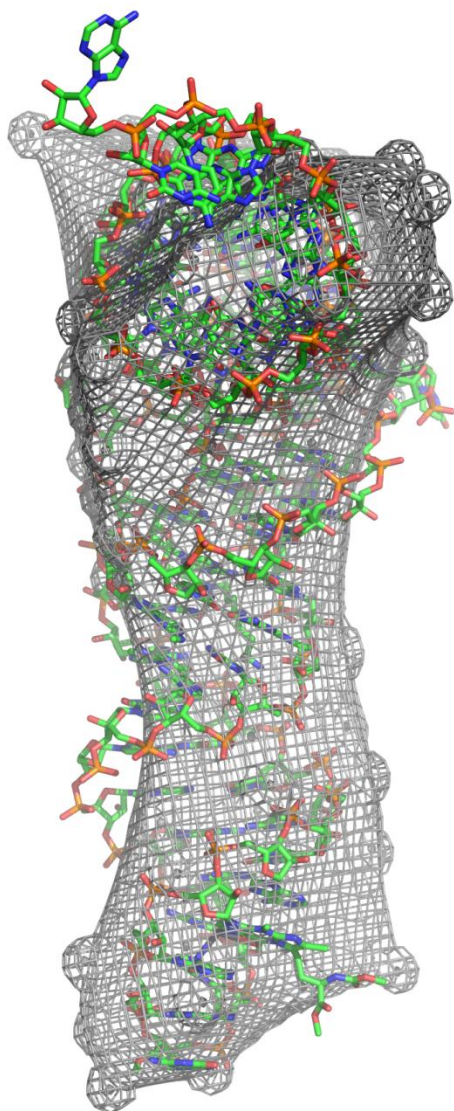


**Figure 70** Bead model of tRNA<sup>Phe</sup> derived from SAXS data compared with the crystal structure. The tRNA<sup>Phe</sup> was manually manoeuvred into the bead model density which demonstrated the accuracy of the generated bead model.

### Section 3.2.4.2 SAXS Analysis: sIIB-tRNA<sup>Phe</sup>

SEC and AUC experiments demonstrated that the sIIB-tRNA<sup>Phe</sup> monomer and Rev:sIIB-tRNA<sup>Phe</sup> complexes have large hydrodynamic radii and that both the monomer and the complex are oblong in shape. In order to determine if the conclusions about molecular shape inferred by previous experiments and modeling, SAXS experiments were performed on the sIIB-tRNA<sup>Phe</sup> monomer to generate a bead model that could be compared to the model we had built by superimposing RNA elements. Preliminary scattering experiments and analysis have also been undertaken for the Rev:sIIB-tRNA<sup>Phe</sup> complex.

The sIIB-tRNA<sup>Phe</sup> was prepared by overnight dialysis into 200 mM NaCl, 50 mM Tris, 5 mM MgCl<sub>2</sub>, pH 7.2 followed by concentration to 5 mg/ml for experiments. Data was collected on a Rigaku BioSAXS-1000 camera on a Rigaku FRD generator using CuK<sub>α</sub> radiation at UTMB-Galveston. A theoretical scattering profile generated from the sIIB-tRNA<sup>Phe</sup> model using CRY SOL was compared to the experimental scattering profile as Log (I) vs.  $s$  and Kratky plots (Figures 71 and 72) [99,103,105]. The Kratky plot comparison shows that the global architecture of the sIIB-tRNA<sup>Phe</sup> and the sIIB-tRNA<sup>Phe</sup> model match reasonably well (Figure 72). A slight amount of aggregation may be present, given the slight upturn of the plotted data at low  $s$  in the Guinier region (Figure 73), which complicates the determination of  $R_g$ . The  $D_{max}$  was estimated to be 155 Å with a  $R_g$  of 41.4 Å, which closely match the model  $R_g$  (42.2Å) and  $D_{max}$  (149Å). Based upon the experimental scattering curve, *ab initio* reconstructions of the molecular shape

were performed with the program DAMMIN [97,99,104]. Multiple reconstructions were performed and averaged together to generate the final bead model. The atomic model for sIIB-tRNA<sup>Phe</sup> was manually maneuvered into the bead model density and corresponded closely to the experimentally generated bead model.

SAXS data analysis on the sIIB-tRNA<sup>Phe</sup> monomer revealed an oblong-shaped electron density which fit precisely with the model (Figure 75). This finding agreed with the solution behavior as observed with SEC and AUC experiments with the monomer (40.31 kDa) eluting as a spherical RNA with a mass of ~183 kDa. The oblong shape of the monomer may also explain the solution behavior of the putative Rev-mediated dimer of sIIB-tRNA<sup>Phe</sup>.

. The experimental elution volume of the Rev:RNA complex was measured at 6.98 mL and suggested that the complex eluted as a spherical RNA of mass ~600 kDa. This data led to the construction of a Rev-mediated sIIB-tRNA<sup>Phe</sup> dimer using the crystal structure of the Rev dimer. The model suggested that the oblong sIIB-tRNA<sup>Phe</sup> monomers superposed onto the Rev dimer structure in a fashion which would result in the complex having a very large hydrodynamic radius consistent with the experimentally measured elution volumes and sedimentation rates. Elution volumes for the Rev-mediated sIIB-tRNA<sup>Phe</sup> dimer were calculated using Hydropro and determined to be 7.04 mL, in excellent agreement with the experimentally measured value of 6.98 mL (Table 1). Confirmation of the oblong shape of the monomer using SAXS would explain the large hydrodynamic radius of the Rev-mediated dimer of sIIB-tRNA<sup>Phe</sup>

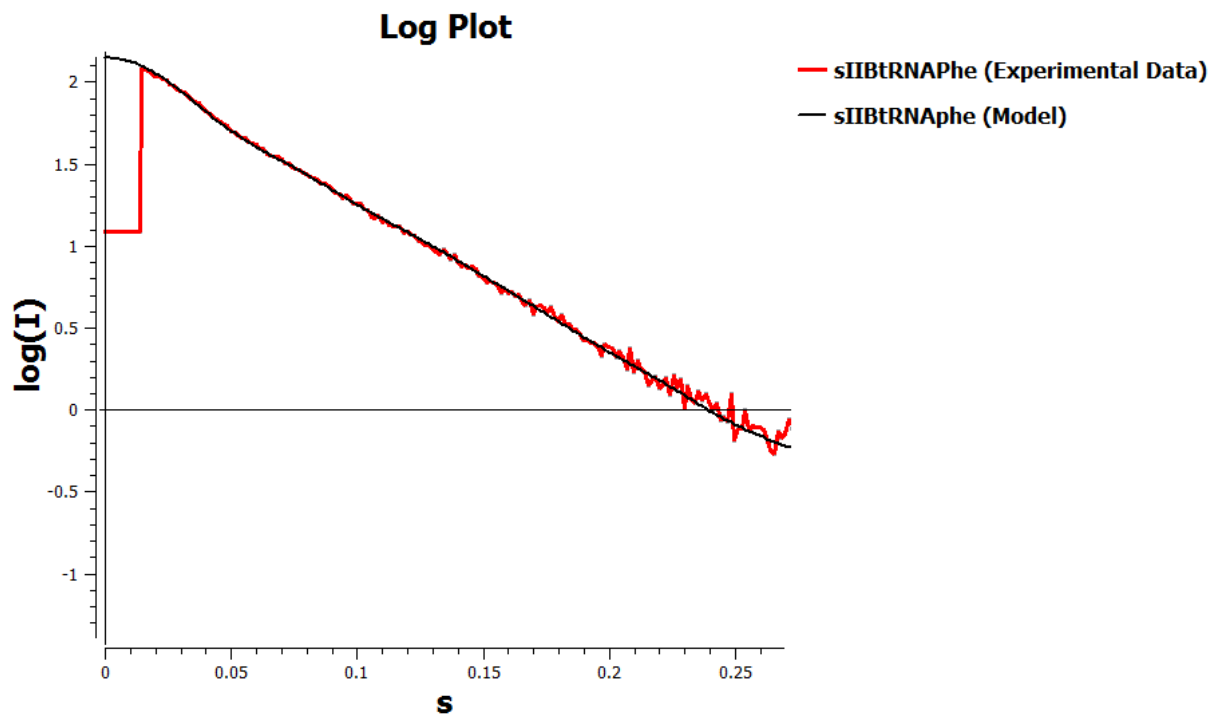


**Figure 71** Log(I) vs.  $s$  plot(s) from X-ray scattering curves on sIIB-tRNA<sup>Phe</sup>. Overlay of Log(I) vs.  $s$  plots of experimental (red) and theoretical (black) data of sIIB-tRNA<sup>Phe</sup>. The theoretical scattering curve was generated using CRY SOL from the sIIB-tRNA<sup>Phe</sup> model.

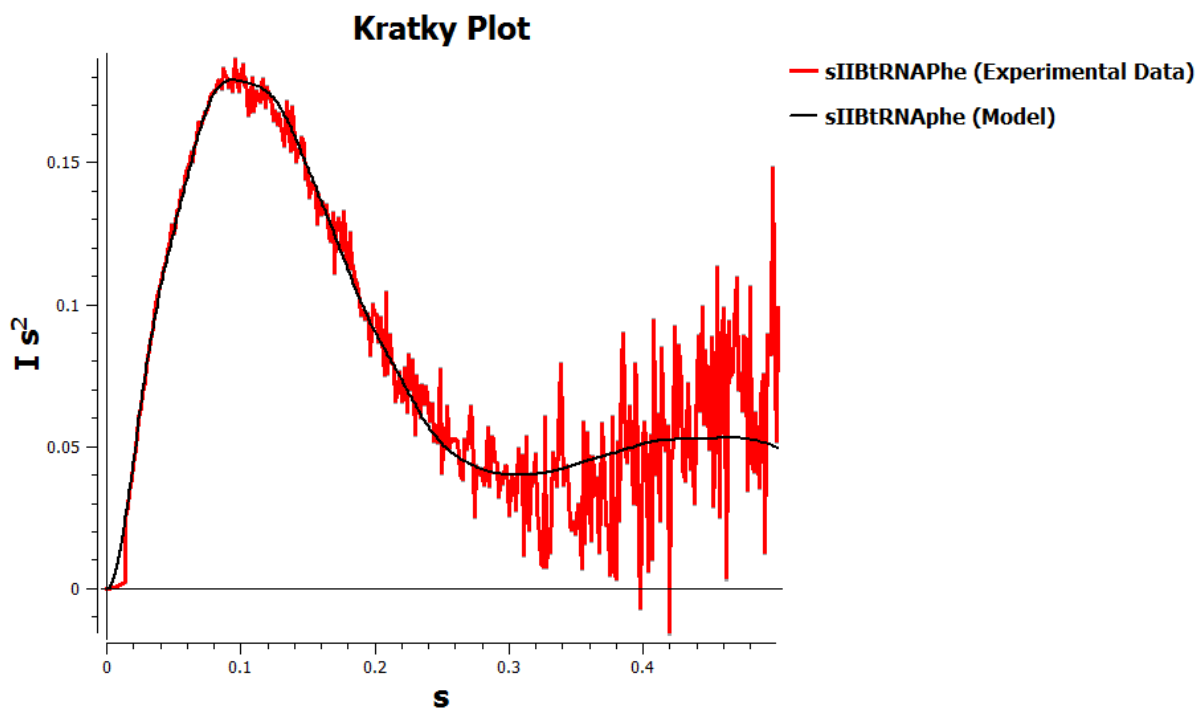
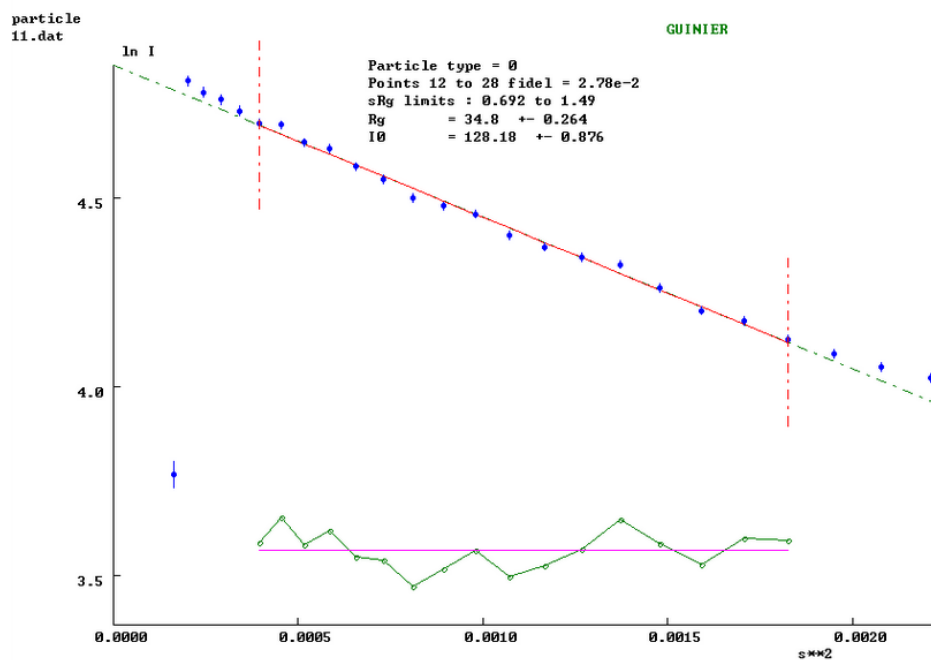


**Figure 72 Kratky Plot ( $I \cdot s^2$  vs.  $s$ ).** Overlay of Kratky plots ( $I \cdot s^2$  vs.  $s$ ) plots of experimental and theoretical scattering curves of tRNA<sup>Phe</sup>. The theoretical scattering curve was generated using CRY SOL from the model of sIIB-tRNA<sup>Phe</sup>.



81

**Figure 73 Guinier plot for sIIB-tRNA<sup>Phe</sup>.** The Guinier plot revealed that there was no significant aggregation in the RNA sample as evidenced by the data points resting on the best fit line.

---

Input file(s) : S5avg-Baug11.dat \*\*\* JOB = 0  
Real space: Rg = 41.39 , I(0) = 0.1396E+03

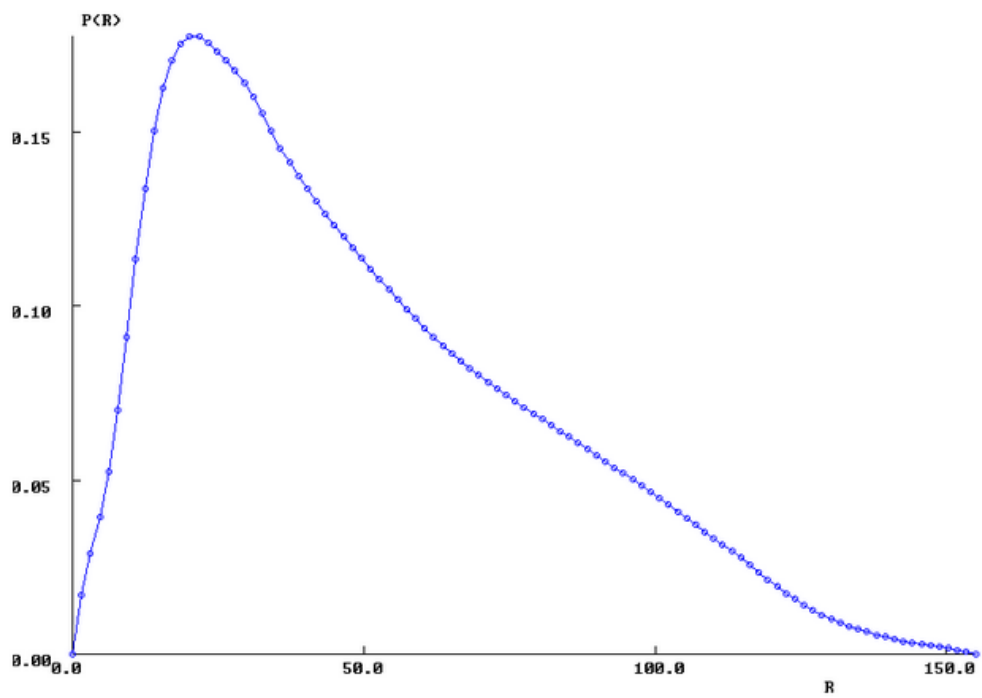


**Figure 74**  $P(r)$  Curve for sIIB-tRNA<sup>Phe</sup>. The radius of gyration ( $R_g$ ) as calculated from the  $P(r)$  curve was determined to be 41.4Å.

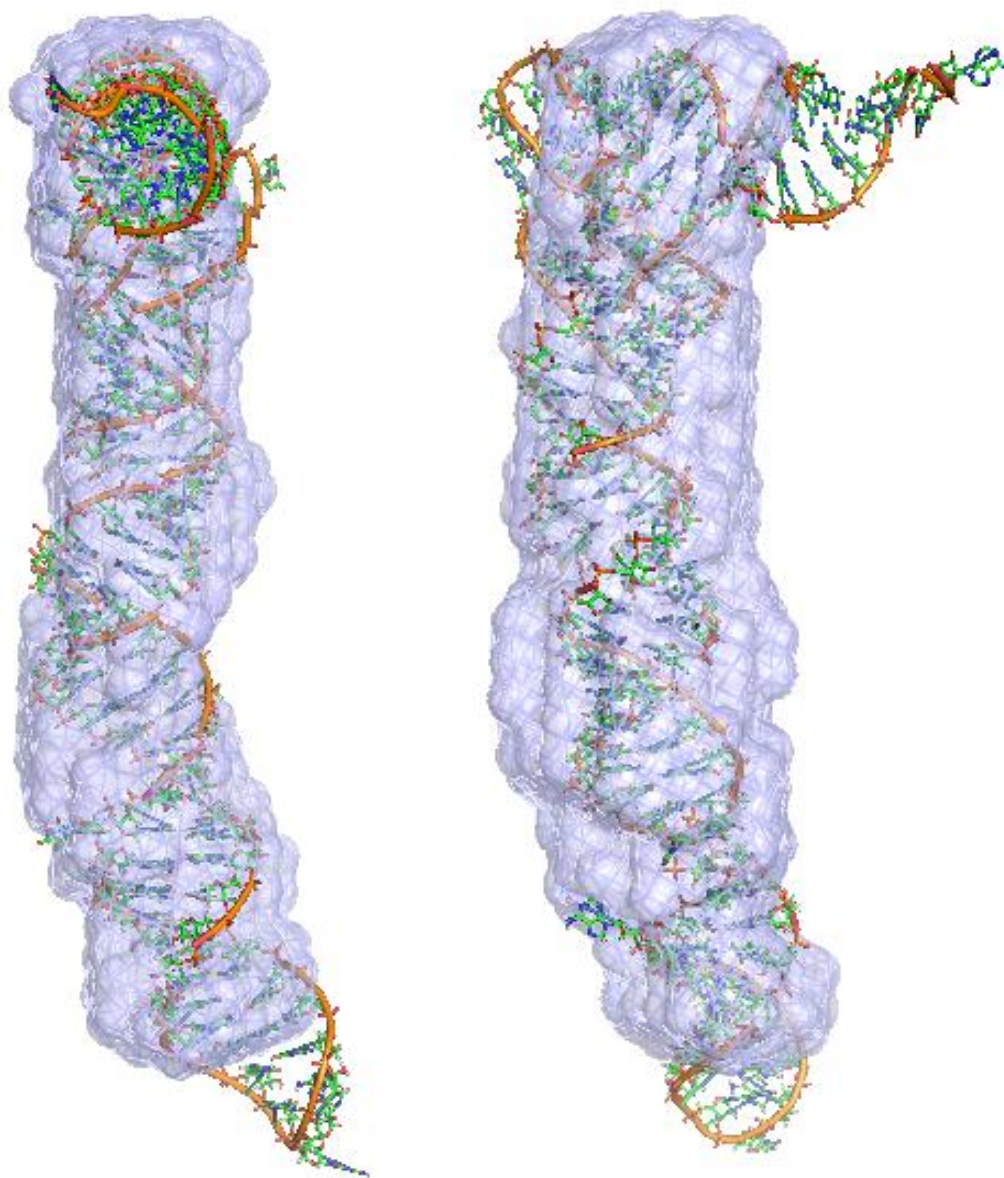


**Figure 75** Bead model of sIIB-tRNA<sup>Phe</sup>. Atomic model of sIIB-tRNA<sup>Phe</sup> superposed onto bead model.

## CHAPTER 4: SUMMARY AND IMPLICATIONS

Current models of the Rev:RRE interaction indicate that Rev:RRE complexes contain one RNA and many copies of the Rev protein. It is believed that Rev initially interacts with the high-affinity binding site called stem loop-IIB into 8-11 monomers and subsequently polymerize along stem I of the same RRE (putatively). This is followed by the Rev binding of cellular cofactors which facilitate the transport of the Rev:RRE complex from the nucleus to the cytoplasm. Results from this dissertation suggest an alternative quaternary structure in which two or more Rev monomers hold together two copies of RRE RNA. This finding is based upon solution biophysical studies performed for this work and is consistent with recent crystal structures of the Rev dimer.

Size-exclusion chromatography experiments revealed that the Rev:sIIB-tRNA<sup>Phe</sup> complex eluted as a 640 kDa spherical RNA or 460 kDa protein. The monomer (40.31 kDa) elution position corresponded to a 115 kDa protein or 158 kDa spherical RNA. This data suggested that the sIIB-tRNA<sup>Phe</sup> monomer was either very oblong in shape or migrated as an oligomer, and that the Rev:sIIB-tRNA<sup>Phe</sup> complex contained more than two RNA. The data collected on the Rev<sup>Fluo</sup>:sIIB-tRNA<sup>Phe</sup> complexes showed that A<sub>495</sub> was only detected in the Rev:RNA complex peak. In order to confirm the solution behavior and the oligomeric state of the two species, SEC experiments were followed up with analytical ultracentrifugation experiments.

Analytical ultracentrifugation experiments were initially performed on sIIB-tRNA<sup>Phe</sup> monomer at two separate magnesium concentrations. The RNA sedimented

with a value of 4.8S at both magnesium concentrations. Subsequently, Rev:sIIB-tRNA<sup>Phe</sup> complexes were prepared at Rev:RNA ratios of 1:1, 2:1, and 3:1. The data revealed two species at all Rev:RNA ratios which correlated with the two species revealed by size-exclusion chromatography. One species corresponded to a monomer of sIIB-tRNA<sup>Phe</sup> which sedimented at a rate of 4.8S. The Rev:sIIB-tRNA<sup>Phe</sup> complex sedimented at 9.8S. Following the determination of experimental sedimentation rates for the sIIB-tRNA<sup>Phe</sup> alone and Rev:sIIB-tRNA<sup>Phe</sup> complex, SEDFIT was used to determine possible oligomeric states consistent with the two species. For sIIB-tRNA<sup>Phe</sup> alone, molar masses for the monomer (40.31 kDa) and dimer (80.62 kDa) were used in the SEDFIT calculation for the comparison of the physical parameters, frictional and axial ratios. Only when the molar mass of 40.31 kDa was used in the calculation did the frictional and axial ratios make physical sense.

In order to determine the oligomeric state and preliminary stoichiometry of, SEDFIT calculations were done. Initial calculations were performed using the molecular weight for monomeric RNA and molecular weights for increasing equivalents of Rev bound to the RNA. However, the frictional ratios ( $f/f_0$ ) and axial ratios ( $a/b$ ) values were not physically realistic. Subsequently, calculations using molecular weights for two RNAs and increasing equivalents of Rev produced results that were physically possible. From these calculations, it was reasonable to conclude that the Rev:RNA complex is a Rev-mediated sIIB-tRNA<sup>Phe</sup> dimer, however, the number of Revs mediating the RNA dimer remains unclear.

SEC and AUC data led to the 3D modeling of the sIIB-tRNA<sup>Phe</sup> monomer and the Rev:sIIB-tRNA<sup>Phe</sup> complex. The rationale was to determine how well the SEC and AUC calculated data from the models fit the determined experimental values. The model of sIIB-tRNA<sup>Phe</sup> was built as a module and consisted of the crystal structure for the phenylalanyl tRNA (Yeast) serving as the scaffold (Shi and Moore 2000), and two segments of identical A-form RNAs connecting the NMR structure of the 34-nucleotide stem loop-IIB RRE fragment which served as the sIIB insert [21,90]. Calculations using Hydropro showed the elution volume of the monomer model was in excellent agreement with the experimental data. The calculated sedimentation coefficient and the experimentally derived value were also in excellent agreement. These calculations confirmed the accuracy of the sIIB-tRNA<sup>Phe</sup> monomer model, and it was reasonable to use in modeling the Rev-mediated sIIB-tRNA<sup>Phe</sup> dimer.

Two separate models for the Rev-mediated sIIB-tRNA<sup>Phe</sup> dimer were constructed using the crystal structure(s) of the Rev dimer. One of the crystal structures featured Rev interacting via A:A, and the second structure shows the dimer interacting via the B:B interface. Both of the structures show the RNA binding residues (34-50) of the ARM region protruding from each monomer in a prong-like manner at a 140° angle from each other. The positions of the RNA binding residues suggested that Rev could bind two copies of RRE RNA and that sIIB-tRNA<sup>Phe</sup> positioned on each side of the dimers. Since the 34-nt stem loop-IIB NMR structure was solved complexed with the ARM peptide, sIIB-tRNA<sup>Phe</sup> (containing the ARM peptide) was maneuvered onto each of the Rev dimer

crystal structures. In the first model, sIIB-tRNA<sup>Phe</sup> was maneuvered on each side of the Rev dimer with the monomers interacting via the A:A interface. In the second model, sIIB-tRNA<sup>Phe</sup> was maneuvered on the Rev dimer with monomers interacting via the B:B interface. Calculations using Hydropro demonstrated that only the model sIIB-tRNA<sup>Phe</sup> dimer using the Rev dimer interacting via the A:A interface was consistent elution volume of the Rev:sIIB-tRNA<sup>Phe</sup> complex. The calculated sedimentation coefficient for the Rev<sub>2</sub>:sIIB-tRNA<sup>Phe</sup><sub>2</sub> (A:A) model was very disparate from the experimentally measured value. This disparity in sedimentation rates between calculated data from the model and experimental data could be explained by the fact that the stoichiometry of the Rev:sIIB-tRNA<sup>Phe</sup> remains unknown and the diffusion coefficient (D) would be dependent on the number of Rev's mediating the RNA dimer. Small changes in the diffusion coefficient would be reflected in the calculated sedimentation rate.

SAXS experiments were performed on the sIIB-tRNA<sup>Phe</sup> monomer. Theoretical scattering curves were generated for the monomer model and compared to the experimental data. An overlay of Log (I) vs. s and Kratky plots from the experimental and theoretical data demonstrated that the low q (higher resolution) and mid q (global fold) were in agreement. Multiple *ab initio* bead models were generated from the experimental scattering data, averaged, and refined against the 3D model of sIIB-tRNA<sup>Phe</sup> to generate the final bead model electron density. The sIIB-tRNA<sup>Phe</sup> model fit remarkably well into the bead model density, confirming the oblong, cylindrical shape of the RNA.

. This sequence direct comparison of the calculated and experimental SEC, AUC, and SAXS data confirm the hydrodynamic behavior, size, and oblong, cylindrical shape of the sIIB-tRNA<sup>Phe</sup> monomer. Calculated and experimental SEC and AUC data on the Rev-sIIB-tRNA<sup>Phe</sup> complexes combined with data on the sIIB-tRNA<sup>Phe</sup> monomer suggest that Rev is mediating a dimer of the RRE-containing RNA. Recently published SEC data on Rev:stem loop-IIB complexes suggested that multiple Rev's bound a single RNA [75]. However, after 3-dimensional modeling of the this Rev:stem loop-IIB complex for this work and calculating elution volumes for the complex, it was clear that the complex observed in SEC experiments was in fact a Rev-mediated dimer of stem loop-IIB.

Most recently in 2010, Daugherty and colleagues performed gel shift experiments with Rev bound to stem loop-IIB constructs and suggest that Rev binds the RNA as a dimer [70]. Additionally, Dimattia, *et al.* suggest that based on the position of the RNA binding residues of the RNA residues in the Rev dimer crystal structure that stem loop-I may “wrap” around and interact with Rev on opposing sides of the Rev oligomer [69]. Our solution biophysical data on the Rev:sIIB-tRNA<sup>Phe</sup> complex establishes that Rev mediates a dimer of RRE containing RNA. The implications of this finding that may help explain the efficiency in which Rev exports intron containing HIV transcripts during viral replication. Additionally, it was recently discovered that the Rev/RRE system in combination with 5' UTR dimerization signals, dramatically enhances the encapsidation of a diploid copy of HIV RNA into a mature virion confirming the putative role of Rev functioning to mediate RRE dimers [79,106,107,108].

In conclusion, we have successfully designed, expressed, and purified a RRE RNA related sequence via a tRNA scaffold. The chimeric tRNA was shown to bind the Rev protein in such a manner that offered insight into how Rev may interact with the full length RRE *in vivo*. This work provides a framework for expressing longer sequences of the RRE via a tRNA scaffold(s) with known atomic structures to be used in X-ray crystallographic or solution biophysical experiments to better understand the Rev/RRE interaction.

## REFERENCES

- [1] B.K. Felber, C.M. Drysdale, G.N. Pavlakis, Feedback regulation of human immunodeficiency virus type 1 expression by the Rev protein., *J Virol* 64 (1990) 3734-3741.
- [2] D.F. Purcell, M.A. Martin, Alternative splicing of human immunodeficiency virus type 1 mRNA modulates viral protein expression, replication, and infectivity., *J Virol* 67 (1993) 6365-6378.
- [3] M.O. McClure, Q.J. Sattentau, P.C. Beverley, J.P. Hearn, A.K. Fitzgerald, A.J. Zuckerman, R.A. Weiss, HIV infection of primate lymphocytes and conservation of the CD4 receptor., *Nature* 330 (1987) 487-489.
- [4] L.J. Lowenstine, N.C. Pedersen, J. Higgins, K.C. Pallis, A. Uyeda, P. Marx, N.W. Lerche, R.J. Munn, M.B. Gardner, Seroepidemiologic survey of captive Old-World primates for antibodies to human and simian retroviruses, and isolation of a lentivirus from sooty mangabeys (*Cercocebus atys*). *Int J Cancer* 38 (1986) 563-574.
- [5] H. Kornfeld, N. Riedel, G.A. Viglianti, V. Hirsch, J.I. Mullins, Cloning of HTLV-4 and its relation to simian and human immunodeficiency viruses., *Nature* 326 (1987) 610-613.
- [6] V.M. Hirsch, G.A. Dapolito, S. Goldstein, H. McClure, P. Emau, P.N. Fultz, M. Isahakia, R. Lenroot, G. Myers, P.R. Johnson, A distinct African lentivirus from Sykes' monkeys., *J Virol* 67 (1993) 1517-1528.
- [7] C.O. Agboghorama, Contraception in the context of HIV/AIDS: a review., *Afr J Reprod Health* 15 (2011) 15-23.
- [8] D. Gilden, When HAART is not enough., *GMHC Treat Issues* 10 (1996) 1-6.
- [9] D.I. Abrams, Current therapeutic options for Kaposi's sarcoma., *Oncology (Williston Park)* 10 (1996) 24-27; discussion 37-28.
- [10] D.C. Bright, Antiretroviral therapy for HIV infection: a review of current medications and therapies., *J Am Optom Assoc* 70 (1999) 355-383.
- [11] J.A. Turpin, The next generation of HIV/AIDS drugs: novel and developmental antiHIV drugs and targets., *Expert Rev Anti Infect Ther* 1 (2003) 97-128.
- [12] X.F. Lu, Z.W. Chen, The development of anti-HIV-1 drugs., *Yao Xue Xue Bao* 45 (2010) 165-176.
- [13] E.J. Arts, D.J. Hazuda, HIV-1 Antiretroviral Drug Therapy., *Cold Spring Harb Perspect Med* 2 (2012) a007161.
- [14] D.P. Bartel, M.L. Zapp, M.R. Green, J.W. Szostak, HIV-1 Rev regulation involves recognition of non-Watson-Crick base pairs in viral RNA., *Cell* 67 (1991) 529-536.
- [15] M.L. Zapp, M.R. Green, Sequence-specific RNA binding by the HIV-1 Rev protein., *Nature* 342 (1989) 714-716.

- [16] Y.F. Ahmed, S.M. Hanly, M.H. Malim, B.R. Cullen, W.C. Greene, Structure-function analyses of the HTLV-I Rex and HIV-1 Rev RNA response elements: insights into the mechanism of Rex and Rev action., *Genes Dev* 4 (1990) 1014-1022.
- [17] M.H. Malim, S. Böhnlein, J. Hauber, B.R. Cullen, Functional dissection of the HIV-1 Rev trans-activator--derivation of a trans-dominant repressor of Rev function., *Cell* 58 (1989) 205-214.
- [18] M.H. Malim, J. Hauber, S.Y. Le, J.V. Maizel, B.R. Cullen, The HIV-1 rev trans-activator acts through a structured target sequence to activate nuclear export of unspliced viral mRNA., *Nature* 338 (1989) 254-257.
- [19] M.H. Malim, L.S. Tiley, D.F. McCarn, J.R. Rusche, J. Hauber, B.R. Cullen, HIV-1 structural gene expression requires binding of the Rev trans-activator to its RNA target sequence., *Cell* 60 (1990) 675-683.
- [20] T.J. Daly, K.S. Cook, G.S. Gray, T.E. Maione, J.R. Rusche, Specific binding of HIV-1 recombinant Rev protein to the Rev-responsive element in vitro., *Nature* 342 (1989) 816-819.
- [21] J.L. Battiste, R. Tan, A.D. Frankel, J.R. Williamson, Binding of an HIV Rev peptide to Rev responsive element RNA induces formation of purine-purine base pairs., *Biochemistry* 33 (1994) 2741-2747.
- [22] E.O. Freed, HIV-1 replication., *Somat Cell Mol Genet* 26 (2001) 13-33.
- [23] V.W. Pollard, M.H. Malim, The HIV-1 Rev protein., *Annu Rev Microbiol* 52 (1998) 491-532.
- [24] A.D. Frankel, J.A. Young, HIV-1: fifteen proteins and an RNA., *Annu Rev Biochem* 67 (1998) 1-25.
- [25] J.L. Battiste, H. Mao, N.S. Rao, R. Tan, D.R. Muhandiram, L.E. Kay, A.D. Frankel, J.R. Williamson, Alpha helix-RNA major groove recognition in an HIV-1 rev peptide-RRE RNA complex., *Science* 273 (1996) 1547-1551.
- [26] J.A. Turpin, R.W. Buckheit, D. Derse, M. Hollingshead, K. Williamson, C. Palamone, M.C. Osterling, S.A. Hill, L. Graham, C.A. Schaeffer, M. Bu, M. Huang, W.M. Cholody, C.J. Michejda, W.G. Rice, Inhibition of acute-, latent-, and chronic-phase human immunodeficiency virus type 1 (HIV-1) replication by a bistriazolacridone analog that selectively inhibits HIV-1 transcription., *Antimicrob Agents Chemother* 42 (1998) 487-494.
- [27] T. Van Neck, C. Pannecouque, E. Vanstreels, M. Stevens, W. Dehaen, D. Daelemans, Inhibition of the CRM1-mediated nucleocytoplasmic transport by N-azolylacrylates: structure-activity relationship and mechanism of action., *Bioorg Med Chem* 16 (2008) 9487-9497.
- [28] R. Wagner, M. Graf, K. Bieler, H. Wolf, T. Grunwald, P. Foley, K. Uberla, Rev-independent expression of synthetic gag-pol genes of human immunodeficiency virus type 1 and simian immunodeficiency virus: implications for the safety of lentiviral vectors., *Hum Gene Ther* 11 (2000) 2403-2413.

- [29] A.M. Ward, D. Rekosh, M.L. Hammarskjold, Trafficking through the Rev/RRE pathway is essential for efficient inhibition of human immunodeficiency virus type 1 by an antisense RNA derived from the envelope gene., *J Virol* 83 (2009) 940-952.
- [30] J.M. Watts, K.K. Dang, R.J. Gorelick, C.W. Leonard, J.W. Bess, R. Swanstrom, C.L. Burch, K.M. Weeks, Architecture and secondary structure of an entire HIV-1 RNA genome., *Nature* 460 (2009) 711-716.
- [31] H. Wodrich, H.G. Kräusslich, Nucleocytoplasmic RNA transport in retroviral replication., *Results Probl Cell Differ* 34 (2001) 197-217.
- [32] C.S. Adamson, E.O. Freed, Novel approaches to inhibiting HIV-1 replication., *Antiviral Res* 85 (2010) 119-141.
- [33] B.R. Cullen, HIV-1 auxiliary proteins: making connections in a dying cell., *Cell* 93 (1998) 685-692.
- [34] C.M. Wright, B.K. Felber, H. Paskalis, G.N. Pavlakis, Expression and characterization of the trans-activator of HTLV-III/LAV virus., *Science* 234 (1986) 988-992.
- [35] J. Berger, C. Aepinus, M. Dobrovnik, B. Fleckenstein, J. Hauber, E. Böhnlein, Mutational analysis of functional domains in the HIV-1 Rev trans-regulatory protein., *Virology* 183 (1991) 630-635.
- [36] A.W. Cochrane, K.S. Jones, S. Beidas, P.J. Dillon, A.M. Skalka, C.A. Rosen, Identification and characterization of intragenic sequences which repress human immunodeficiency virus structural gene expression., *J Virol* 65 (1991) 5305-5313.
- [37] D.A. Mann, I. Mikaélian, R.W. Zimmell, S.M. Green, A.D. Lowe, T. Kimura, M. Singh, P.J. Butler, M.J. Gait, J. Karn, A molecular rheostat. Co-operative rev binding to stem I of the rev-response element modulates human immunodeficiency virus type-1 late gene expression., *J Mol Biol* 241 (1994) 193-207.
- [38] L.K. Venkatesh, S. Mohammed, G. Chinnadurai, Functional domains of the HIV-1 rev gene required for trans-regulation and subcellular localization., *Virology* 176 (1990) 39-47.
- [39] P.J. Dillon, P. Nelbock, A. Perkins, C.A. Rosen, Structural and functional analysis of the human immunodeficiency virus type 2 Rev protein., *J Virol* 65 (1991) 445-449.
- [40] F. Bachelierie, M.S. Rodriguez, C. Dargemont, D. Rousset, D. Thomas, J.L. Virelizier, F. Arenzana-Seisdedos, Nuclear export signal of IkappaBalpha interferes with the Rev-dependent posttranscriptional regulation of human immunodeficiency virus type I., *J Cell Sci* 110 ( Pt 22) (1997) 2883-2893.
- [41] E. Berthold, F. Maldarelli, cis-acting elements in human immunodeficiency virus type 1 RNAs direct viral transcripts to distinct intranuclear locations., *J Virol* 70 (1996) 4667-4682.

- [42] B.R. Henderson, P. Percipalle, Interactions between HIV Rev and nuclear import and export factors: the Rev nuclear localisation signal mediates specific binding to human importin-beta., *J Mol Biol* 274 (1997) 693-707.
- [43] E. Izaurralde, U. Kutay, C. von Kobbe, I.W. Mattaj, D. Görlich, The asymmetric distribution of the constituents of the Ran system is essential for transport into and out of the nucleus., *EMBO J* 16 (1997) 6535-6547.
- [44] P. Askjaer, T.H. Jensen, J. Nilsson, L. Englmeier, J. Kjems, The specificity of the CRM1-Rev nuclear export signal interaction is mediated by RanGTP., *J Biol Chem* 273 (1998) 33414-33422.
- [45] U. Fischer, V.W. Pollard, R. Lührmann, M. Teufel, M.W. Michael, G. Dreyfuss, M.H. Malim, Rev-mediated nuclear export of RNA is dominant over nuclear retention and is coupled to the Ran-GTPase cycle., *Nucleic Acids Res* 27 (1999) 4128-4134.
- [46] D. Daelemans, E. Afonina, J. Nilsson, G. Werner, J. Kjems, E. De Clercq, G.N. Pavlakakis, A.M. Vandamme, A synthetic HIV-1 Rev inhibitor interfering with the CRM1-mediated nuclear export., *Proc Natl Acad Sci U S A* 99 (2002) 14440-14445.
- [47] T.J. Daly, R.C. Doten, J.R. Rusche, M. Auer, The amino terminal domain of HIV-1 Rev is required for discrimination of the RRE from nonspecific RNA., *J Mol Biol* 253 (1995) 243-258.
- [48] S. Heaphy, C. Dingwall, I. Ernberg, M.J. Gait, S.M. Green, J. Karn, A.D. Lowe, M. Singh, M.A. Skinner, HIV-1 regulator of virion expression (Rev) protein binds to an RNA stem-loop structure located within the Rev response element region., *Cell* 60 (1990) 685-693.
- [49] Y. Hakata, M. Yamada, N. Mabuchi, H. Shida, The carboxy-terminal region of the human immunodeficiency virus type 1 protein Rev has multiple roles in mediating CRM1-related Rev functions., *J Virol* 76 (2002) 8079-8089.
- [50] M. Floer, G. Blobel, Putative reaction intermediates in Crm1-mediated nuclear protein export., *J Biol Chem* 274 (1999) 16279-16286.
- [51] C.F. Zanelli, S.R. Valentini, Is there a role for eIF5A in translation?, *Amino Acids* 33 (2007) 351-358.
- [52] M. Ruhl, M. Himmelspach, G.M. Bahr, F. Hammerschmid, H. Jaksche, B. Wolff, H. Aschauer, G.K. Farrington, H. Probst, D. Bevec, Eukaryotic initiation factor 5A is a cellular target of the human immunodeficiency virus type 1 Rev activation domain mediating trans-activation., *J Cell Biol* 123 (1993) 1309-1320.
- [53] D. Bevec, J. Hauber, Eukaryotic initiation factor 5A activity and HIV-1 Rev function., *Biol Signals* 6 (1997) 124-133.
- [54] O. Rosorius, B. Reichart, F. Krätzer, P. Heger, M.C. Dabauvalle, J. Hauber, Nuclear pore localization and nucleocytoplasmic transport of eIF-5A: evidence for direct interaction with the export receptor CRM1., *J Cell Sci* 112 ( Pt 14) (1999) 2369-2380.

- [55] G. Farjot, A. Sergeant, I. Mikaélian, A new nucleoporin-like protein interacts with both HIV-1 Rev nuclear export signal and CRM-1., *J Biol Chem* 274 (1999) 17309-17317.
- [56] M. Suhasini, T.R. Reddy, Cellular proteins and HIV-1 Rev function., *Curr HIV Res* 7 (2009) 91-100.
- [57] Z. Yu, N. Sánchez-Velaz, I.E. Catrina, E.L. Kittler, E.B. Udofia, M.L. Zapp, The cellular HIV-1 Rev cofactor hRIP is required for viral replication., *Proc Natl Acad Sci U S A* 102 (2005) 4027-4032.
- [58] J.J. He, J. Henao-Mejia, Y. Liu, Sam68 functions in nuclear export and translation of HIV-1 RNA., *RNA Biol* 6 (2009) 384-386.
- [59] M. McLaren, K. Asai, A. Cochrane, A novel function for Sam68: enhancement of HIV-1 RNA 3' end processing., *RNA* 10 (2004) 1119-1129.
- [60] S. Modem, K.R. Badri, T.C. Holland, T.R. Reddy, Sam68 is absolutely required for Rev function and HIV-1 production., *Nucleic Acids Res* 33 (2005) 873-879.
- [61] T.R. Reddy, A single point mutation in the nuclear localization domain of Sam68 blocks the Rev/RRE-mediated transactivation., *Oncogene* 19 (2000) 3110-3114.
- [62] J. Li, H. Tang, T.M. Mullen, C. Westberg, T.R. Reddy, D.W. Rose, F. Wong-Staal, A role for RNA helicase A in post-transcriptional regulation of HIV type 1., *Proc Natl Acad Sci U S A* 96 (1999) 709-714.
- [63] M. Ishaq, J. Hu, X. Wu, Q. Fu, Y. Yang, Q. Liu, D. Guo, Knockdown of cellular RNA helicase DDX3 by short hairpin RNAs suppresses HIV-1 viral replication without inducing apoptosis., *Mol Biotechnol* 39 (2008) 231-238.
- [64] V.S. Yedavalli, C. Neuveut, Y.H. Chi, L. Kleiman, K.T. Jeang, Requirement of DDX3 DEAD box RNA helicase for HIV-1 Rev-RRE export function., *Cell* 119 (2004) 381-392.
- [65] M. Auer, H.U. Gremlich, J.M. Seifert, T.J. Daly, T.G. Parslow, G. Casari, H. Gstach, Helix-loop-helix motif in HIV-1 Rev., *Biochemistry* 33 (1994) 2988-2996.
- [66] T.J. Daly, J.R. Rusche, T.E. Maione, A.D. Frankel, Circular dichroism studies of the HIV-1 Rev protein and its specific RNA binding site., *Biochemistry* 29 (1990) 9791-9795.
- [67] T.J. Daly, P. Rennert, P. Lynch, J.K. Barry, M. Dundas, J.R. Rusche, R.C. Doten, M. Auer, G.K. Farrington, Perturbation of the carboxy terminus of HIV-1 Rev affects multimerization on the Rev responsive element., *Biochemistry* 32 (1993) 8945-8954.
- [68] C. Jain, J.G. Belasco, Structural model for the cooperative assembly of HIV-1 Rev multimers on the RRE as deduced from analysis of assembly-defective mutants., *Mol Cell* 7 (2001) 603-614.
- [69] M.A. DiMattia, N.R. Watts, S.J. Stahl, C. Rader, P.T. Wingfield, D.I. Stuart, A.C. Steven, J.M. Grimes, Implications of the HIV-1 Rev dimer structure at 3.2 Å resolution for multimeric binding to the Rev response element., *Proc Natl Acad Sci U S A* 107 (2010) 5810-5814.

- [70] M.D. Daugherty, B. Liu, A.D. Frankel, Structural basis for cooperative RNA binding and export complex assembly by HIV Rev., *Nat Struct Mol Biol* 17 (2010) 1337-1342.
- [71] N. Lewis, J. Williams, D. Rekosh, M.L. Hammarskjöld, Identification of a cis-acting element in human immunodeficiency virus type 2 (HIV-2) that is responsive to the HIV-1 rev and human T-cell leukemia virus types I and II rex proteins., *J Virol* 64 (1990) 1690-1697.
- [72] R.W. Zemmel, A.C. Kelley, J. Karn, P.J. Butler, Flexible regions of RNA structure facilitate co-operative Rev assembly on the Rev-response element., *J Mol Biol* 258 (1996) 763-777.
- [73] W.C. Lam, J.M. Seifert, F. Amberger, C. Graf, M. Auer, D.P. Millar, Structural dynamics of HIV-1 Rev and its complexes with RRE and 5S RNA., *Biochemistry* 37 (1998) 1800-1809.
- [74] S.J. Pond, W.K. Ridgeway, R. Robertson, J. Wang, D.P. Millar, HIV-1 Rev protein assembles on viral RNA one molecule at a time., *Proc Natl Acad Sci U S A* 106 (2009) 1404-1408.
- [75] M.D. Daugherty, D.S. Booth, B. Jayaraman, Y. Cheng, A.D. Frankel, HIV Rev response element (RRE) directs assembly of the Rev homooligomer into discrete asymmetric complexes., *Proc Natl Acad Sci U S A* 107 (2010) 12481-12486.
- [76] T. Vercruysse, S. Pawar, W. De Borggraeve, E. Pardon, G.N. Pavlakis, C. Pannecoque, J. Steyaert, J. Balzarini, D. Daelemans, Measuring cooperative Rev protein-protein interactions on Rev responsive RNA by fluorescence resonance energy transfer., *RNA Biol* 8 (2011) 316-324.
- [77] M. Laughrea, L. Jetté, Kissing-loop model of HIV-1 genome dimerization: HIV-1 RNAs can assume alternative dimeric forms, and all sequences upstream or downstream of hairpin 248-271 are dispensable for dimer formation., *Biochemistry* 35 (1996) 1589-1598.
- [78] J.C. Paillart, R. Marquet, E. Skripkin, C. Ehresmann, B. Ehresmann, Dimerization of retroviral genomic RNAs: structural and functional implications., *Biochimie* 78 (1996) 639-653.
- [79] R.S. Russell, C. Liang, M.A. Wainberg, Is HIV-1 RNA dimerization a prerequisite for packaging? Yes, no, probably?, *Retrovirology* 1 (2004) 23.
- [80] K. Moehle, Z. Athanassiou, K. Patora, A. Davidson, G. Varani, J.A. Robinson, Design of beta-hairpin peptidomimetics that inhibit binding of alpha-helical HIV-1 Rev protein to the rev response element RNA., *Angew Chem Int Ed Engl* 46 (2007) 9101-9104.
- [81] T.A. Wilkinson, M.V. Botuyan, B.E. Kaplan, J.J. Rossi, Y. Chen, Arginine side-chain dynamics in the HIV-1 rev-RRE complex., *J Mol Biol* 303 (2000) 515-529.
- [82] K. Fineberg, T. Fineberg, A. Graessmann, N.W. Luedtke, Y. Tor, R. Lixin, D.A. Jans, A. Loyter, Inhibition of nuclear import mediated by the Rev-arginine rich motif by RNA molecules., *Biochemistry* 42 (2003) 2625-2633.

- [83] L. Chaloin, F. Smagulova, E. Hariton-Gazal, L. Briant, A. Loyter, C. Devaux, Potent inhibition of HIV-1 replication by backbone cyclic peptides bearing the Rev arginine rich motif., *J Biomed Sci* 14 (2007) 565-584.
- [84] L. Ponchon, G. Beauvais, S. Nonin-Lecomte, F. Dardel, A generic protocol for the expression and purification of recombinant RNA in *Escherichia coli* using a tRNA scaffold., *Nat Protoc* 4 (2009) 947-959.
- [85] L. Ponchon, F. Dardel, Recombinant RNA technology: the tRNA scaffold., *Nat Methods* 4 (2007) 571-576.
- [86] C.M. Dunham, G.L. Conn, Recombinant RNA expression., *Nat Methods* 4 (2007) 547-548.
- [87] X.J. Huang, T.J. Hope, B.L. Bond, D. McDonald, K. Grahl, T.G. Parslow, Minimal Rev-response element for type 1 human immunodeficiency virus., *J Virol* 65 (1991) 2131-2134.
- [88] J. Karn, C. Dingwall, J.T. Finch, S. Heaphy, M.J. Gait, RNA binding by the tat and rev proteins of HIV-1., *Biochimie* 73 (1991) 9-16.
- [89] P. Bénas, G. Bec, G. Keith, R. Marquet, C. Ehresmann, B. Ehresmann, P. Dumas, The crystal structure of HIV reverse-transcription primer tRNA(Lys,3) shows a canonical anticodon loop., *RNA* 6 (2000) 1347-1355.
- [90] H. Shi, P.B. Moore, The crystal structure of yeast phenylalanine tRNA at 1.93 Å resolution: a classic structure revisited., *RNA* 6 (2000) 1091-1105.
- [91] E. Schmitt, M. Panvert, S. Blanquet, Y. Mechulam, Crystal structure of methionyl-tRNA<sup>fMet</sup> transformylase complexed with the initiator formyl-methionyl-tRNA<sup>fMet</sup>., *EMBO J* 17 (1998) 6819-6826.
- [92] H.P. Erickson, Size and shape of protein molecules at the nanometer level determined by sedimentation, gel filtration, and electron microscopy., *Biol Proced Online* 11 (2009) 32-51.
- [93] J. Lebowitz, M.S. Lewis, P. Schuck, Modern analytical ultracentrifugation in protein science: a tutorial review., *Protein Sci* 11 (2002) 2067-2079.
- [94] M.X. Fernandes, A. Ortega, M.C. López Martínez, J. García de la Torre, Calculation of hydrodynamic properties of small nucleic acids from their atomic structure., *Nucleic Acids Res* 30 (2002) 1782-1788.
- [95] A.M. Joubert, A.S. Byrd, V.J. LiCata, Global conformations, hydrodynamics, and X-ray scattering properties of Taq and *Escherichia coli* DNA polymerases in solution., *J Biol Chem* 278 (2003) 25341-25347.
- [96] L. Kisselev, T. Venkster, tRNA: Structure and functions Report of a Pre-Symposium held in Riga, U.S.S.R., on June 19 and 20, 1970, within the scope of the VII International Symposium on the Chemistry of Natural Products., *FEBS Lett* 11 (1970) 73-77.
- [97] J. Lipfert, S. Doniach, Small-angle X-ray scattering from RNA, proteins, and protein complexes., *Annu Rev Biophys Biomol Struct* 36 (2007) 307-327.
- [98] L. Pollack, SAXS studies of ion-nucleic acid interactions., *Annu Rev Biophys* 40 (2011) 225-242.

- [99] S. Yang, M. Parisien, F. Major, B. Roux, RNA structure determination using SAXS data., *J Phys Chem B* 114 (2010) 10039-10048.
- [100] J.M. Blose, S.A. Pabit, S.P. Meisburger, L. Li, C.D. Jones, L. Pollack, Effects of a protecting osmolyte on the ion atmosphere surrounding DNA duplexes., *Biochemistry* 50 (2011) 8540-8547.
- [101] R.P. Rambo, J.A. Tainer, Improving small-angle X-ray scattering data for structural analyses of the RNA world., *RNA* 16 (2010) 638-646.
- [102] C.D. Putnam, M. Hammel, G.L. Hura, J.A. Tainer, X-ray solution scattering (SAXS) combined with crystallography and computation: defining accurate macromolecular structures, conformations and assemblies in solution., *Q Rev Biophys* 40 (2007) 191-285.
- [103] K. Stovgaard, C. Andreetta, J. Ferkinghoff-Borg, T. Hamelryck, Calculation of accurate small angle X-ray scattering curves from coarse-grained protein models., *BMC Bioinformatics* 11 (2010) 429.
- [104] H.B. Stuhmann, Small-angle scattering and its interplay with crystallography, contrast variation in SAXS and SANS., *Acta Crystallogr A* 64 (2008) 181-191.
- [105] R. Russell, I.S. Millett, S. Doniach, D. Herschlag, Small angle X-ray scattering reveals a compact intermediate in RNA folding., *Nat Struct Biol* 7 (2000) 367-370.
- [106] J.L. Darlix, C. Gabus, M.T. Nugeyre, F. Clavel, F. Barré-Sinoussi, Cis elements and trans-acting factors involved in the RNA dimerization of the human immunodeficiency virus HIV-1., *J Mol Biol* 216 (1990) 689-699.
- [107] E.S. DeJong, C.E. Chang, M.K. Gilson, J.P. Marino, Proflavine acts as a Rev inhibitor by targeting the high-affinity Rev binding site of the Rev responsive element of HIV-1., *Biochemistry* 42 (2003) 8035-8046.
- [108] A.S. Cockrell, H. van Praag, N. Santistevan, H. Ma, T. Kafri, The HIV-1 Rev/RRE system is required for HIV-1 5' UTR cis elements to augment encapsidation of heterologous RNA into HIV-1 viral particles., *Retrovirology* 8 (2011) 51.

## **VITA**

Jason Kelly Allison was born in Meridian, Mississippi on February 14, 1974 to parents Buford Henry and Mary Glen Allison. Jason completed his undergraduate degree in Biomedical Science at Texas A&M University. While attending Texas A&M University, Jason worked in the Laboratory of Dr. J. Martin Scholtz on protein folding. He was accepted to the Molecular Biophysics Educational Track (MBET) at the University of Texas Medical Branch-Galveston in 2005.

Jason can be contacted at 2319 Creekhickory Rd., Houston, TX, 77068

### **Education**

B.S., Biomedical Science, Texas A&M University, College Station, TX

### **Publications**

Design, Expression, and Characterization of a RRE-containing Chimeric tRNA

(Manuscript in preparation)

## **Summary of Dissertation**

This dissertation investigated the Rev Response Element (RRE) binding properties of the HIV Rev protein. The HIV-1 Rev is a regulatory protein which is critical for the late-phase development of the Human Immunodeficiency Virus-1 (HIV-1). During early-phase development of HIV-1, Rev accumulates in the cytoplasm and is transported into the nucleus through interactions with Importin- $\beta$  via its Nuclear Localization Sequence (NLS). Following sufficient accumulation in the nucleus, Rev recognizes and assembles on the Rev Response Element (RRE), a 351nt region contained within singly and unspliced HIV RNAs. This ribonucleoprotein (RNP) complex allows for the export of these RNA transcripts encoding viral structural proteins and genomic RNA to the cytoplasm. Of particular interest is the interaction of Rev with the Rev Response Element (RRE) RNA. It is known that Rev initially binds to a structured Stem Loop-IIB on the RRE and subsequently assembles along flanking sequences of the RRE; however, details of this interaction are not completely understood. I designed RRE-containing tRNAs for biophysical studies of the Rev:RRE complexes. The tRNA chimeras employed natural tRNA from human lysyl tRNA, bacterial initiator methionyl tRNA, and baker's yeast (*S. cerevisiae*) phenylalanyl tRNA for use as scaffolds to express RRE sequences. Using size-exclusion (SEC), analytical ultracentrifugation (AUC), and small angle X-ray scattering (SAXS) I demonstrated the formation of a discrete Rev:RRE RNA complex. Data analysis presented in this work suggests that Rev is mediating a dimer of RRE RNA.

---